4. Generation of Runoff Data by Tank Model

4.1 Purpose

Generation of runoff data of Yuam river aimed to examine reasonability of the runoff data which was actually observed and employed as a basic information in energy computation.

4.2 Observed data utilized in the generation

The observed daily runoff data collected at Ban Tha Rua was available for eleven years from 1970 to 1980, while daily rainfall was observed at Mae Saviang for thirty-one years from 1950 to 1980 and other four observatories, i.e. Ban Tha Rua, Chom Chaeng, Sop Han and Mae La Luang for fourteen years or so.

In the generating process, however, those four rainfall observatories were not taken into consideration because the observing periods are much shorter than of Mae Saviang, and most of the periods are overlapping with the period of runoff data at Ban Tha Rua, thus no point to be used in generating the runoff of Yuam river. Consequently runoff data was generated on the basis of the thirty-one year daily rainfall at Mae Sariang which overlaps for the full period of eleven years of daily runoff at Ban Tha Rua and, in addition, extends twenty years more to the past till 1950.

The generating model, i.e. the tank model, was first adjusted during the overlapping period and then generated the runoff of the river taking the daily rainfall as input.

4.3 Tank model

1) General

Tank model is one method of runoff analysis, being widely adopted in the world. Tank model applicable to both flood and daily runoff analysis can estimate runoff of a river by taking rainfall as input. Basically the model is composed of several tanks combined each other in series or parallel, each tank of which has outlets in the bottom or side corresponding to seepage to the ground or discharge to a river. The conceptional illustration is given Fig. 4.1(a).

Function of tank model is explained as follows, taking simplest component (one tank with two outlets in the bottom and side) as an example. See Fig. 4.1(b).

In the model, section of all tanks is 1, thus storage volume can be simply expressed by height of the water stored in the tank. All the inputs and outputs are considered in time series and expressed by unit of millimeter (mm).

Rainfall	$\{x_n\}$	
Storage	$\{X_n\}$	
Discharge	$\{y_n\}$	
Seepage	$\{z_n\}$	$n = 1, 2, 3, \cdots\cdots$

The outlets equipped in the side and bottom have respective coefficient α and β adjusting the discharge or seepage rate. The side outlet is usually equipped above the bottom with certain distance H which also enables to adjust the discharge and seepage rate.

The output from the tank can be expressed as follows.

$$y_n = \begin{cases} 0 & \text{if } 0 \leq Xn \leq H \\ \alpha(Xn - H) & \text{if } H < Xn \end{cases}$$

$$z_n = \beta Xn$$

Considering the process in time series, time n and n+1, as shown Fig. 4.1(c), outputs are then expressed in the following way.

time n;

$y_n = \alpha(Xn - H)$, since Xn>H in the figure

$z_n = \beta Xn$

then

$X'n = Xn - y_n - z_n$

time n+1;

$X_{n+1} = X'n + x_{n+1}$

$y_{n+1} = \alpha(X_{n+1} - H)$

$z_{n+1} = \beta X_{n+1}$

then

$X'_{n+1} = X_{n+1} - y_{n+1} - z_{n+1}$

This process is repeated afterwards as time proceeds.

In ordinary tank model shown in Fig. 4.1(a), the said tanks are combined each other vertically in series. In such case, discharge to a river is summation of all the output from the side outlets, while output from the bottom outlet is regarded as seepage to the ground, which is trapped in the lower tank.

Structure of the ordinary tank model is also understood on the analogy of real structure of the ground. Fig. 4.2 shows the correspondence between them.

Rainfall falls into the top tank. Lower tanks receive the water coming out of the upper tank through the bottom outlet. On the other hand, a part of water stored in each tank is discharged to a river through the side outlet. This process is seemed resemble to the real structure of the ground shown in left-hand side, figure (a).

Rainfall falling on the surface of the ground is partially discharged immediately, while the rest seepages to the ground. Outflow from the side outlet of each tank shown in the figure (b) can be considered discharge from each permeable layer of the ground as shown in the figure (a). On the other hand outflow from the bottom outlet of each tank can be thought infiltration from upper permeable layer to lower permeable layer. In the model, outlets of lower tanks are made narrower, i.e. smaller coefficient α or β, because discharge rates in real situation are smaller in lower layers.

This model can well reflect variety of discharge pattern resulted from rainfall pattern. For example, continuous rainfall could cause floods, even if the rainfall is less intensified, while highly intensified rainfall could cause floods even if the whole amount of precipitation is small. In this tank model, if the rainfall continues at a rate exceeding the infiltration rate of the bottom outlet of the top tank, storage in the top tank increases gradually and it causes a large amount of discharge from the top tank where side outlet is wide and enables to release water quickly. If the rainfall occured in short period with high intensity, it also causes a large amount of discharge because storage in the top tank increases rapidly and most of the water trapped in the tank is released from the side outlet.

Generally speaking, if the tank model is composed of three or four tanks combined vertically in series, the top tank is considered corresponding to surface runoff, the second tank is to be subsurface flow and the third and fourth tanks are to be base flow. The tank model where each tank has differet discharge rate, α and β, is, thus, considered to represent the actual physical characteristics of the phenomenon.

Problem of the tank model is to decide the parameters of the model. As seen in the previous figures, the model consists of several tanks and each tank has parameters of outflow rate α and β and the distance of the side outlet from the bottom. These parameters have to be decided by trial and error, namely taking rainfall data as input, the parameters are so adjusted that the model as a whole can generate runoff well-matched to the observed runoff.

2) Tank model considered in the study

Tank model has variety in its structure, reflecting basin condition. Following three types were considered in this study.

(i) Ordinary series combination of four tanks
(ab. ordinary model, see Fig. 4.3(a))

(ii) Ordinary model equipped with soil moisture function in the top tank
(ab. soil moisture model, see Fig. 4.3(b))

(iii) Parallel combination of four soil moisture models
(ab. 4 x 4 model, see Fig. 4.3(c))

It is generally said that the ordinary model is suitable for such region that climate is mild and there is moderate rainfall throughout a year rendering the ground always wet. On the other hand, the soil moisture model is said appropriate for such region where long dry season exists and thus the ground becomes dry for certain period in a year. If the dry condition of climate is much severer, the 4x4 model is considered suitable.

All the simulation by these three models had been conducted by computer and the soil moisture model was eventually employed in analysis in this study.

3) Soil moisture model

Fig. 4.4 shows detail of the soil moisture function equipped in the top tank.

The soil moisture function consists of two components, the primary and the secondary, which have saturation capacity of S1 and S2, respecttively Symbols appearing in the figure have the following meanings.

S1: Saturation Capacity of the primary soil moisture function

S2: Saturation Capacity of the secondary soil moisture function

XP: Actual Storage in the primary soil moisture function

XS: Actual Storage in the secondary soil moisture function

XF: Free Water stored above the primary soil moisture function, learing the primary function full.

$$XA = XP + XF$$

$$T1 = K1\left(1 - \frac{XP}{S1}\right)$$

$$T2 = K2\left(\frac{XP}{S1} - \frac{XS}{S2}\right)$$

Rainfall is accumulated into XA. If XA is less than S1, whole XA is considered XP. If XA is greater than S1, XP is saturated (XP=S1) and the rest is considered free water (XF=XA-S1). Thus, seepage and discharge from the top tank is caused by the free water XF.

In additrion to the ordinary process of the tank model, this model allows water to move between S1 and S2, and between the top tank and the second tank. It is shown in Fig. 4.4 (3). If S1 portion is not saturated and there is free water left in the second tank, water is supplyed to the S1 portion from the second tank. This water movement is expressed by the equation below.

$$T1 = K1(1 - \frac{XP}{S1})$$

where K1 is a coefficient.

As seen in the equation, water moves only from the second tank to the S1 portion in proportion to XP/S1 which is relative humidity of the S1 portion.

On the other hand, water moves between S1 and S2 portions in a manner expressed by the following equation;

$$T2 = K2(\frac{XP}{S1} - \frac{XS}{S2})$$

If T2 is positive, water moves from the second to the top tank, on the contrary if T2 is negative, water moves from the top to the second tank. This means, in other words, water moves from dry portion to wet portion in proportion to the difference of relative humidities between the two portions.

As described above, the soil moisture function can be controlled by the four parameters, i.e. S1, S2, K1, K2.

Fig. 4.5 shows the soil moisture model with the parameters which were finally employed in the analysis. As seen in the figure, there are totally eighteen (18) parameters to be decided. These parameters were decided by trial and error. That is, under certain value of parameters given, runoff was generated by taking Mae Saviang rainfall as input, and hydrograph was then synthesized. Comparing these synthetic hydrograph with the observed hydrograph at Ban Tha Rua, parameters had been adjusted little by little so as to make the synthetic hydrograph more fit to observed.

Fig. 4.6 gives the result, where solid line in the observed hydrograph and dot line is the synthetic one.

Based on the synthetic hydrograph, periodic feature of Yuam river was studyed by spectlum analysis.

References

(1) Sugawara, M., (1978): "Zoku Ryushitsu Kaisekiho", Kyoritsu Shuppan, Tokyo

(2) Sugawara, M., Ozaki, E., Watanabe, I. & Katsuyama, Y.: "On A Method of Forecasting The Daily Discharge of The Mae Nam Chao Phraya and Its Tributaries at Several Points by Means of Tank Model", Research Notes of The National Research Center for Disaster Prevention No.24, July 1976.

(3) Sugawara, M., Ozaki, E., Watanabe, I. & Katsuyama, Y.: "Tank Model and Its Application to Bird Creek, Wollombi Brook, Bikin River, Kitsu River, Sanaga River and Nam Mune", Research Notes of The National Research Center for Disaster Prevention No.11, June 1974.

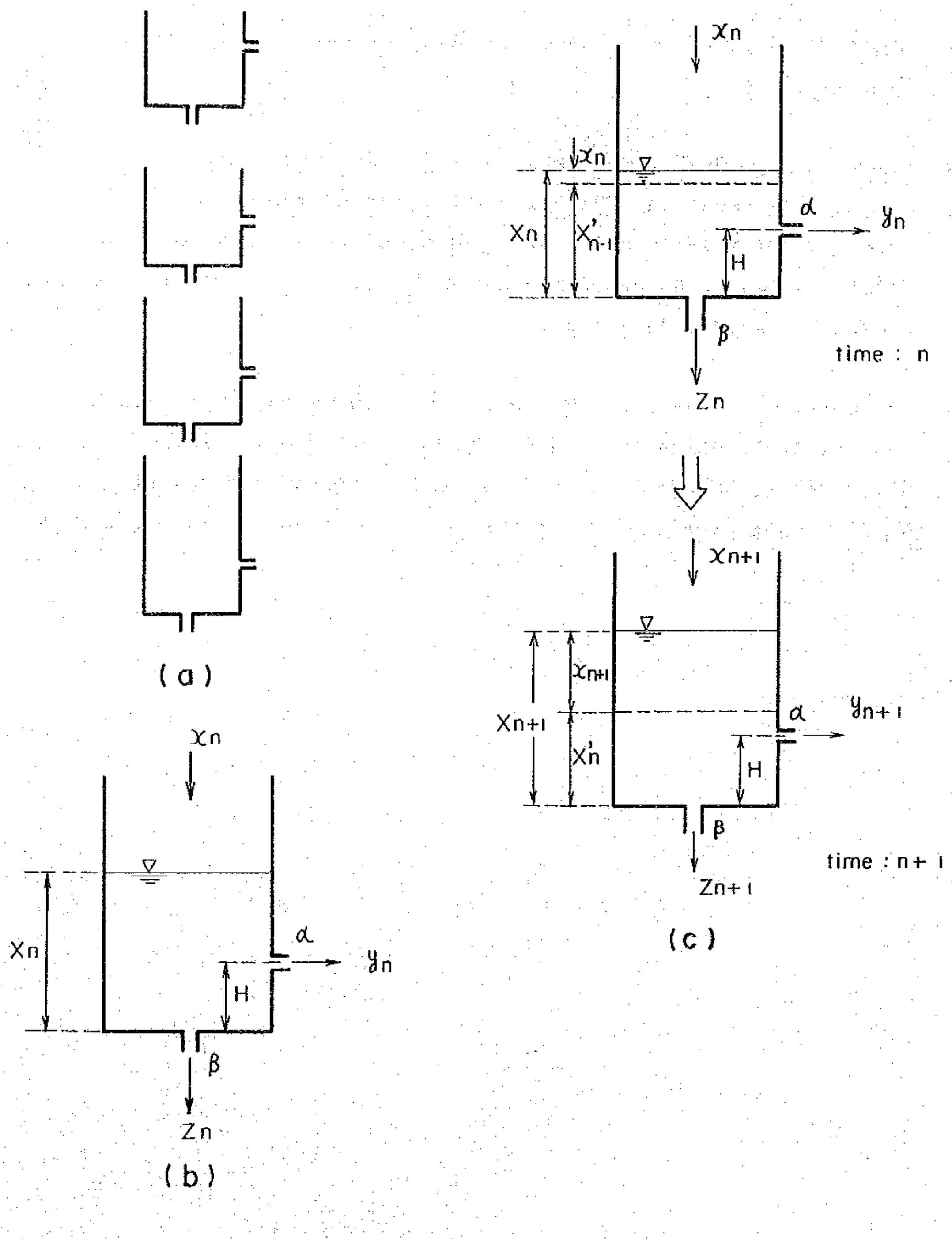

Fig. 4.1 Tank Model, Conceptional Illustration

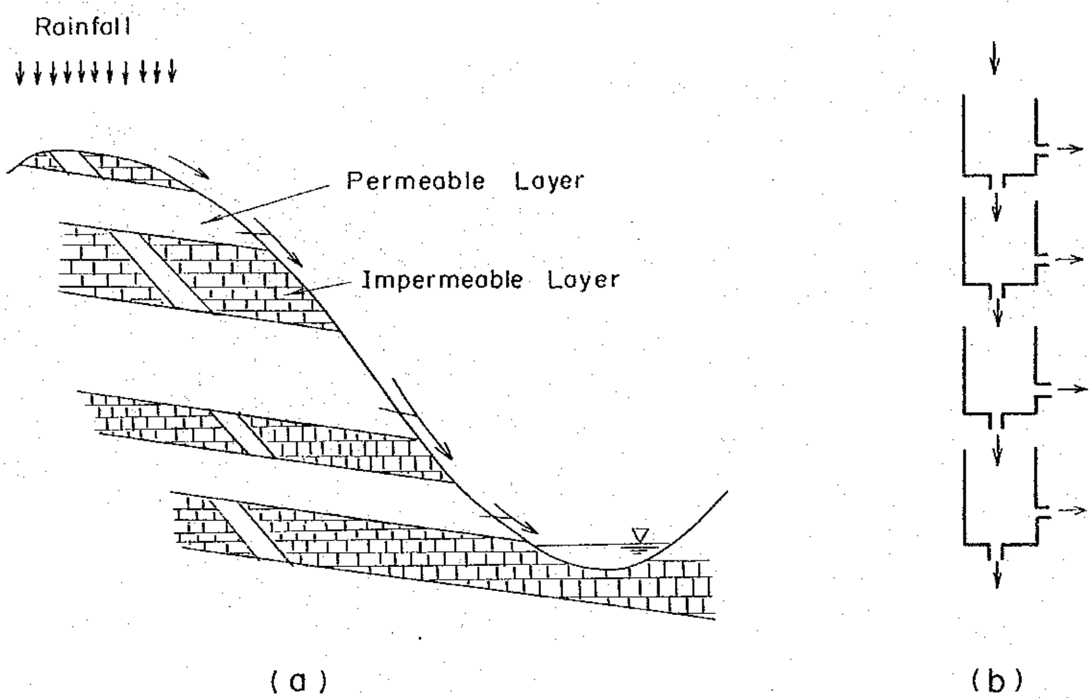

Fig. 4.2 Tank Model, Analogy to the Ground

Fig. 4-3 Estimated and Observed Runoff of Yuam River

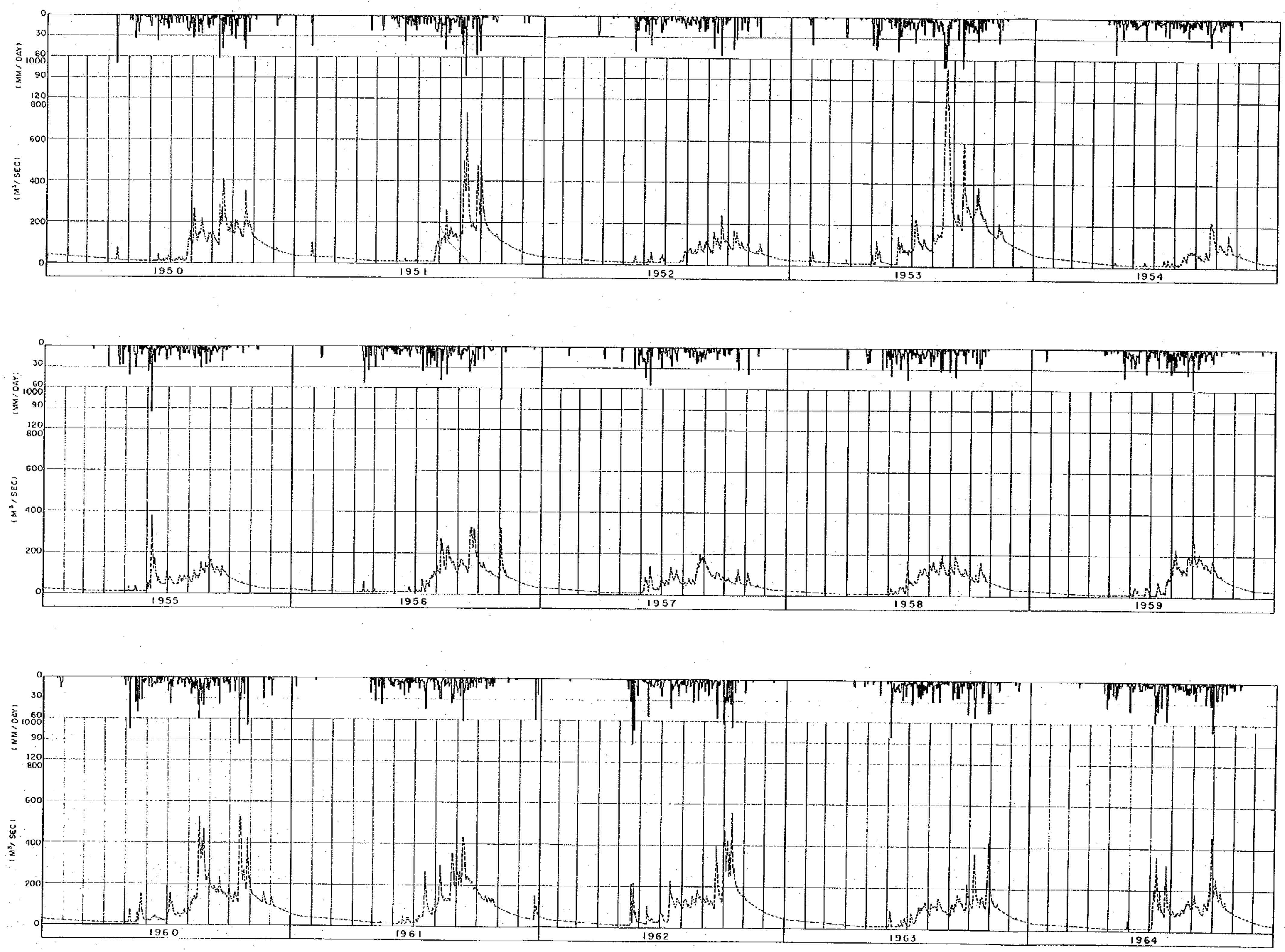

Fig. 4-3 Estimated and Observed Runoff of Yuam River (cont'd.)

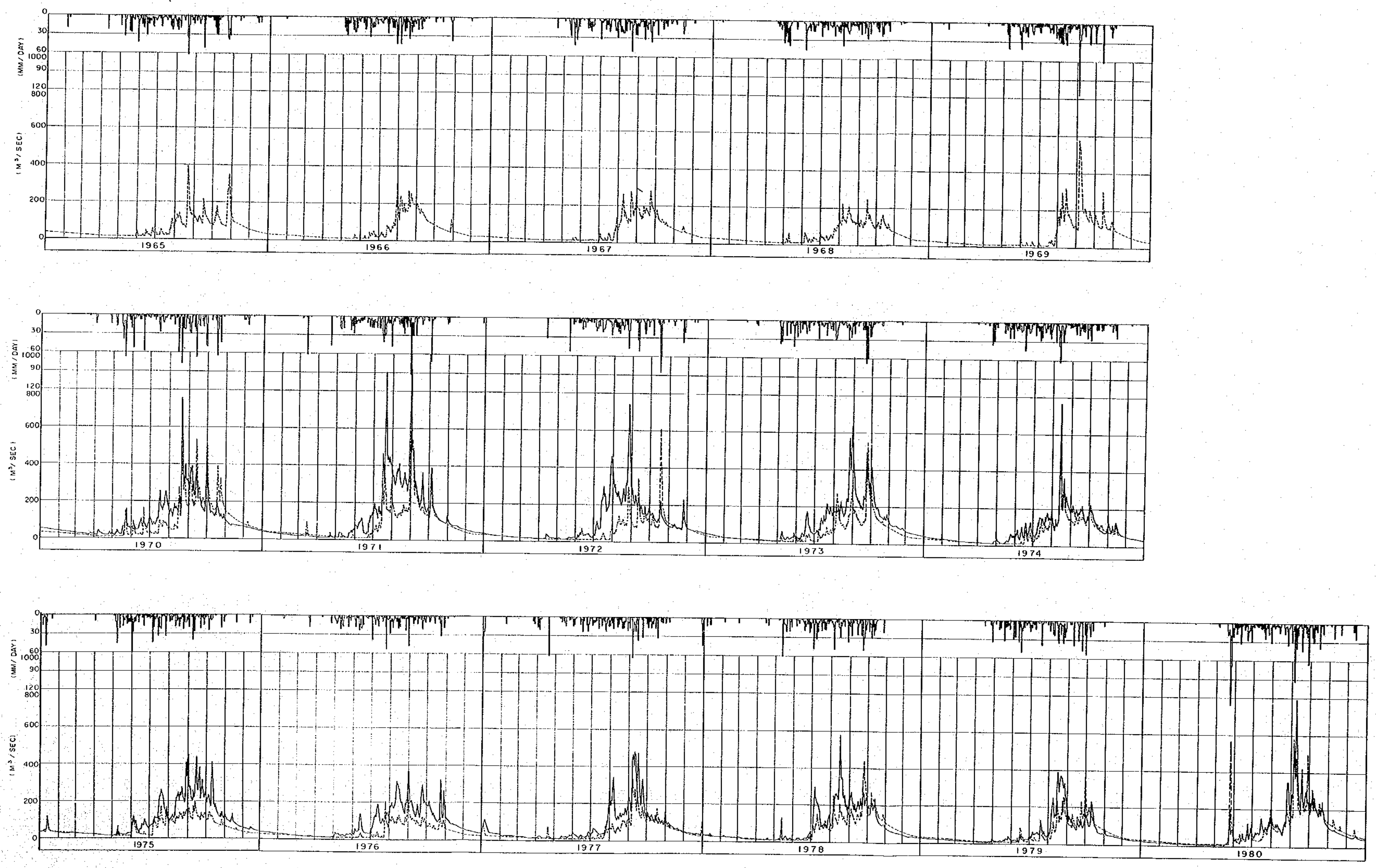

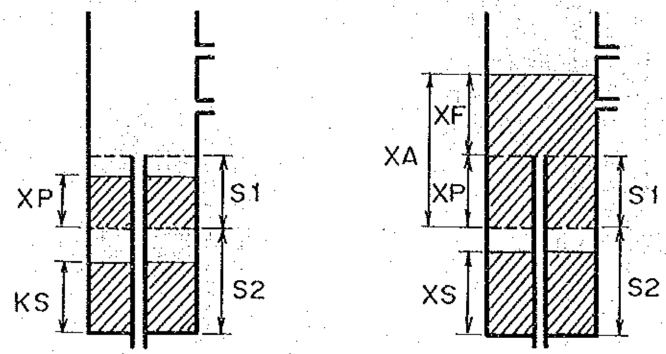

(1) (2)

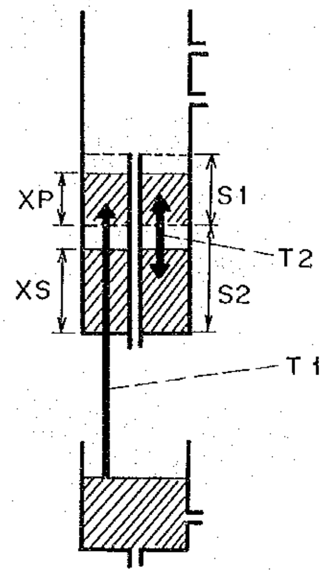

$$T1 = K1\left(1 - \frac{XP}{S1}\right)$$

$$T2 = K2\left(\frac{XP}{S1} - \frac{XS}{S2}\right)$$

(3)

S1 : Saturation Capacity of the primary soil moisture function

S2 : Saturation Capacity of the secondary soil moisture function

XP : Actual Storage in the primary soil moisture function

XS : Actual Storage in the secondary soil moisture function

XF : Free Water stored abone the primary soil moisture function, leaving the primary function full.

$XA = XP + XF$

Fig. 4.4 Detail of Soil Moisture Function

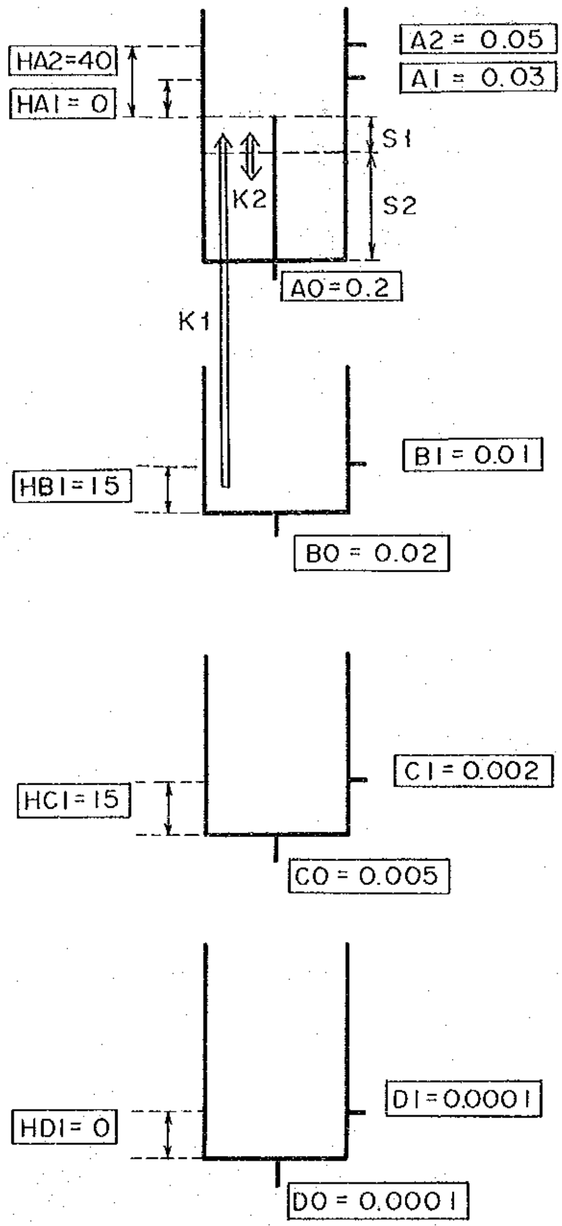

K1=	2
K2=	20
S1=	50
S2=	250

Fig. 4. 5 Tank Model Eventually Employed in the Study

5. Derivation of PMF (Probable Maximum Flood)

5.1 General Procedure of PMF

PMF analysis aims to estimate the maximum flood considered probable in a particular basin. In the analysis, in general, typical storms which have been taken place in the past are collected in the area covering not only the basin in question but also adjacent areas, or in the area where the climate condition is similar. Then such collected storms are adjusted and maximized so as to be adaptable in the said basin. The maximized storms are called PMP (Probable Maximum Precipitation). Based on the PMP derived, PMF is estimated.

In this Nam Yuam project, since most of the data collected were limited within the basin itself, the typical storms were searched for mainly in the basin and were adjusted.

5.2 Selection of precedent typical storms

Storms here are defined that s sequence of rainfall taking for a certain period with considerable amount of precipitation. Twenty-five storms were selected, looking over the past daily precipitation data recorded at four observatories in the basin as shown in Fig. 5.1 (Mas La Luang, Cham Chaeng, Sop Han and Ban Tha Rua) as well as another observatory in the adjacent basin (Salween). In the selection, following points were considered.

- ° The storm should be relatively independent from the sequence.
- ° The storm should contain sufficient amount of precipitation.
- ° The storm should be the one occuring in wide area preferably covering the whole basin.
  (In other words, such storms that found at the five observatories on the same day, during the same period in a similar patter of sequence)

Followings are the storms picked up from the past rainfall data, judging from the said condition.

1.	1967,	Aug. 1	to	Aug. 9
2.	1968,	Jul. 24	to	Jul. 30
3.	"	Aug. 10	to	Aug. 17
4.	1969,	May 26	to	Jun. 2
5.	"	Sep. 2	to	Sep. 7
6.*	1970,	May 15	to	May 18
7.*	1971,	Jul. 16	to	Jul. 22
8.	1972,	Jul. 9	to	Jul. 18
9.	"	Aug. 21	to	Aug. 26
10.	1973,	May 3	to	May 7
11.*	1974,	Aug. 8	to	Aug. 13
12.	1975,	Jul. 13	to	Jul. 18
13.	1976,	Jul. 2	to	Jul. 11
14.	1977,	Jun. 21	to	Jun. 27
15.	"	Jul. 20	to	Jul. 24
16.*	"	Sep. 4	to	Sep. 8
17.*	1978,	Aug. 12	to	Aug. 16
18.*	"	Sep. 20	to	Sep. 23
19.	1979,	Aug. 2	to	Aug. 8
20.*	"	Aug. 11	to	Aug. 17
21.(1)*	1980,	May 20	to	May 25
21.(2)	"	May 26	to	May 28
22.	"	Aug. 22	to	Aug. 27
23.(1)	"	Aug. 31	to	Sep. 5
23.(2)*	"	Sep. 6	to	Sep. 9

Upon these twenty-five storms, average precipitation during the storm period and daily total precipitation of all obser-vaatories were respectively examined so that more competent storms were chosen to the nine storms indicated above by "*".

5.3 DAD (Depth-Area-Duration) analysis

DAD operation was conducted for the selected nine storms, thus the original spot precipitation was converted to areal precipitation. In the operation, hypothetical isohyetal map was elaborated as shown in Fig. 5.2, taking into account rainfall distribution pattern in the basin. An assumption was set that the isohyets would not change the shape regardless of storms or days in the sequence of a storm. On the other hand, rainfall amount represented by the isohyets was properly given in each day in the sequence of a storm. This means that the area surrounded by the isohyet was represented by the observatory located solely in the area and was assumed to have precipitation given as an average of the observatory's and isohyet's.

Fig. 5.3 shows an instance of the DAD operation together with the isohyetal map, which was performed upon the assumption described above. Fig. 5.4 gives an example of DAD curves which was obtained in the analysis.

5.4 Dew point

The observatories in the basin are not recording dew points. Therefore, dew points were obtained from relative humidity and temperature which were available as data, making use of table 5.1. The equation below is the definition of relative humidity.

$$H = \frac{e}{e_s} \times 100\%$$

where, H: relative humidity
e: vapour pressure
e_s: saturation vapor pressure at a particular temperature

Since relative humidity H and temperature are known, vapour pressure e could be obtained, refering saturation vapour pressure e_s at the temperature to the said table. Then, knowing e, dew point could be found, refering again to the table, for dew point is the temperature where the said vapour pressure e is to be saturation vapour pressure e_s.

Temperature data available in this study was daily max. or min., therefore the average of them was utilized in the said procedure.

As a result, dew points had been obtained at three observatories; Sop Han, Ban Tha Rua and Salween. However dew point at Ban Tha Rua was decided to be used in the analysis, considering length of data period and rainfall pattern of the baisn.

5.5 Adjustment and maximization of the storms

Since the typical storms were in this study selected from the rainfalls taking place in the basin now in consideration, the elevation adjustment and barrier adjustment were judged unnecessary, which are taken into account in general procedure of PMP analysis. Another adjustmenth; moisture adjustment, was considered, but was in fact involved in the maximization, because the selected storms were ones in the basin itself.

This maximization of the storms were achieved on the basis of precipitable water (total amount of moisture contained in a column stood vertically on the ground surface of unit area), which was derived from dew point. This precipitable water was known by the figure prepared by the U.S. National Weather Service.

An example of maximization is shown in Table 5.2. In the table, precipitation of line (1) is the one conducted DAD operation, thus, having been converted to areal precipitation. Dew point of line (3) is the highest one taking place at Ban Tha Rua during the particular storm interval. Line (5) indicated the highest dew point having occurred at Ban Tha Rau in the past. Corresponding the dew points given in the line (3) and (5), precipitable waters were respectively obtained. Then, by the propotion between (3) and (5), the observed precipitation in the line (1) was maximized.

The maximized precipitation was shown in the Fig. 5.5 in terms of the persistent period. As seen in the figure, the Storm No.21(1) (1980, May 21 to 24) gives extraordinary large magnitude, thus this storm was employed as PMP.

5.6 Estimation of daily runoff caused by PMP

While searching for PMP as mentioned above, relationship between a sequence of rainfall and the resultant runoff was studied based on the past recorded data of daily precipitation and discharge.

Here, the term "a sequence of rainfall" means the rainfall lasted for several days with remarkable amount and thus caused considerable discharge in the river. Looking over the past records, remarkable sequences of rainfall and the following discharges were selected. And the total amount of rainfall in the sequence and the maximum daily discharge in the discharges followingly caused were studied. Taking unit rainfall to be 10 mm, the resultant maximum daily discharge is 93 m^3/s as an average, is 128 m^3/s as the highest, which occurred generally with time lag of one day. It is shown in Fig. 5.6 and 5.7. Discharge against the unit rainfall varies greatly with the seasons, i.e. rainy and dry seasons. In other words, it varies with the amount of moisture kept in the ground. Fig.5.7 clearly shows that discharges taken place in July and August indicated by circle are consisting a group in the figure. since the PMP is now considered occur in July and August which are middle of rainy season, the ground is to be fully saturated. Therefore, the resultant maximum daily discharge was decided to be 128 m^3/s of the highest against the unit rainfall.

Assuming basin retention of 5% for the four-day persistent rainfall of PMP, rainfall excess becomes 257 mm. the maximum daily discharge thereby is then 3,290 m^3/s. On the other hand, it is notable that the sequence of rainfall takes place continually in July and August where the present study focusses. Therefore a precedent storm and the following discharge should be involved. As the precedent discharge, the maximum experienced discharge at Ban Tha Rua (1791, Aug. 30, Q = 925 m^3/s) was considered. Setting the precedent discharge three days before, the maximum daily discharge becomes 3,790 m^3/s resulted from PMP.

It should be reminded that all the analyses described above are based upon the daily data, thus the obtained maximum discharge is also a daily average. However, it is obvious that flood discharge in fact changes the amount considerably in hours so that actual peak discharge is much larger than the daily average. Examination of observed record at Ban Tha Rua revealed that the ratio between daily average and hourly peak discharges is 1.17 as an average, and is 1.64 as the maximum. Taking the maximum of 1.64, the PMF is concluded to be 6,216 $m^3/s \fallingdotseq$ 6,200 m^3/s as an hourly peak discharge.

Hydrograph of the PMF was formed in the similitude of the envelop of floods recorded in the past. The obtained PMF is given in Fig. 5.8.

References

(1) "Manual for Estimation of Probable Maximum Precipitation", WMO-No.332, Operational Hydrology Report No.1, 1973, WMO, Geneva, Switzerland.

(2) "Hydrological Survey of Iraq, Probable Maximum Flood at Bekhme damsite", EPDC Ltd. Design Sec., Dec. 1979, Tokyo.

(3) "Huai Saphan Hin Project Feasibility Report", Appendix C, Hydrology Part II, Probable Maximum Precipitation, National Energy Administration, Aug. 1977, Thailand.

Table 5.1 Relationship between Temperature and Saturated Vapour Pressure

(Unit: mb)

Temperature (°C)	x 0.1 °C									
	0	1	2	3	4	5	6	7	8	9
50	123.40	124.01	124.63	125.25	125.87	126.49	127.12	127.75	128.38	129.01
49	117.40	117.99	118.58	119.17	119.77	120.37	120.97	121.57	122.18	122.79
48	111.66	112.22	112.79	113.36	113.93	114.50	115.07	115.65	116.23	116.82
47	106.16	106.70	107.24	107.78	108.33	108.88	109.43	109.98	110.54	111.10
46	100.89	101.41	101.93	102.45	102.97	103.50	104.03	104.56	105.09	105.62
45	95.86	96.35	96.85	97.34	97.84	98.34	98.85	99.36	99.87	100.38
44	91.03	91.51	91.98	92.46	92.94	93.42	93.90	94.39	94.87	95.36
43	86.42	86.88	87.33	87.79	88.24	88.70	89.17	89.63	90.10	90.56
42	82.02	82.45	82.88	83.32	83.75	84.19	84.64	85.08	85.53	85.97
41	77.80	78.22	78.63	79.05	79.46	79.88	80.31	80.73	81.63	81.59
40	73.78	74.17	74.57	74.97	75.37	75.77	76.17	76.58	76.98	77.39
39	69.93	70.31	70.69	71.07	71.45	71.83	72.22	72.61	73.00	73.39
38	66.26	66.62	66.98	67.35	67.71	68.08	68.45	68.82	69.19	69.56
37	62.76	63.11	63.45	63.80	64.14	64.49	64.84	65.20	65.55	65.91
36	59.42	59.75	60.08	60.41	60.74	61.07	61.41	61.74	62.08	62.42
35	56.24	56.55	56.86	57.18	57.49	57.81	58.13	58.45	58.77	59.10
34	53.20	53.50	53.80	54.10	54.40	54.70	55.00	55.31	55.62	55.93
33	50.31	50.59	50.87	51.16	51.45	51.74	52.03	52.32	52.61	52.90
32	47.55	47.82	48.09	48.36	48.64	48.91	49.19	49.47	49.75	50.03
31	44.93	45.18	45.44	45.70	45.96	46.22	46.49	46.75	47.02	47.28
30	42.43	42.67	42.92	43.17	43.41	43.66	43.91	44.17	44.42	44.67
29	20.05	40.29	40.52	40.76	40.99	41.23	41.47	41.71	41.95	42.19
28	37.80	38.02	38.24	38.46	38.69	38.91	39.14	39.36	39.59	39.82
27	35.65	35.86	36.07	36.28	36.49	36.71	36.92	37.14	37.36	37.58
26	33.61	33.81	34.01	34.21	34.41	34.62	34.82	35.03	35.23	35.44
25	31.67	31.86	32.05	32.24	32.43	32.63	32.82	33.02	33.21	33.41
24	29.83	30.01	30.19	30.37	30.56	30.74	30.92	31.11	31.30	31.48
23	28.09	28.26	28.43	28.60	28.77	28.95	29.12	29.30	29.48	29.65
22	26.43	26.59	26.75	26.92	27.08	27.25	27.41	27.58	27.75	27.92
21	24.86	25.01	25.17	25.32	25.48	25.64	25.79	25.95	26.11	26.27
20	23.37	23.52	23.66	23.81	23.96	24.11	24.26	24.41	24.56	24.71
19	21.96	22.10	22.24	22.38	22.52	22.66	22.80	22.94	23.08	23.23
18	20.63	20.76	20.89	21.02	21.15	21.29	21.42	21.56	21.69	21.83
17	19.37	19.49	19.61	19.74	19.86	19.99	20.12	20.24	20.37	20.50
16	18.17	18.29	18.41	18.52	18.64	18.76	18.88	19.00	19.12	19.24
15	17.04	17.15	17.46	17.38	17.49	17.60	17.71	17.83	17.94	18.06
14	15.98	16.08	16.19	16.29	16.40	16.50	16.61	16.72	16.83	16.93
13	14.97	15.07	15.17	15.27	15.37	15.47	15.57	15.67	15.77	15.87
12	14.02	14.11	14.20	14.30	14.39	14.49	14.58	14.68	14.77	14.87
11	13.12	13.21	13.29	13.38	13.47	13.56	13.65	13.74	13.83	13.93
10	12.27	12.35	12.44	12.52	12.60	12.69	12.77	12.86	12.95	13.03

Table 5. 2 Maximization of Storms

MAXIMIZATION OF RAINFALL

Storm No.17

Period: 1978, 8/12 - 8/16

		UNIT	STORM PERIOD						REMARKS
			1 day	2 day	3 day	4 day	5 day	6 day	
(1)	Precipitation for C.A. 5,920 km^2	mm	33.2	42.7	52.2	59.0	63.7		
(2)	Date	-	8/14	13 - 14	13 - 15	12 - 15	12 - 16		
(3)	Max. Dew Point at Ban Tha Rua	°C	26.1	26.1	26.1	26.1	26.1		
(4)	Precipitable Water corresp. to the dew point (3) above	mm	90.2	90.2	90.2	90.2	90.2		
(5)	Max. recorded dew point in the whole data (Ban Tha Rua)	°C	33.6	33.6	33.6	33.6	33.6	33.6	
(6)	Precipitable Water corresp. to the dew point in (5) above	mm	164.8	164.8	164.8	164.8	164.8	164.8	
(7)	Max. Factor		1.827	1.827	1.827	1.827	1.827		
(8)	Max. Precipitation	mm	60.7	78.0	95.4	107.8	116.4		

Fig. 5. 1 Observatory and Gaging Stations with the Covering Area

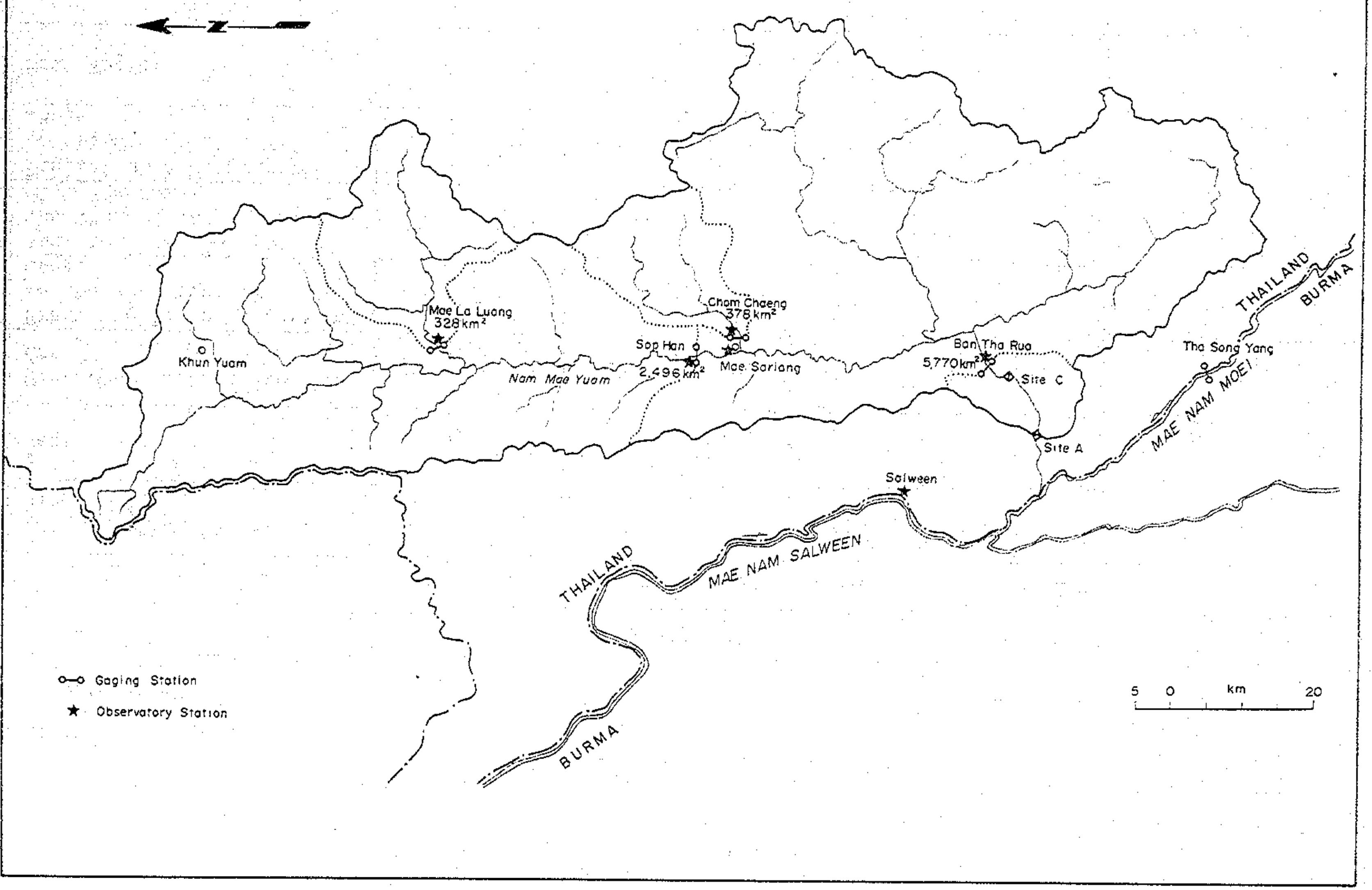

Fig. 5.2 Hypothetical Isohyetal Map with Corresponding O.S.

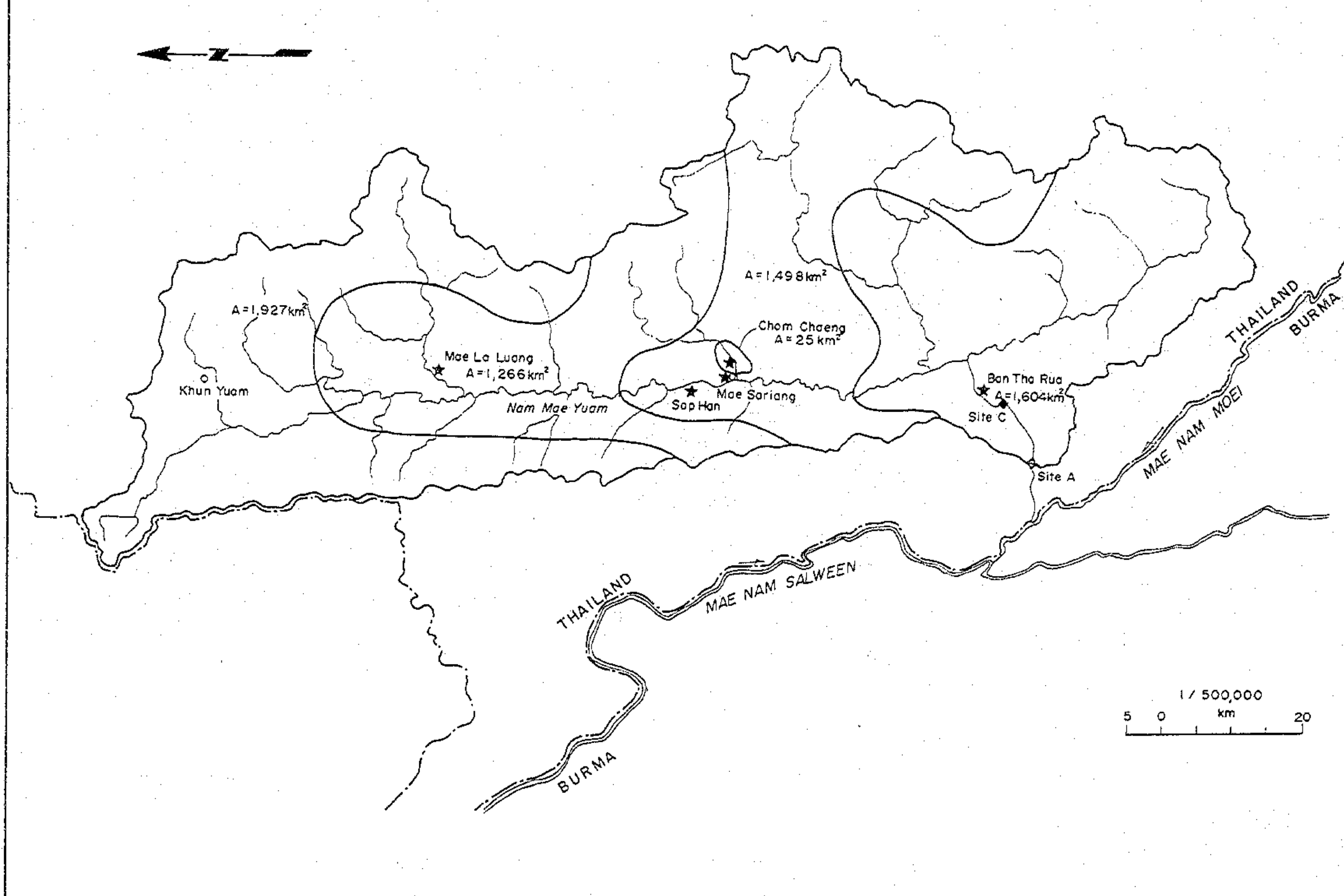

Fig. 5.3 Hypothetical Isohyetal Map with Corresponding O. S.

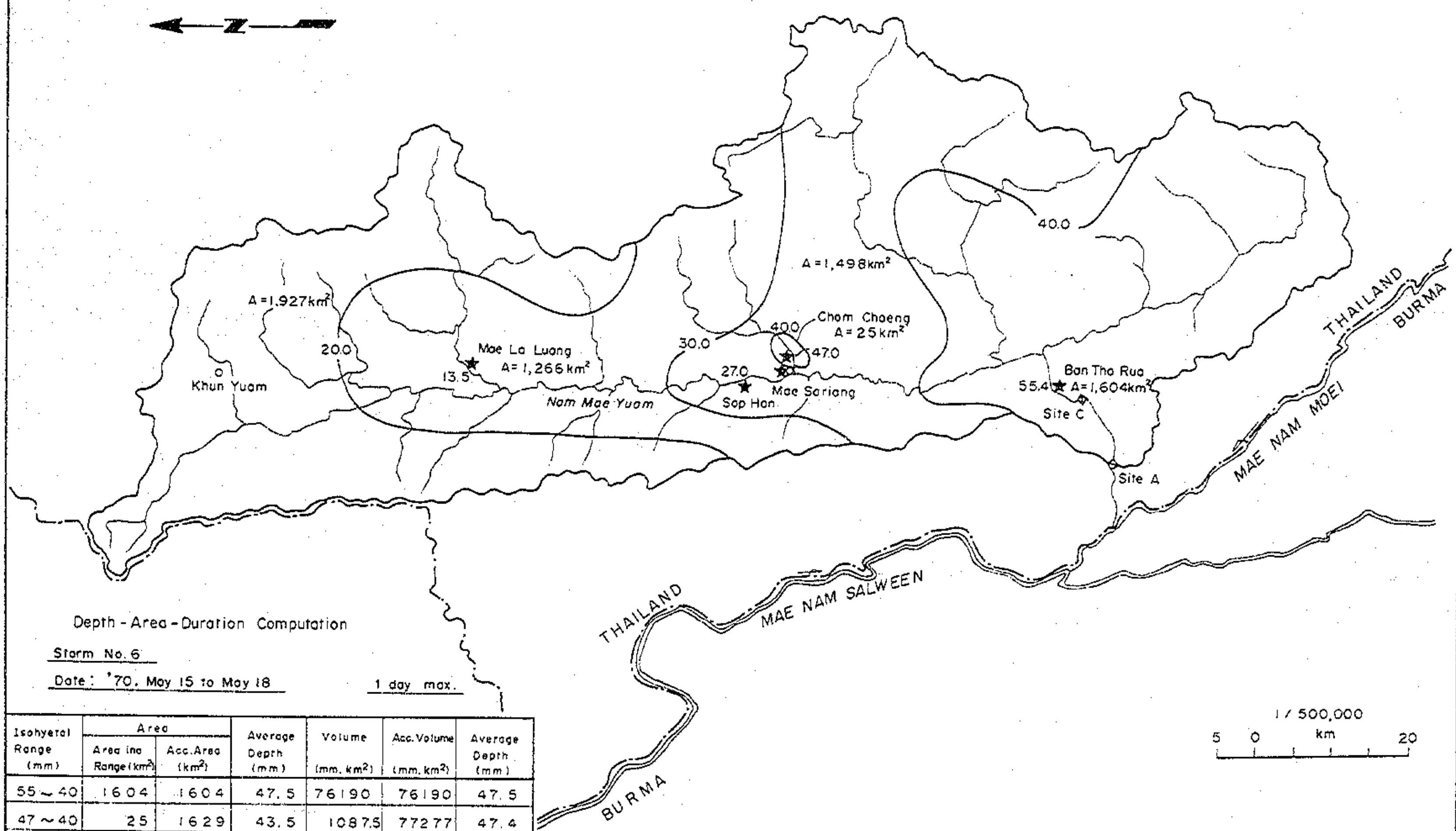

Depth - Area - Duration Computation

Storm No. 6

Date : '70. May 15 to May 18 1 day max.

Isohyetal Range (mm)	Area		Average Depth (mm)	Volume (mm. km²)	Acc. Volume (mm. km²)	Average Depth (mm)
	Area ina Range (km²)	Acc. Area (km²)				
55 ~ 40	1604	1604	47.5	76190	76190	47.5
47 ~ 40	25	1629	43.5	1087.5	77277	47.4
40 ~ 30	1498	3127	35.0	52430	129707	41.5
30 ~ 20	1266	4393	25.0	31650	161357	36.7
20 ~ 0	1527	5920	10.0	15270	176627	29.8

Fig. 5.4 DAD Curves

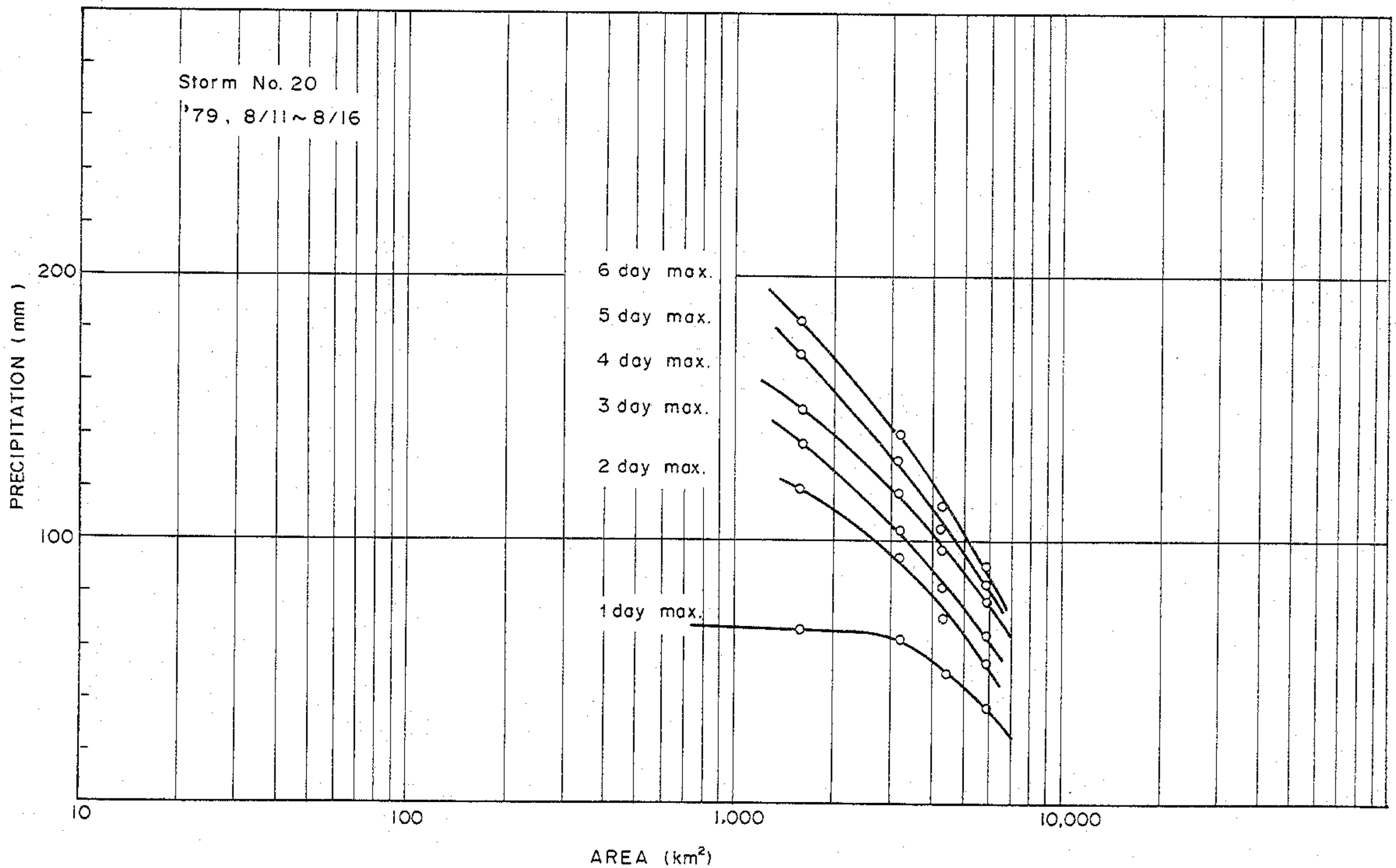

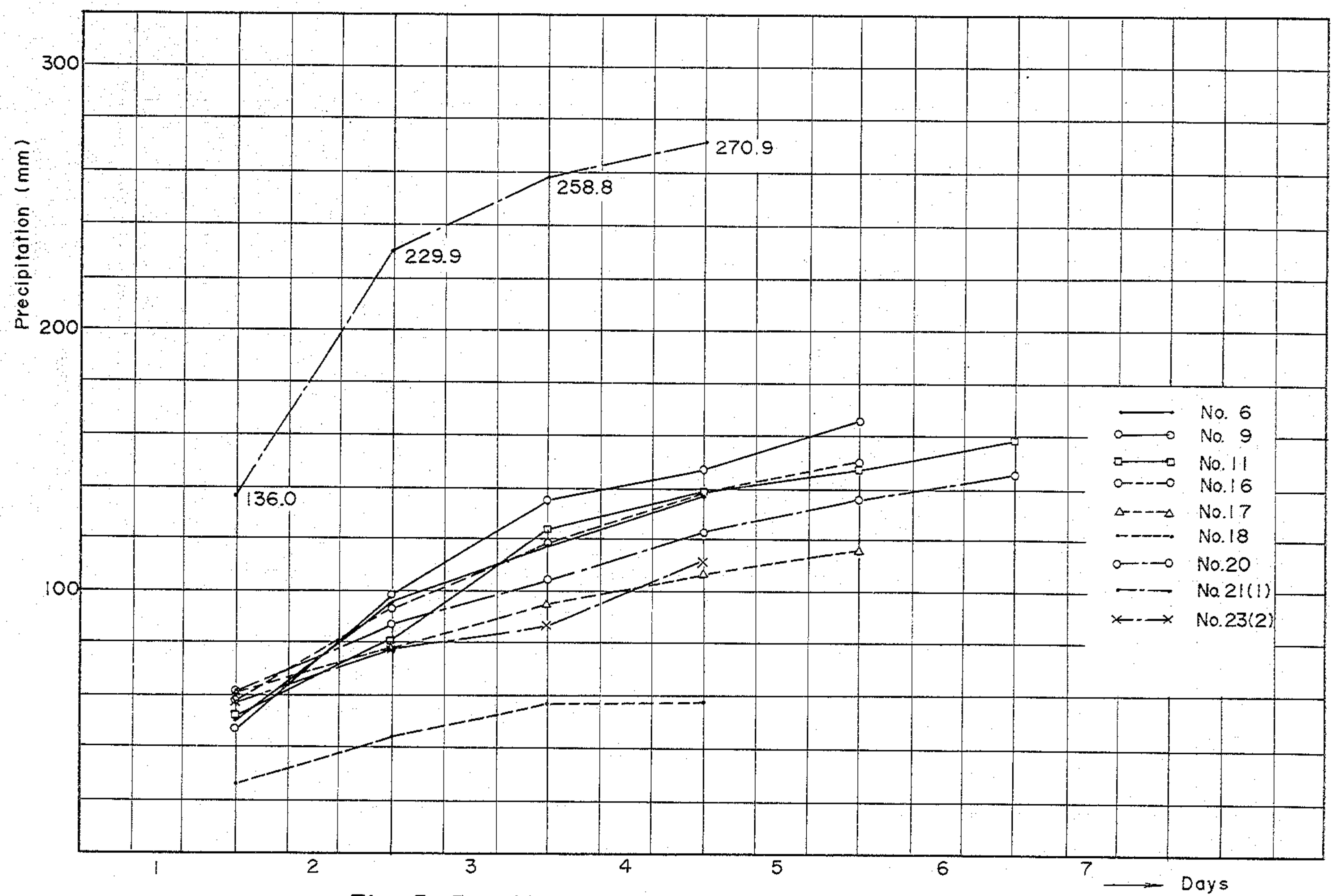

Fig. 5.5 Maximised Precipitation of Storms

Fig. 5. 6 Precipitation and Discharge

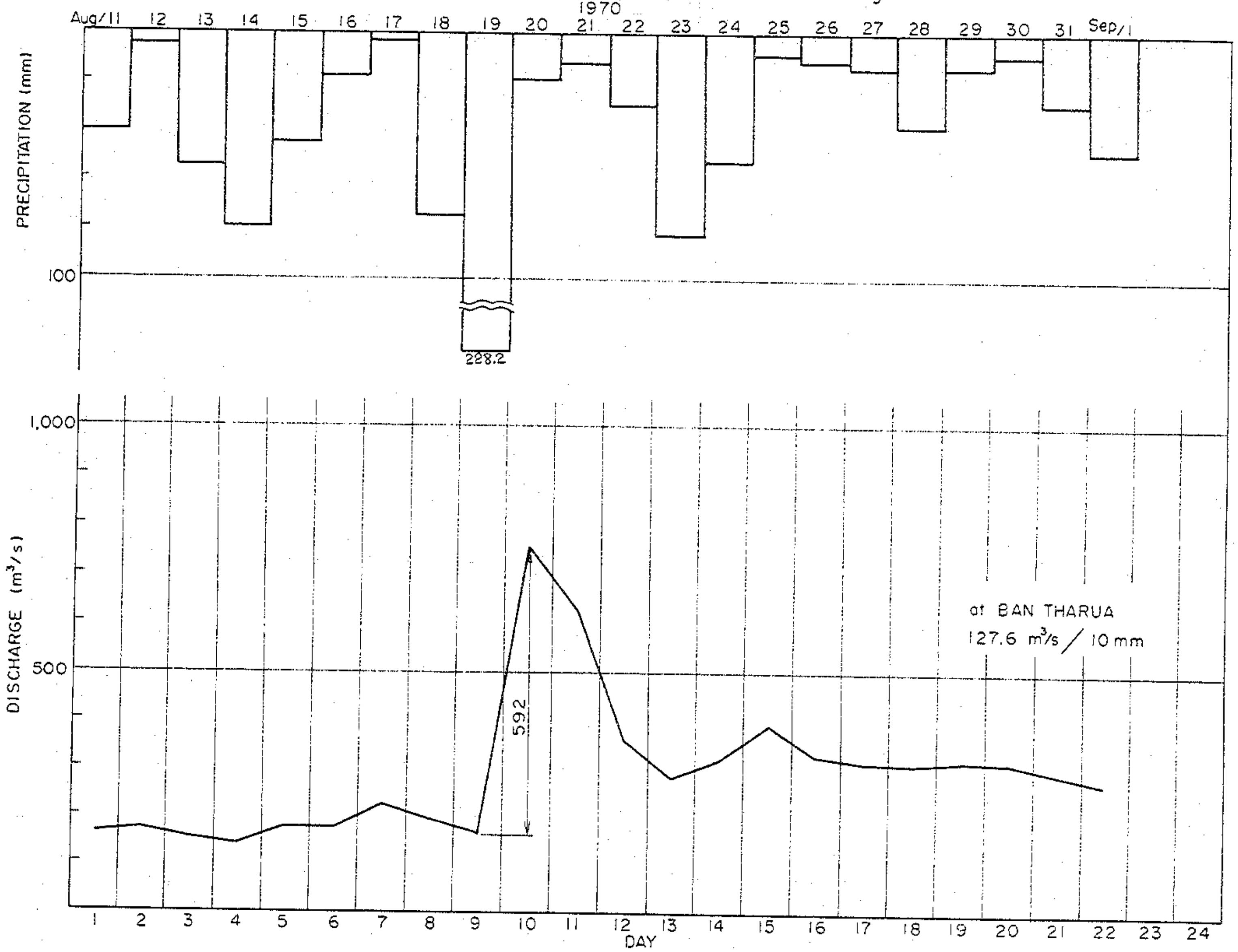

Fig. 5.7 Relationship Between Increment of Discharge and Day Rainfall

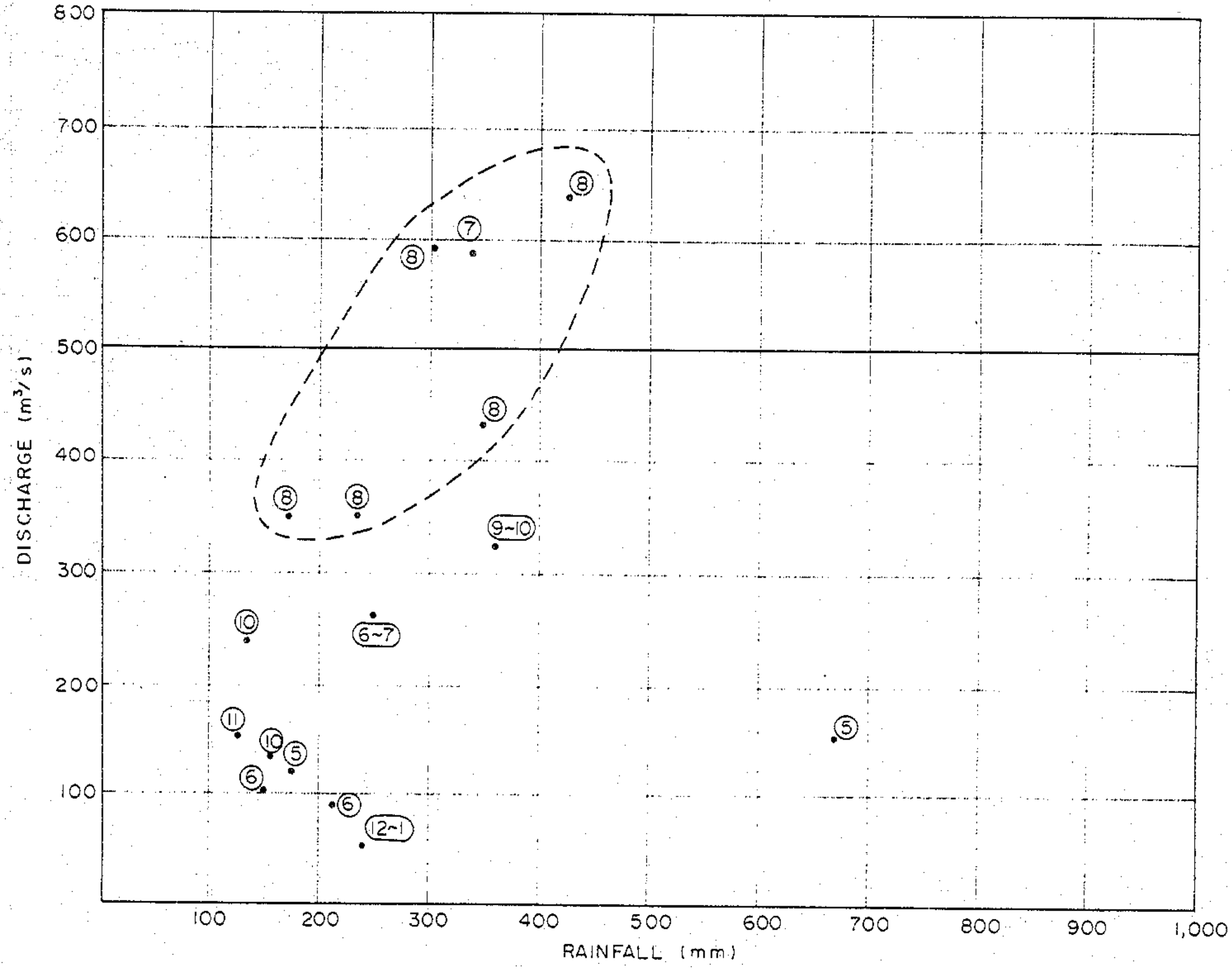

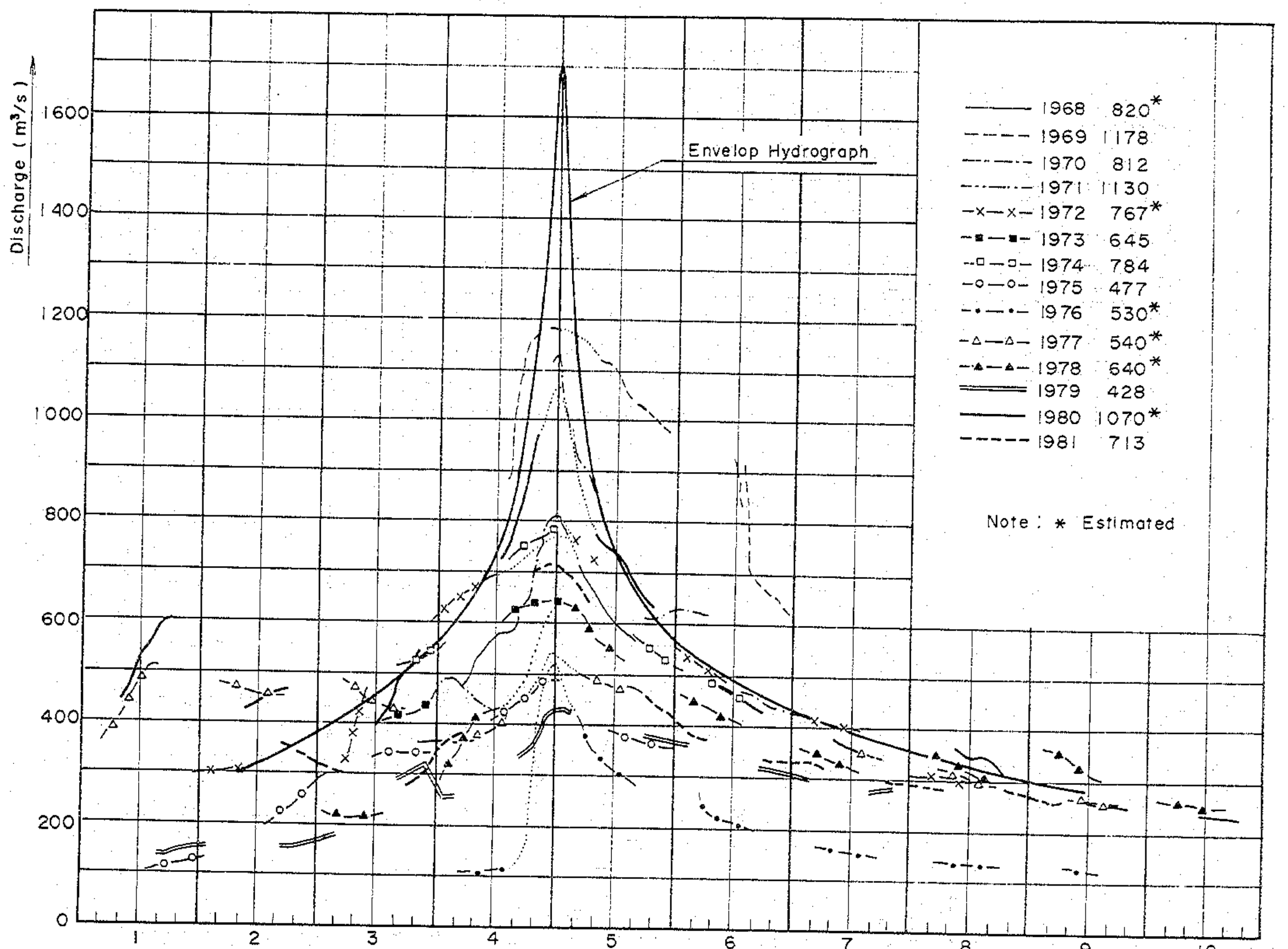

Fig. 5.8 Recorded Flood Discharge

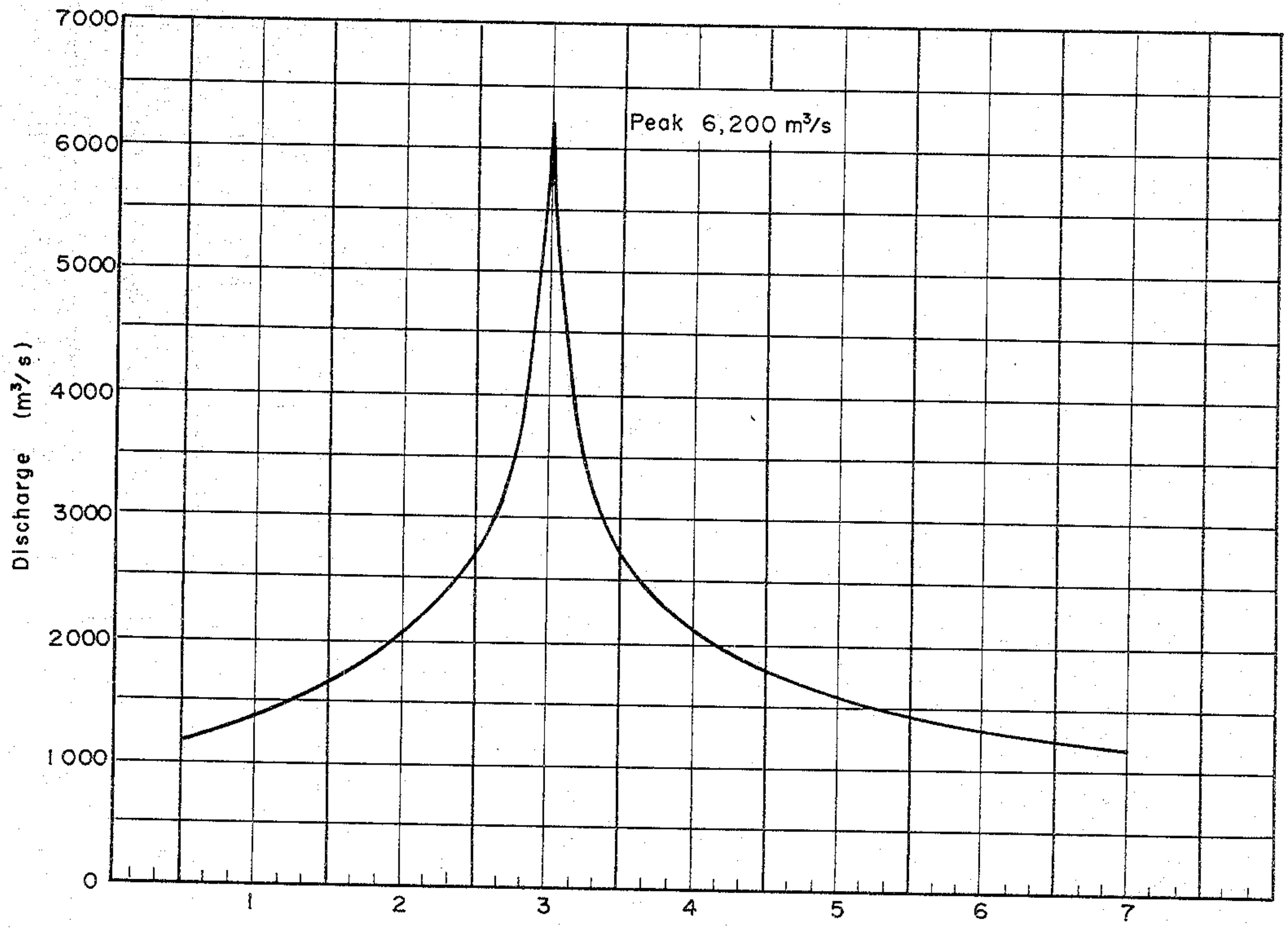

Fig. 5.9 PMF Discharge

A 3 DESIGN

1. Flood Routing

1.1 General

According to the proposed scheme, Nam Yuam dam site has topographical feature of the considerably large reservoir area and hydrological feature of sharpness of the design flood curve. Concerning such a dam site, it is advantageous that the scale of spillway should be reduced to an adequate extent with some of flood volume stored in the reservoir. The flood routing has been done under the below-mentioned conditions.

1.2 Conditions

Design flood inflow

Probable maximum flood (Qmax = 6,200 m^3/sec)

See Fig. 1

Reservoir storage capacity

See Fig. 2

Dimensions of spillway

See Fig. 3, 4

Initial reservoir water level

EL 170.00 (High water level)

Operation rule

i) As far as flood inflow does not exceed discharge capacity of spillway at high water level of EL. 170.00, spillway gates are partially opened with reservoir water level kept the high water level.

ii) If flood inflow exceeds discharge capacity of spillway at high water level, spillway gates are fully opened.

1.3 Calculations

Discharge capacity of spillway is given on the following formula.

$$Q = N \cdot C \cdot (B-2Kh) \cdot h^{3/2}$$

where;

Q: discharge (m^3/sec)

C: coefficient of discharge

K: coefficient of contraction due to pier

N: number of gates = 4

B: width of crest = 12.00 m

h: head on crest (m)

Value of C is determined on Iwasaki's formula in case of idealy shaped crest.

$$C = 1.60 \frac{1 + 2a(h/hd)}{1 + a\ (h/hd)}$$

$$Cd = 2.20 - 0.0416\ (hd/w)^{0.99}$$

where;

hd: design head = 12.00 m

W: height of weir = 8.00 m

Cd: coefficient of overflow at design head

therefore

Cd: 2.138

a = 0.5063

$$C = 1.60 \frac{1 + 1.0126\ (h/12.00)}{1 + 0.5063\ (h/12.00)}$$

Value of K is given on Fig. 5.

Consequently results of calculation of spillway capacity are shown on Table 1 and Fig. 6.

1.4 Results

The results of calculations are shown on Fig. 7. It has been evident that surcharge of 0.88 m at the reservoir enables to reduce needed spillway capacity to 77% of maximum flood discharge.

Table 1.1 Spillway Capacity

Reservoir Water Level(m)	h (m)	h/hd	C	K	2Kh (m)	B-2Kh (m)	Q (m^3/sec)
158.00	0.00	0.000	-	-	-	-	0
159.00	1.00	0.083	1.665	0.126	0.26	1.74	78
160.00	2.00	0.167	1.725	0.105	0.42	1.58	226
161.00	3.00	0.250	1.780	0.087	0.52	1.48	425
162.00	4.00	0.333	1.831	0.071	0.57	1.43	670
163.00	5.00	0.417	1.879	0.056	0.56	1.44	961
164.00	6.00	0.500	1.923	0.046	0.56	1.44	1,294
165.00	7.00	0.583	1.965	0.036	0.51	1.49	1,673
166.00	8.00	0.667	2.004	0.029	0.47	1.53	2,091
167.00	9.00	0.750	2.040	0.023	0.42	1.58	2,552
168.00	10.00	0.833	2.075	0.017	0.35	1.65	3,059
169.00	11.00	0.917	2.107	0.011	0.24	1.76	3,618
170.00	12.00	1.000	2.138	0.004	0.11	1.89	4,229
171.00	13.00	1.083	2.167	0.000	0.00	2.00	4,875
172.00	14.00	1.167	2.194	0.000	0.00	2.00	5,517

Fig. 1.1 Design Flood Inflow

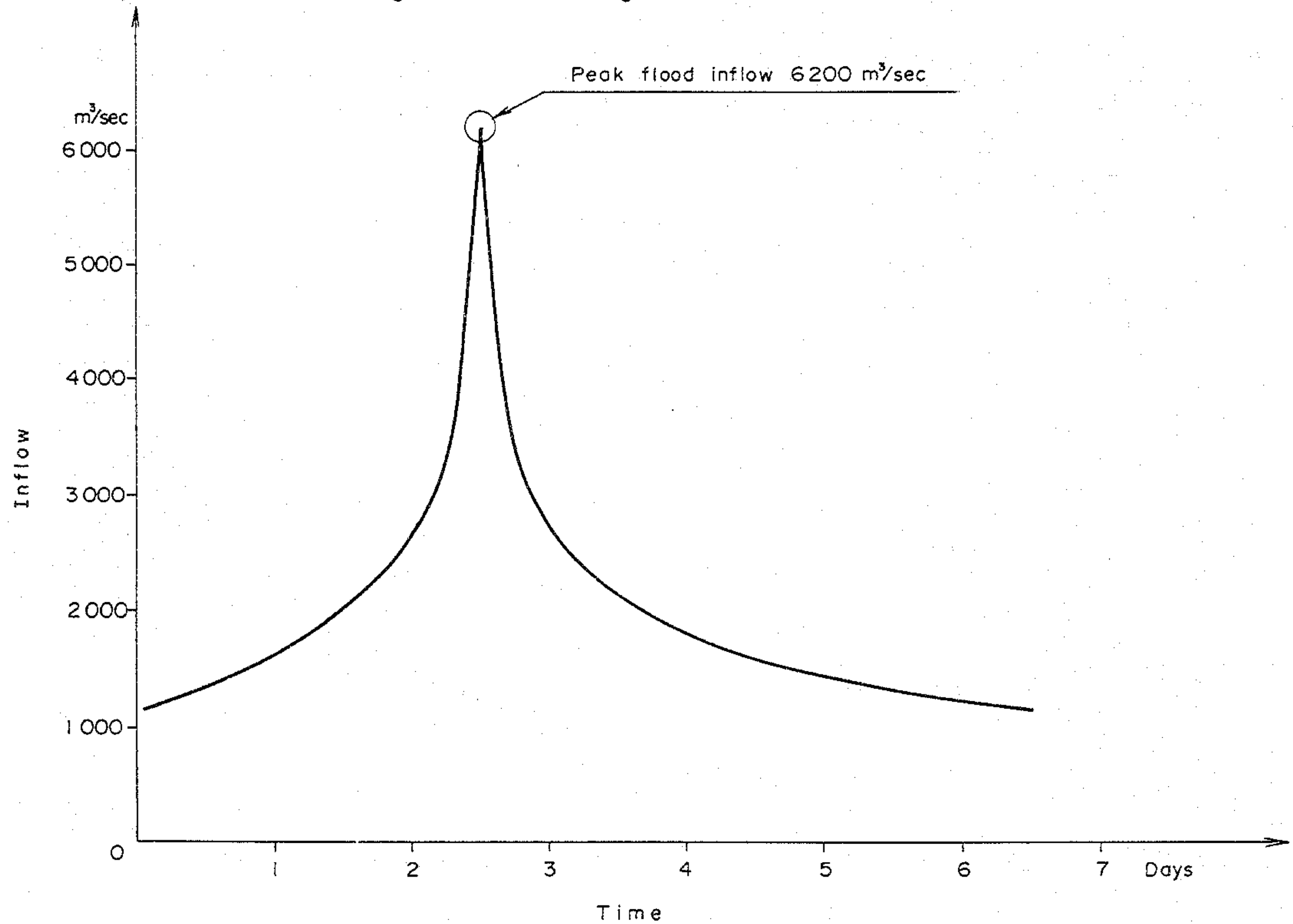

Fig. 1.2 Reservoir Storage Capacity

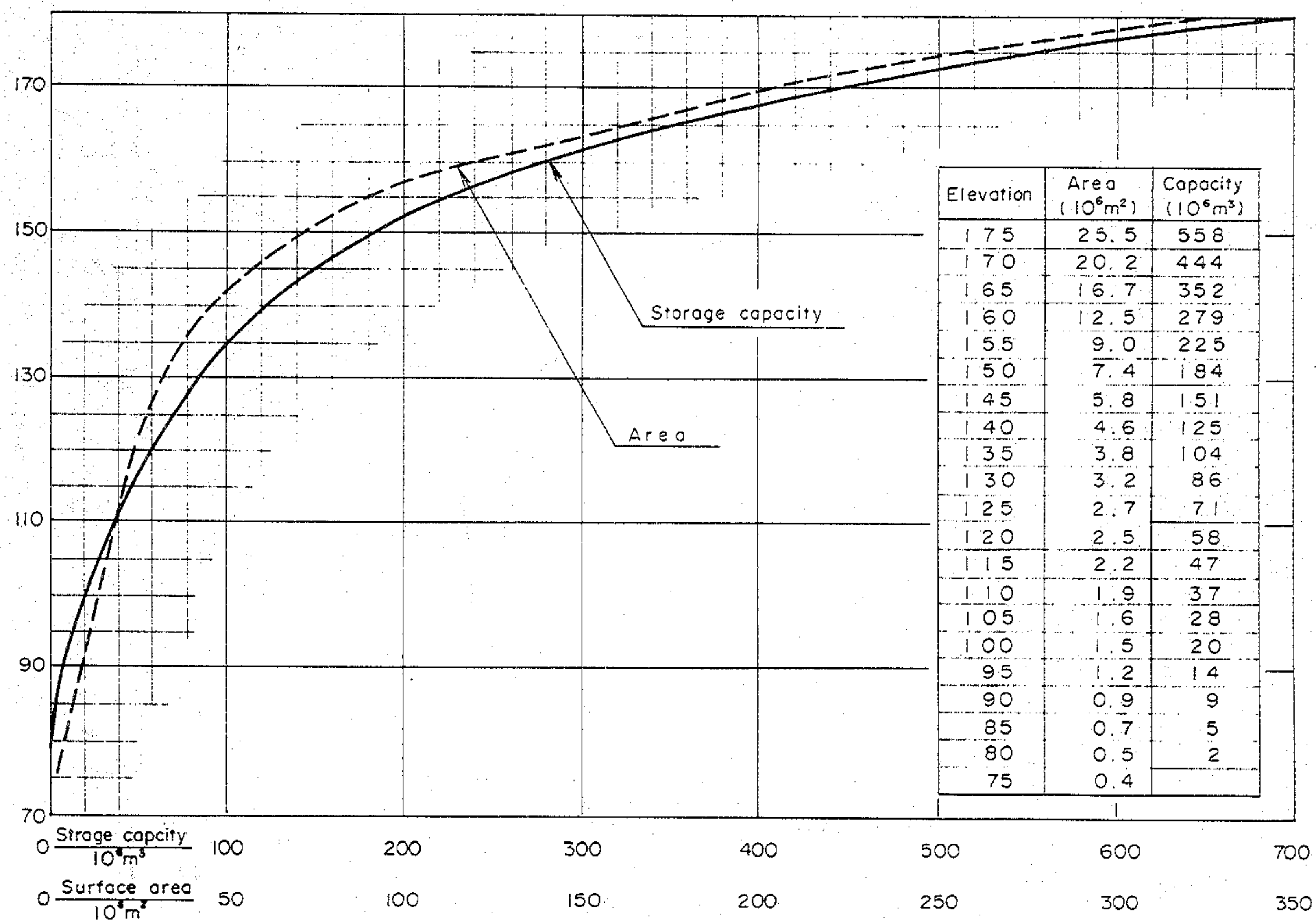

Elevation	Area (10^6m^2)	Capacity (10^6m^3)
175	25.5	558
170	20.2	444
165	16.7	352
160	12.5	279
155	9.0	225
150	7.4	184
145	5.8	151
140	4.6	125
135	3.8	104
130	3.2	86
125	2.7	71
120	2.5	58
115	2.2	47
110	1.9	37
105	1.6	28
100	1.5	20
95	1.2	14
90	0.9	9
85	0.7	5
80	0.5	2
75	0.4	

Fig. 1.3 Upstream View of Spillway

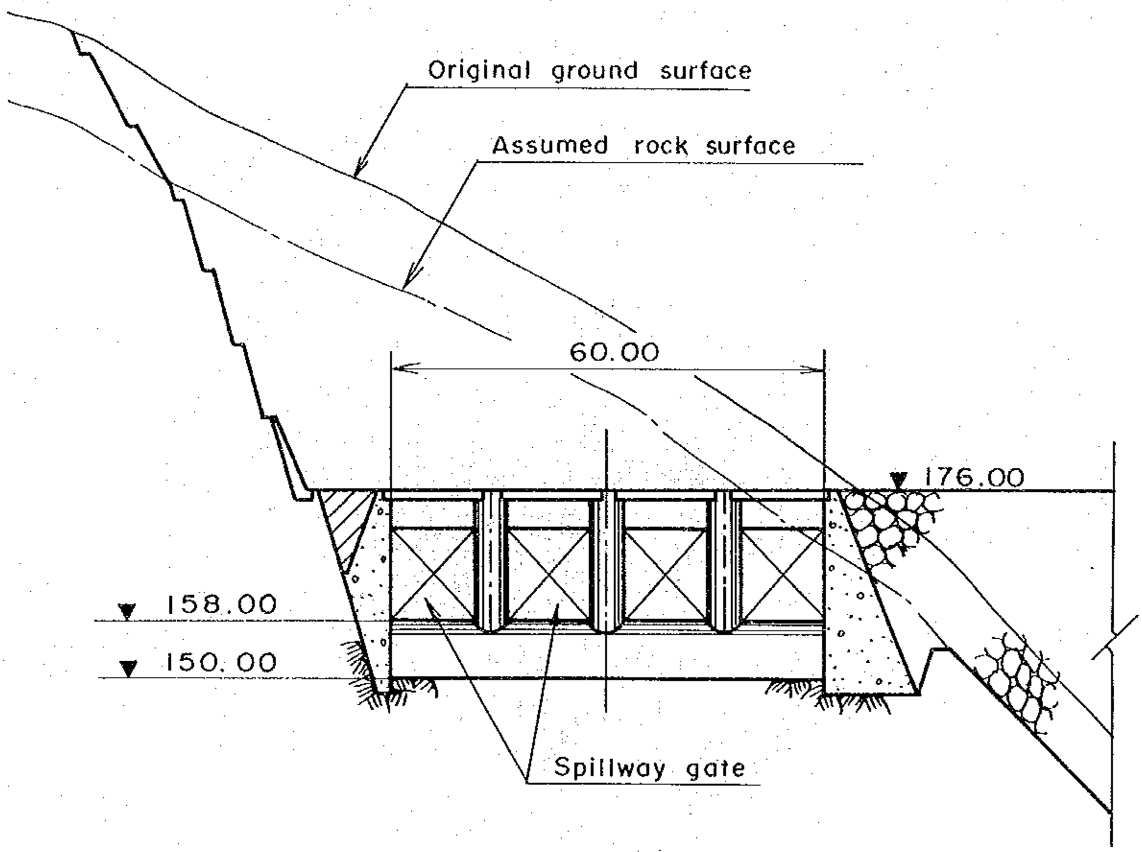

Fig. 1.4 Typical Section of Spillway

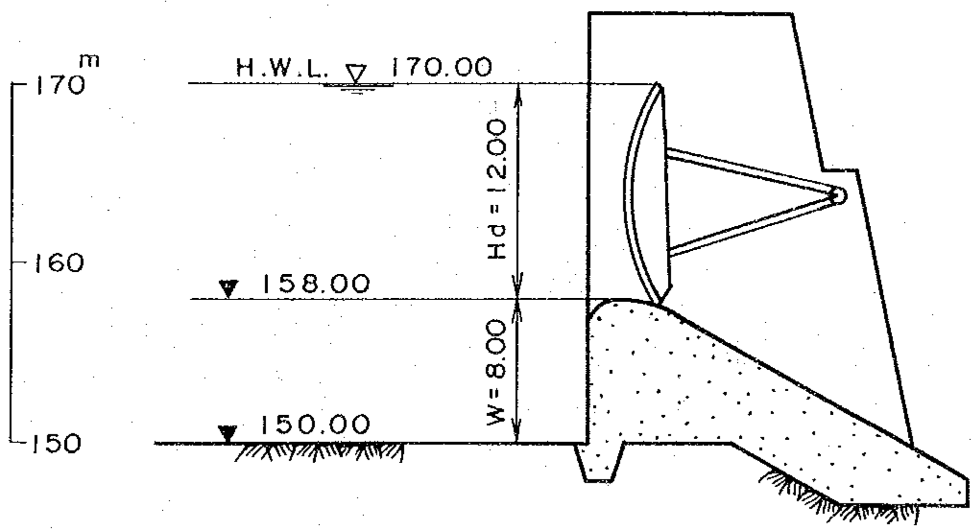

Fig. 1.5 Coefficient of Contraction due to Pier

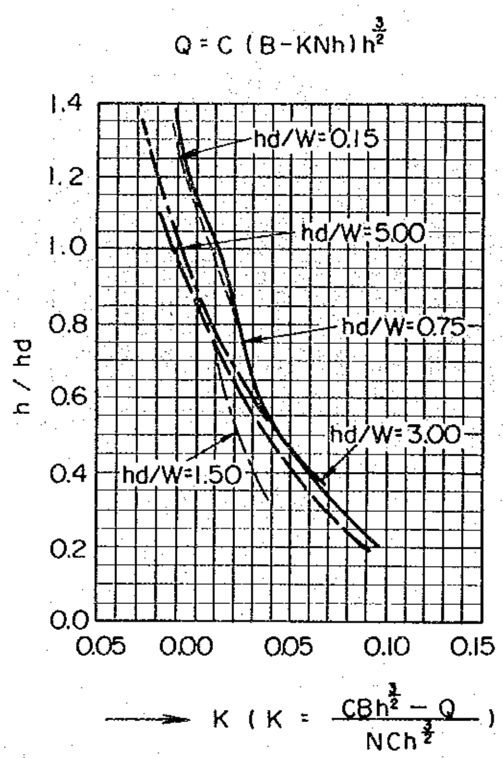

Fig. 1.6 Discharge Capacity of Spillway

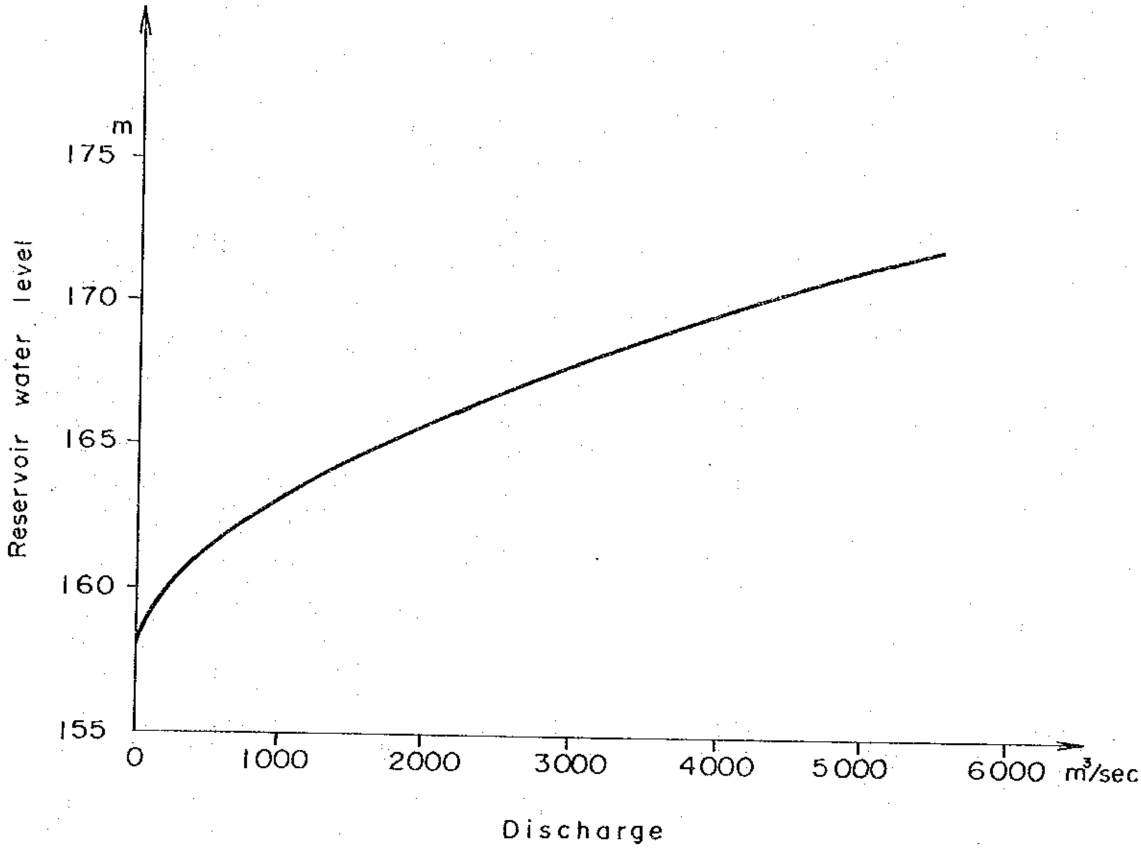

Fig. 1.7 Results of Calculation

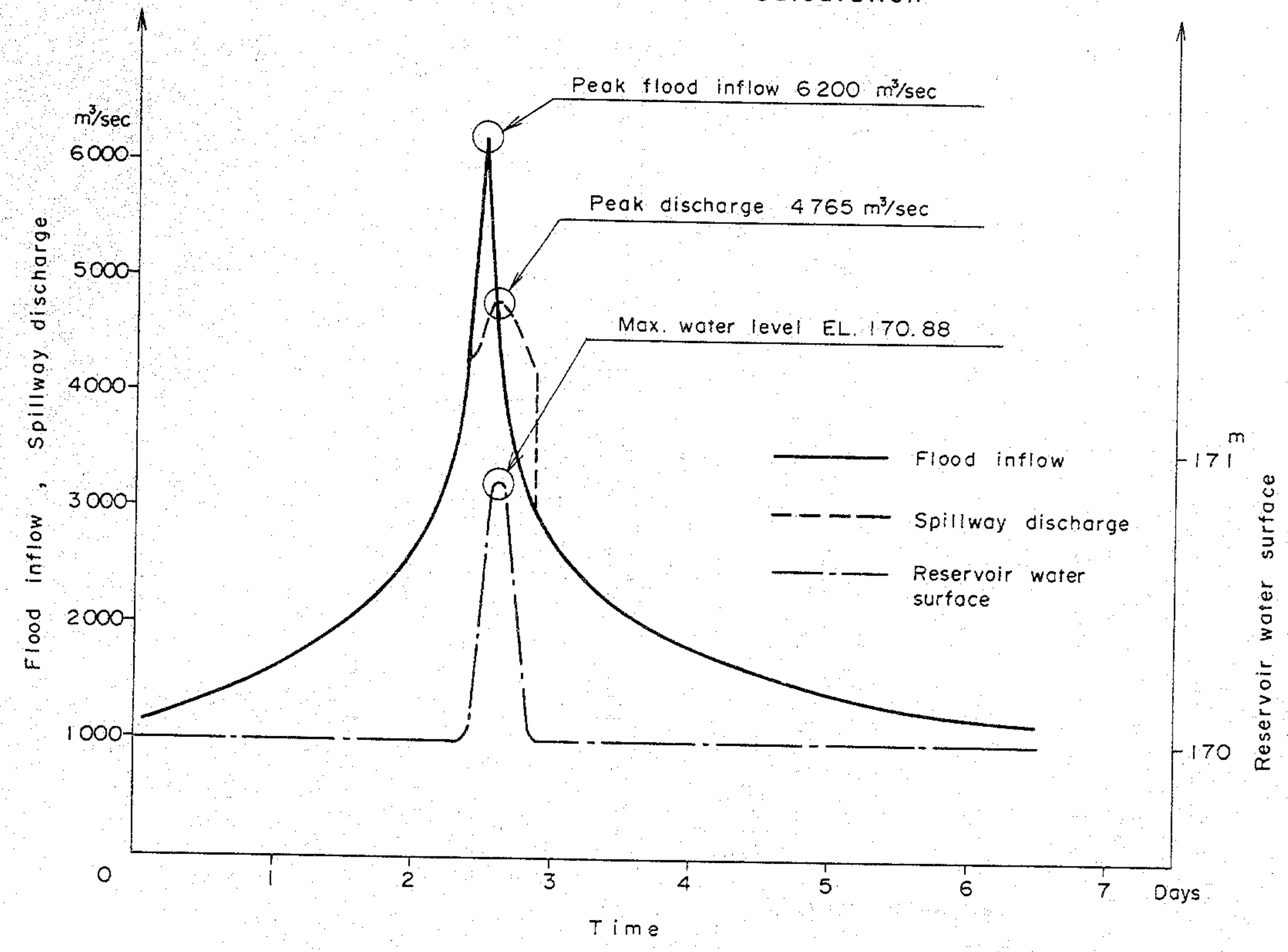

2. Nam Yuam Dam Stability Analysis

2.1 General

Stability analysis was done by the slip circle method for Nam Yuam dam and this analysis was calculated by the computer.

2.2 Stability analysis by slip circle method

The factor of safety against sliding is expressed as follows.

Normal condition:

$$SF(N) = \frac{\Sigma\,(N+Hn-U)\ \text{ton}\,\phi + \Sigma C \cdot L}{\Sigma\,(T - Ht)}$$

Earthquake condition:

$$SF(E) = \frac{\Sigma\,(N+Hn-U)\ \tan\phi - \Sigma\,Ne\ \text{ton}\,\phi + \Sigma C \cdot L}{\Sigma(T - Ht) + \Sigma Te}$$

where,

N : normal force
T : tangential force
$\tan\phi$: coefficient of internal friction
Hn : normal component of hydrostatic pressure
Ht : tangential component of hydrostatic pressure
U : pore water pressure
L : length of sliding circle
Ne : normal component of seismic force
Te : tangential component of seismic force
C : cohesion force

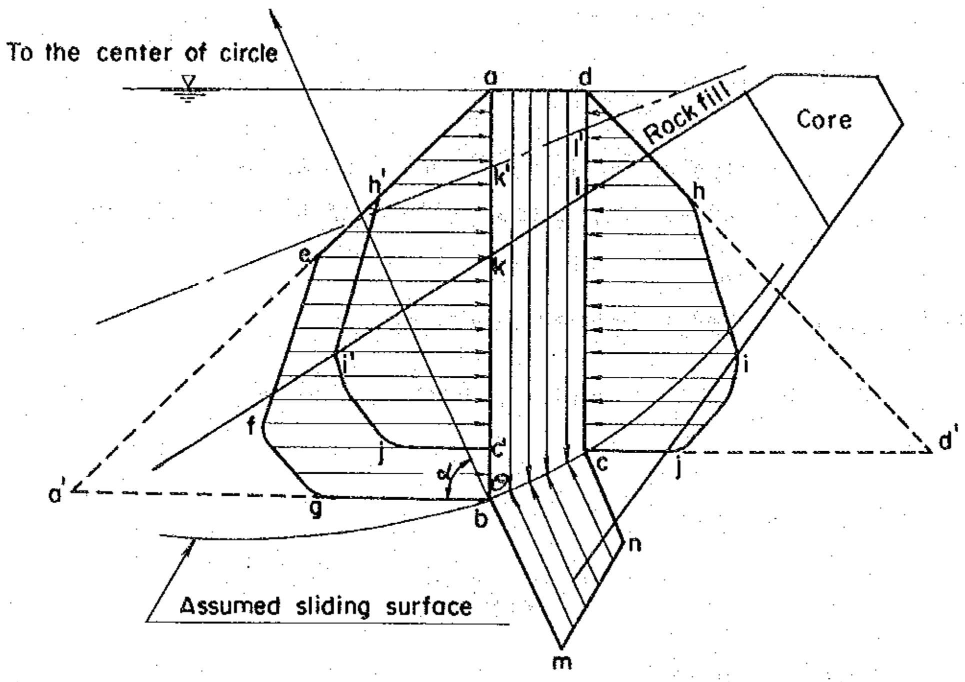

$\Sigma N \cdot \tan\phi = \Sigma\{\gamma(k'bcl') + \gamma w(abcd)\} \cos\theta \tan\phi$

$\Sigma Hn \cdot \tan\phi = \Sigma(efgbc'j'i'j') \cos\alpha \tan\phi$

$\Sigma U \tan\phi = \Sigma(bmnc) \tan\phi$

$\Sigma T = \Sigma\{\gamma(k'bcl') + \gamma n(abcd)\} \sin\theta$

$\Sigma Ht = \Sigma(efgbc'j'i'h') \sin\alpha$

$\Sigma Ne \tan\phi = \Sigma\beta(k'bcl')K \sin\theta \tan\phi$

$\Sigma Te = \Sigma\beta(k'bcl')K \cos\theta$

γ : unit weight in normal condition

β : unit weight in earthquake condition

abcd : a piece of slice

bmnc : porefluid pressure to the sliding surface

efgbc'j'i'h' : total of horizontal hydrostatic pressure to the slice

K : seismic coefficient

2.3 Conditions of Calculation

Design values of embankment materials

Zone	Material	Specific gravity	Unit weight t/m³			Coefficient	
			Dry	Wet	Saturated	tan ø	C
1	Impervious core	2.65	1.80	2.07	2.12	0.45	0
2a	Transition fill	2.63	1.95	2.00	2.20	0.65	0
2b	Filter fill	2.63	1.95	2.00	2.20	0.65	0
3	Smaller size rock fill	2.63	1.80	1.82	2.13	0.70	0
4	Larger size rock fill	2.63	1.75	1.77	2.09	0.80	0

Reservoir water surface level;
EL. 170.00 (Normal high water level)

Seismic coefficient;
K = 0.06

Porefluid pressure;

Porefluid pressure of cofferdam was not taken into account and porefluid pressure in impervious core is assumed as shown in Fig. 1. Materials forms are shown in Fig. 2.

2.4 Result

The safety factor of sliding circles are shown in Fig. 3. From the result of this analysis, the dambody is safe enough under normal and earthquake conditions for assumed design values. But after the determination of the actual design values for the respective tests' results, the safety of dam must be checked in detail.

Fig. 2.1 POREFLUID PRESSURE

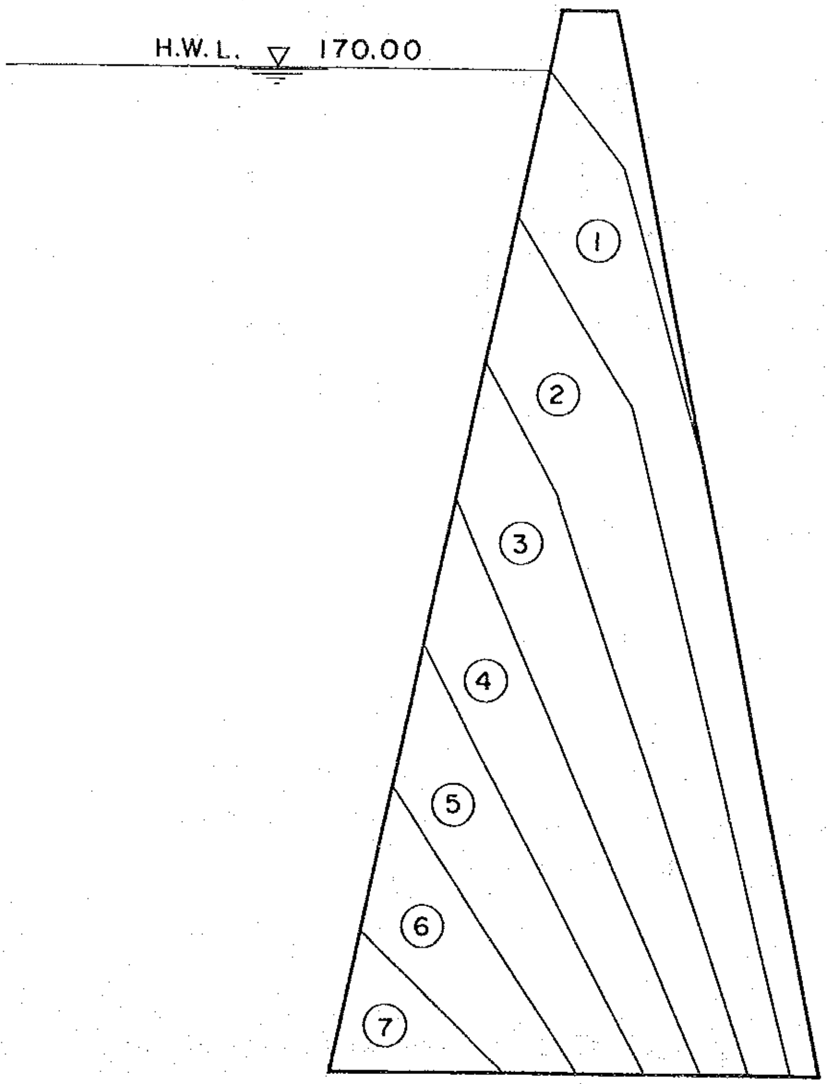

Zone	Porefluid Pressure (t/m²)
①	7.5
②	22.5
③	37.5
④	52.5
⑤	67.5
⑥	82.5
⑦	97.5

Fig. 2.2 TYPICAL SECTION

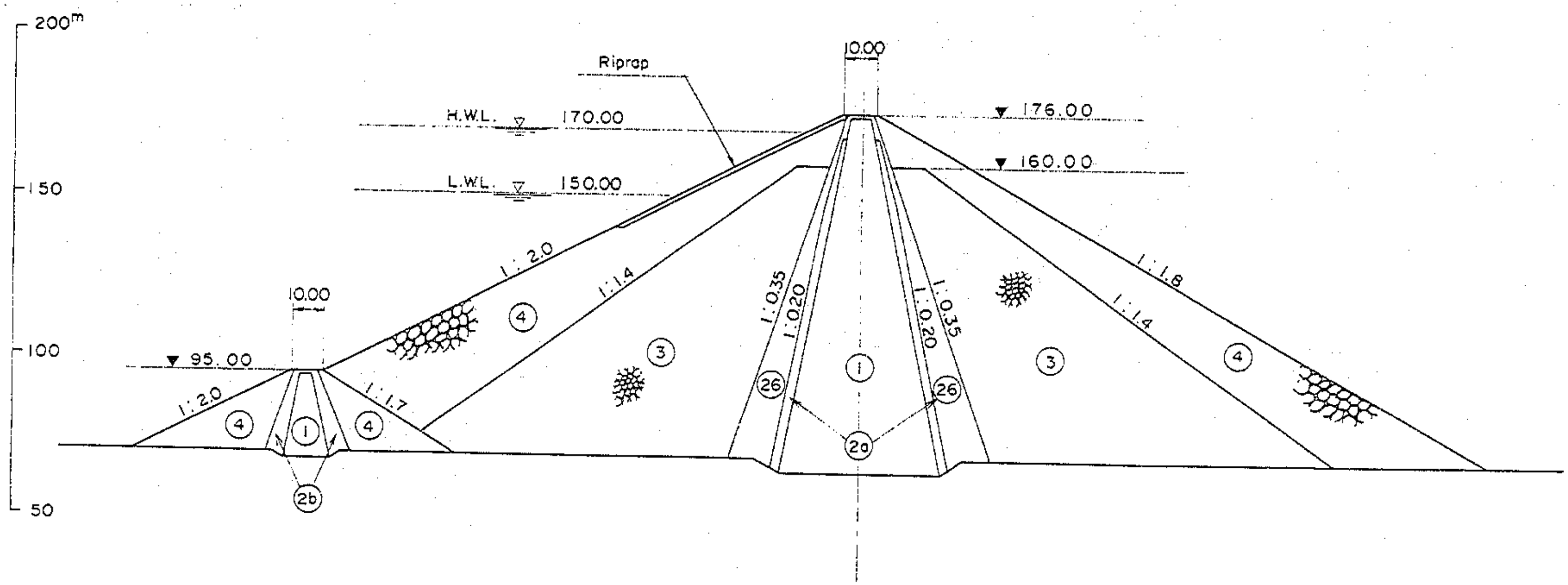

(1) Impervious core

(2a) Transition fill

(2b) Filter fill

(3) Smaller size rock fill

(4) Larger size rock fill

Fig. 2.3 RESULT OF STABILITY ANALYSIS

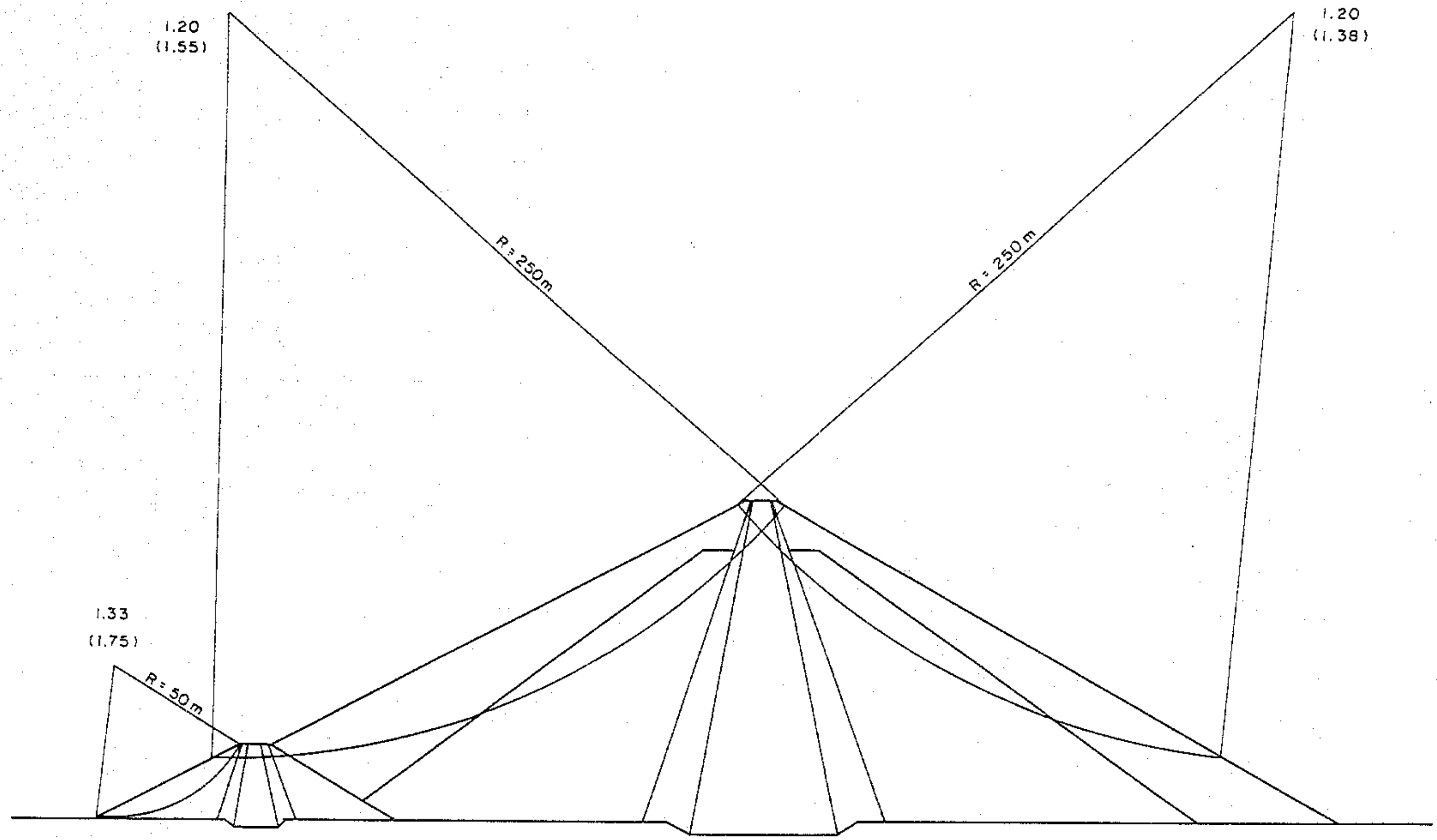

Fafety factor

Earthquake condition
(Normal condition)

3. Tailwater level

Control section was assumed at Section I, where uniform flow would be formed. Tailwater level was obtained by backwater calculations.

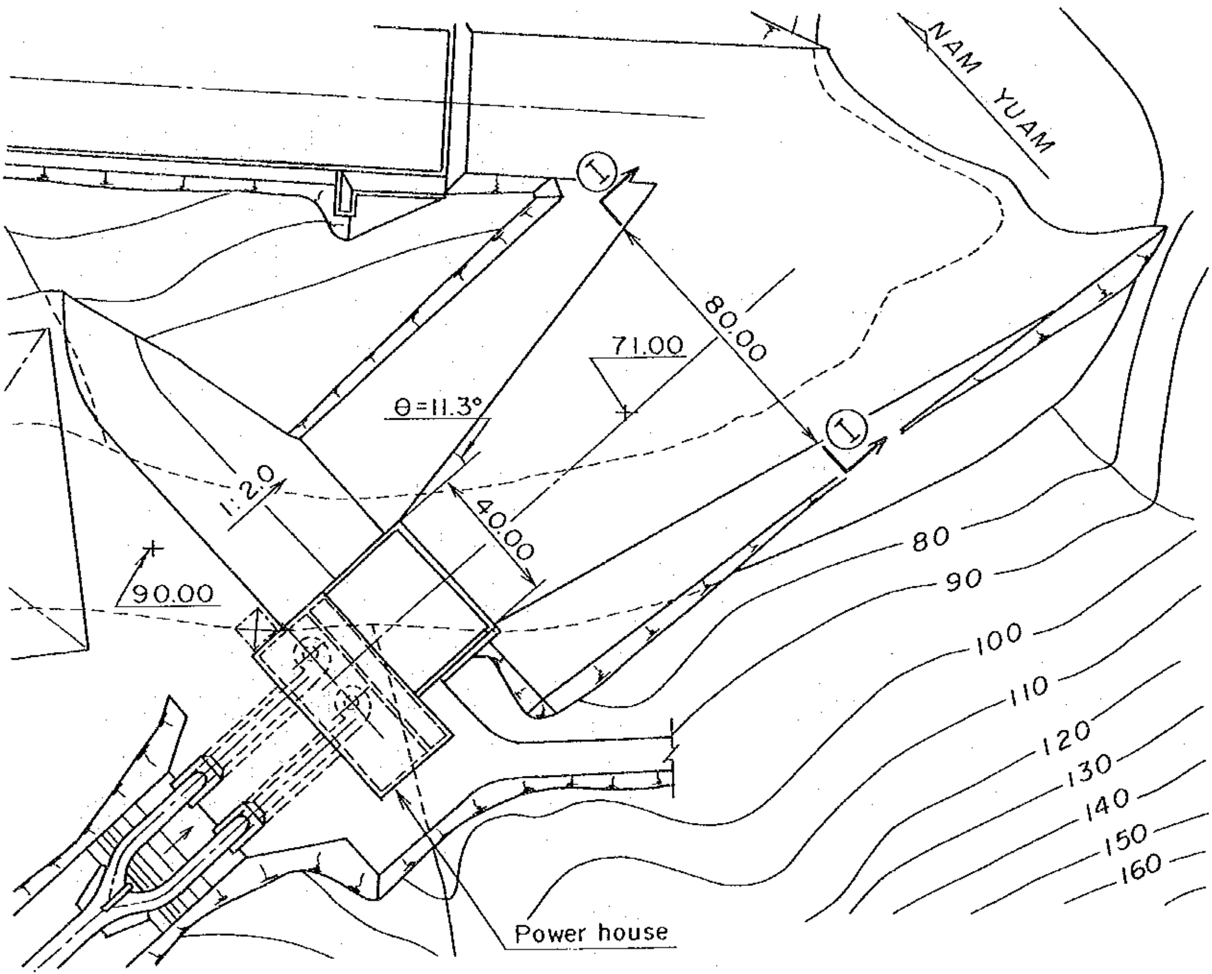

Section I

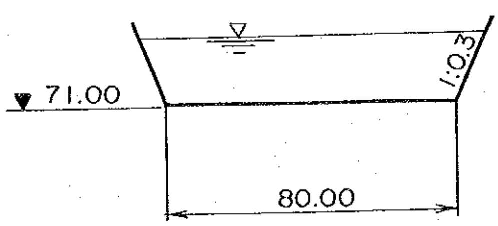

A 4 CONSTRUCTION MATERIAL

Table 4-1 Result of Soil Tests

Sample No.	Depth (m)	Classification of Soils by Unified System	Specific Gravity	Natural Water Content (%)	Atterberg Limits LL (%)	Atterberg Limits PL (%)	Atterberg Limits PI	Gradation Analyses Maximum Grain Size (mm)	Gradation Analyses -38.1 mm (%)	Gradation Analyses -19.1 mm (%)	Gradation Analyses -4.75 mm (%)	Gradation Analyses -0.425 mm (%)	Gradation Analyses -0.075 mm (%)	Gradation Analyses -0.005 mm (%)	Compaction & Permeability Optimum Water Content (%)	Compaction & Permeability Maximum Dry Density (t/m³)	Compaction & Permeability Coefficient of Permeability (cm/sec)	Triaxial Compression Strength ($\overline{CIU}$) Total Stress c (kgf/cm²)	Total Stress ø (deg.)	Effective Stress $\bar{c}$ (kgf/cm²)	Effective Stress $\bar{ø}$ (deg.)
A-1	1	SC	2.688	8.8	28.6	18.5	10.1	25	100	97	86	48	45	30	13.0	1.850	7.9×10^{-5}	0	27.8	0.48	33.8
A-2	1	SC	2.832	14.0	39.0	23.3	15.7	19	100	100	75	50	44	19	18.2	1.695	3.2×10^{-6}	—	—	—	—
	2	ML	2.788	16.9	39.2	27.0	12.2	25	100	99	93	66	56	22	—	—	—	—	—	—	—
	3	SC	2.841	18.6	38.2	22.9	15.3	25	100	97	91	61	47	18	15.7	1.710	4.4×10^{-6}	1.10	18.4	0.56	26.4
	4	CL	2.826	22.1	43.0	23.7	19.3	19	100	100	84	64	58	23	22.4	1.580	6.7×10^{-6}	—	—	—	—
	5	CL	2.839	24.0	40.9	22.8	18.1	25	100	96	94	74	64	27	22.5	1.585	6.3×10^{-6}	1.00	18.8	0.66	25.5
A-3	1	GC	2.733	10.8	41.2	23.0	18.2	38	100	91	65	39	35	21	—	—	—	—	—	—	—
	2	GC	2.734	10.3	40.8	23.6	17.2	38	100	92	59	35	30	18	12.8	1.930	1.7×10^{-5}	1.00	19.7	0.36	33.8
A-4	1	GC	2.660	8.6	26.2	17.2	9.0	25	100	96	54	25	20	13	—	—	—	—	—	—	—
A-5	1	SC	2.687	9.0	35.2	23.5	11.7	25	100	97	74	48	45	24	—	—	—	—	—	—	—
	2	GC	2.720	8.3	32.8	21.9	10.9	25	100	96	63	31	26	17	11.7	1.990	6.5×10^{-5}	0.67	27.2	0.37	34.8
A-7	1	CL	2.694	25.6	49.3	25.8	23.5				90	78	74		—	—	—		—	—	—
	2	ML	2.612	18.6	40.4	26.2	14.2				84	61	56		15.6	1.762	3.9×10^{-7}	(15.4)	—	—	—
	3	ML	2.656	13.5	44.8	28.5	16.3				—	62	52		17.2	1.757	1.1×10^{-7}	(18.9)	—	—	—
A-8	1	GC	2.773	27.6	38.2	24.1	14.1				73	53	48		—	—	—	—	—	—	—
	2	SM	2.779	24.0	39.1	24.0	15.1				82	54	46		13.4	1.807	3.4×10^{-7}	(14.6)	—	—	—
	3	SC	2.752	10.0	37.0	23.8	13.2				79	55	50		14.8	1.803	2.6×10^{-7}	(14.4)	—	—	—
A-9	1	CL	2.709	19.6	33.4	20.1	13.3				83	75	59		—	—	—	—	—	—	—
	2	CL	2.684	15.1	37.9	22.0	15.9				88	64	51		13.8	1.845	1.6×10^{-7}	(14.0)	—	—	—
	3	CL	2.752	24.2	44.2	26.4	17.8				83	66	58		—	—	—	—	—	—	—
	4	CL	2.669	21.9	44.7	23.8	20.9				88	72	65		16.8	1.762	1.4×10^{-7}	(15.8)	—	—	—
A-10	1	CL	2.610	19.1	36.5	20.8	15.7				82	62	54		—	—	—	—	—	—	—
	2	CL	2.628	29.1	38.2	21.2	17.0								—	—	—	—	—	—	—
	3	CL	2.758	25.7	37.9	21.5	16.4				95	83	71		16.1	1.779	3.1×10^{-8}	(17.1)	—	—	—
	4	CL	2.662	18.6	39.6	21.2	18.4				99	87	75		—	—	—	—	—	—	—
	5	CL	2.788	20.6	39.0	21.0	18.0				95	81	69		15.8	1.782	8.9×10^{-8}	(16.8)	—	—	—

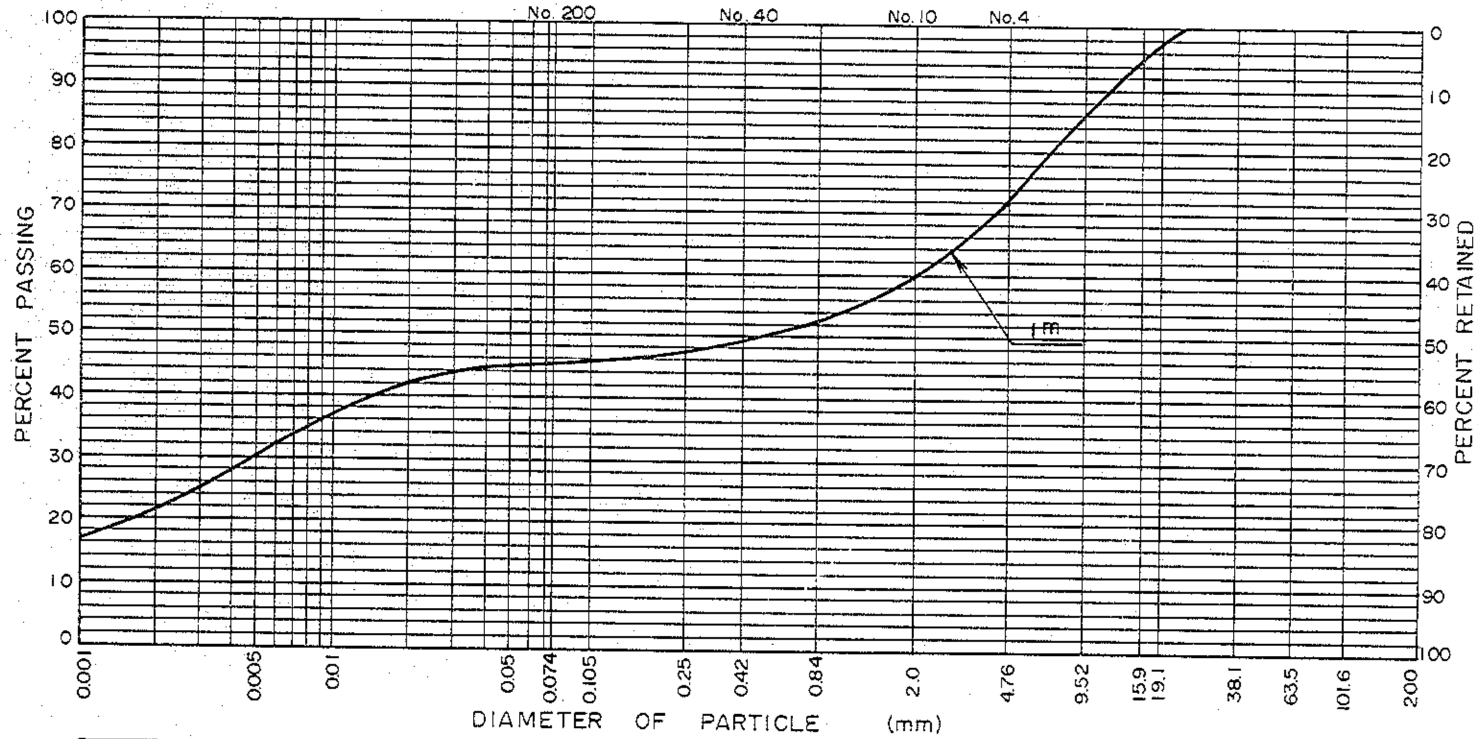

CLAY (PLASTIC) ~ SILT (NON-PLASTIC)	SAND			GRAVEL		COBBLES
	FINE	MEDIUM	COARSE	FINE	COARSE	

SAMPLE NO.		
MAX GRAIN SIZE		
mm (%)		
mm (%)		
mm 46 (%)		
mm 0.074 (%)		
D_{60} (mm)		
D_{30} (mm)		
D_{10} (mm)		
Cu		
Cc		

$Cu = \frac{D_{60}}{D_{10}}$ COEFFICIENT OF UNIFORMITY

$Cc = \frac{(D_{30})^2}{(D_{60}) \times (D_{10})}$ COEFFICIENT OF CURVATURE

SAMPLE		SOIL CLASSIFICATION		SPECIFIC GRAVITY		ATTERBERG LIMITS			
NUMBER	DEPTH (m)	UNIFIED SYSTEM	REVISED PR. SYSTEM			LL	PL	PI	SL

Fig. 1-1 Grain Size Distribution Curve Sample A-1

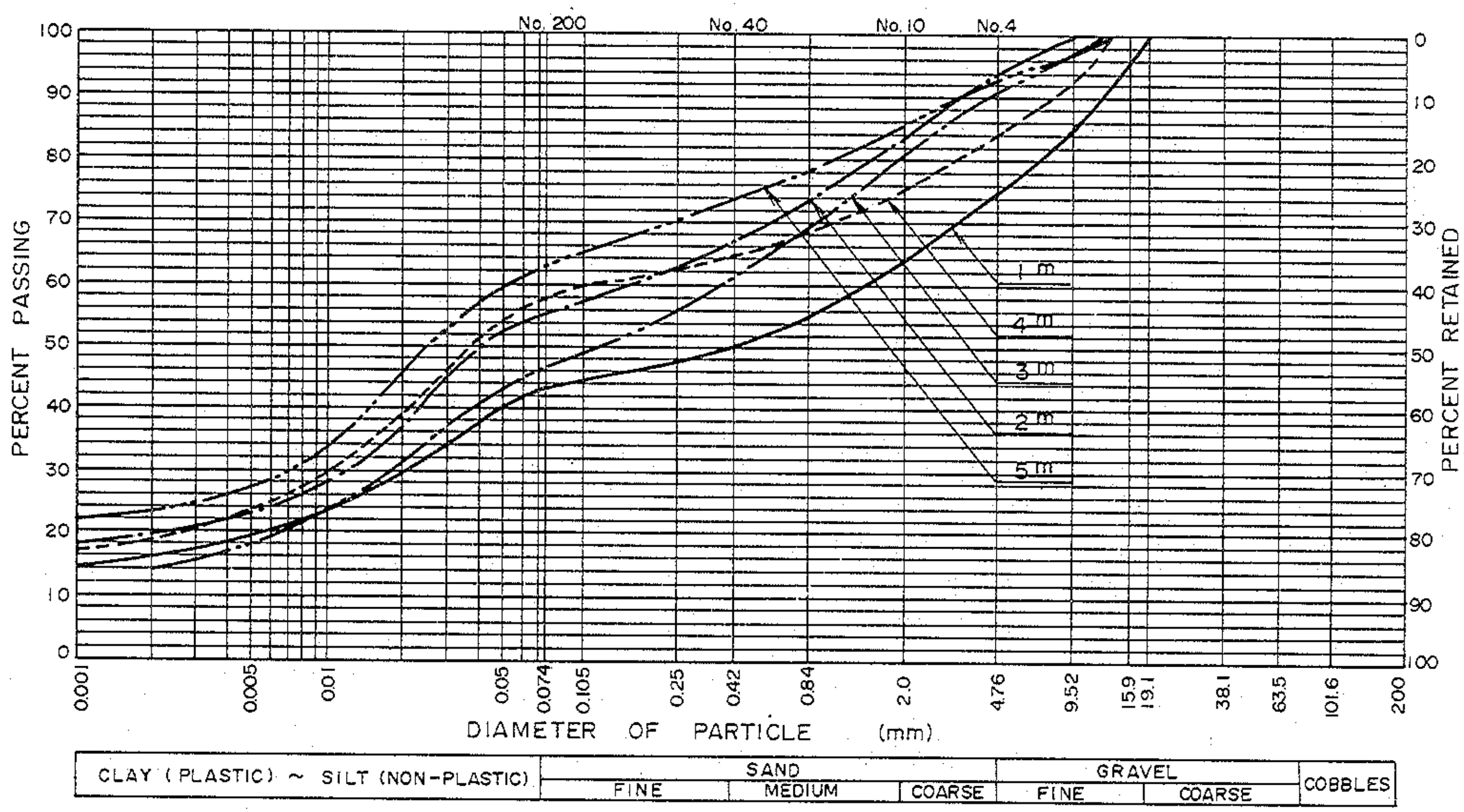

SAMPLE NO.		
MAX GRAIN SIZE		
mm (%)		
mm (%)		
mm 46 (%)		
mm 0.074 (%)		
D_{60} (mm)		
D_{30} (mm)		
D_{10} (mm)		
Cu		
Cc		

$$Cu = \frac{D_{60}}{D_{10}}$$

COEFFICIENT OF UNIFORMITY

$$Cc = \frac{(D_{30})^2}{(D_{60}) \times (D_{10})}$$

COEFFICIENT OF CURVATURE

SAMPLE		SOIL CLASSIFICATION		SPECIFIC GRAVITY		ATTERBERG LIMITS			
NUMBER	DEPTH (m)	UNIFIED SYSTEM	REVISED PR. SYSTEM			LL	PL	PI	SL

Fig. I-2 Grain Size Distribution Curve Sample A-2

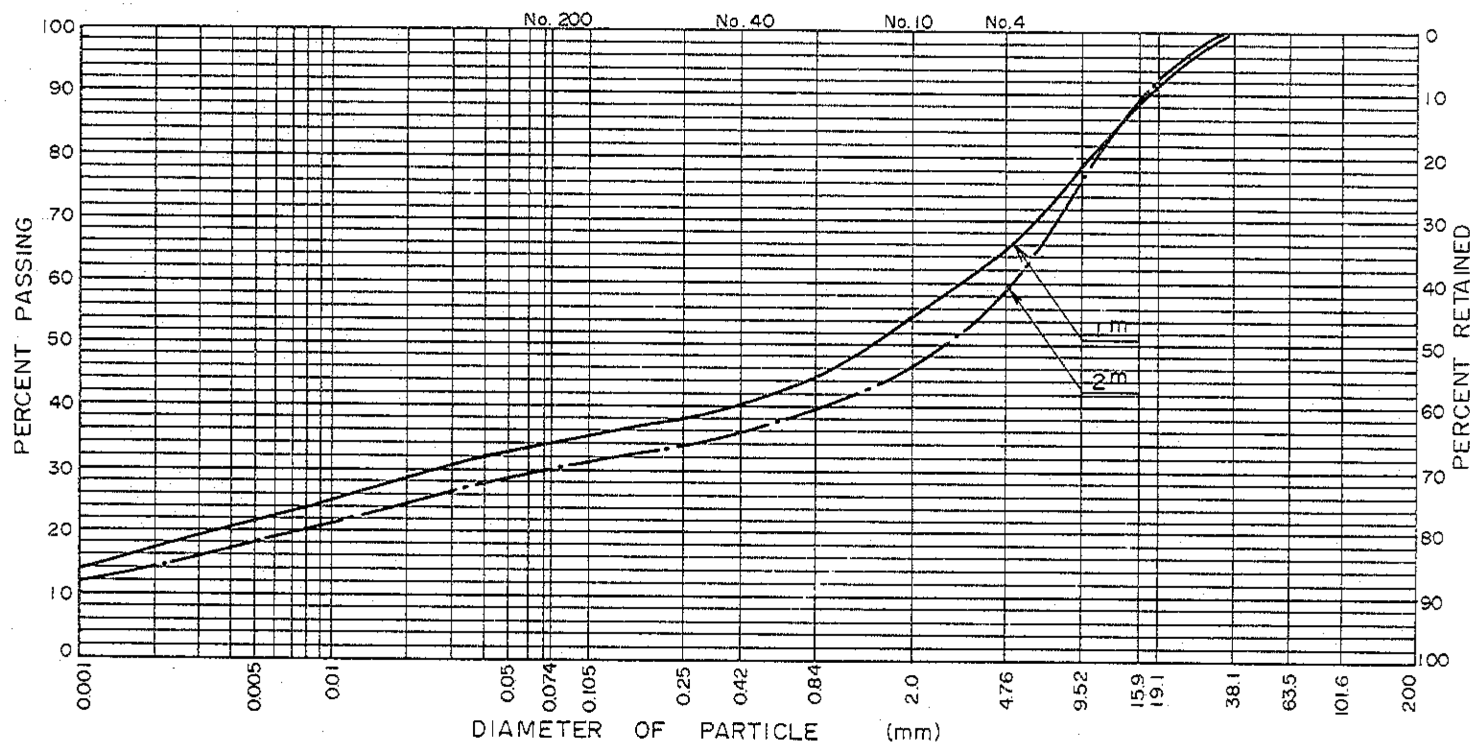

CLAY (PLASTIC) ~ SILT (NON-PLASTIC)	SAND			GRAVEL		COBBLES
	FINE	MEDIUM	COARSE	FINE	COARSE	

SAMPLE		SOIL CLASSIFICATION		SPECIFIC GRAVITY		ATTERBERG LIMITS			
NUMBER	DEPTH (m)	UNIFIED SYSTEM	REVISED P.R. SYSTEM			LL	PL	PI	SL

SAMPLE NO.		
MAX GRAIN SIZE		
mm (%)		
mm (%)		
mm 46 (%)		
mm 0.074 (%)		
D_{60} (mm)		
D_{30} (mm)		
D_{10} (mm)		
Cu		
Cc		

$Cu = \frac{D_{60}}{D_{10}}$ COEFFICIENT OF UNIFORMITY

$Cc = \frac{(D_{30})^2}{(D_{60}) \times (D_{10})}$ COEFFICIENT OF CURVATURE

Fig.1-3 Grain Size Distribution Curve Sample A-3

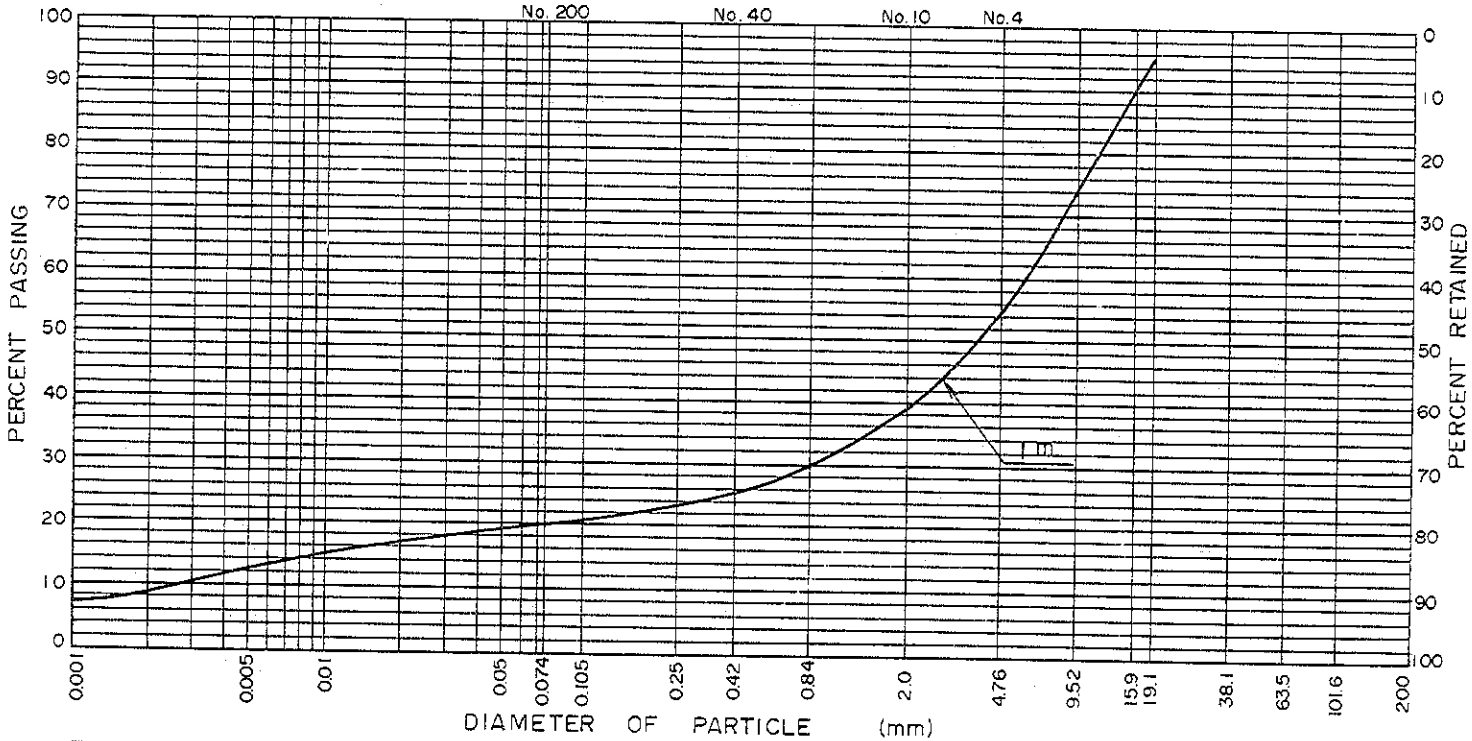

CLAY (PLASTIC) ~ SILT (NON-PLASTIC)	SAND			GRAVEL		COBBLES
	FINE	MEDIUM	COARSE	FINE	COARSE	

SAMPLE NO.		
MAX GRAIN SIZE		
mm (%)		
mm (%)		
mm 46 (%)		
mm 0.074 (%)		
D_{60} (mm)		
D_{30} (mm)		
D_{10} (mm)		
Cu		
Cc		

$$Cu = \frac{D_{60}}{D_{10}}$$

COEFFICIENT OF UNIFORMITY

$$Cc = \frac{(D_{30})^2}{(D_{60}) \times (D_{10})}$$

COEFFICIENT OF CURVATURE

SAMPLE		SOIL CLASSIFICATION		SPECIFIC GRAVITY		ATTERBERG LIMITS			
NUMBER	DEPTH (m)	UNIFIED SYSTEM	REVISED P.R. SYSTEM			LL	PL	PI	SL

Fig. I-4 Grain Size Distribution Curve Sample A-4

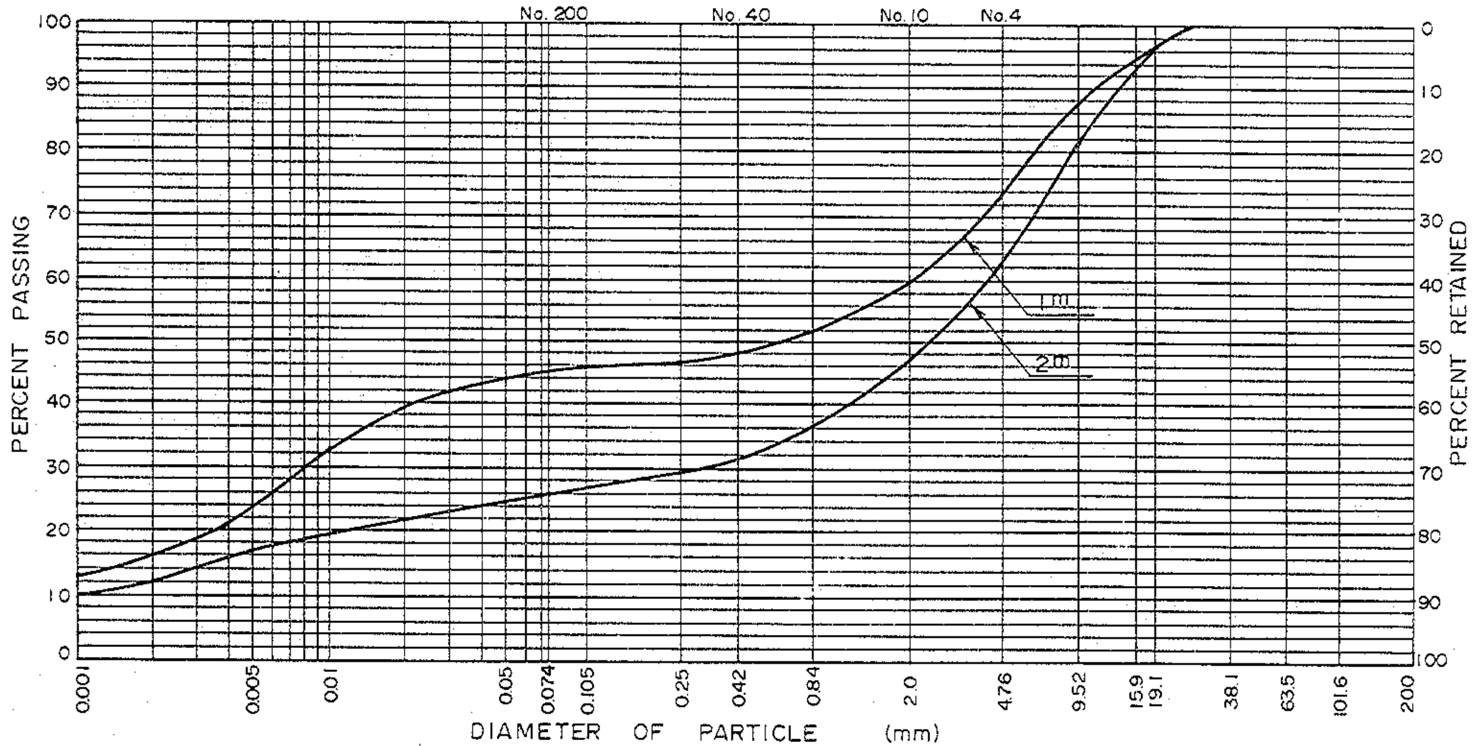

CLAY (PLASTIC) ~ SILT (NON-PLASTIC)	SAND			GRAVEL		COBBLES
	FINE	MEDIUM	COARSE	FINE	COARSE	

SAMPLE NO.		
MAX GRAIN SIZE		
mm (%)		
mm (%)		
mm 46 (%)		
mm 0.074 (%)		
D_{60} (mm)		
D_{30} (mm)		
D_{10} (mm)		
Cu		
Cc		

$Cu = \frac{D_{60}}{D_{10}}$

COEFFICIENT OF UNIFORMITY

$Cc = \frac{(D_{30})^2}{(D_{60}) \times (D_{10})}$

COEFFICIENT OF CURVATURE

SAMPLE		SOIL CLASSIFICATION		SPECIFIC GRAVITY		ATTERBERG LIMITS			
NUMBER	DEPTH (m)	UNIFIED SYSTEM	REVISED P.R. SYSTEM			LL	PL	PI	SL

Fig. I-5 Grain Size Distribution Curve Sample A-5

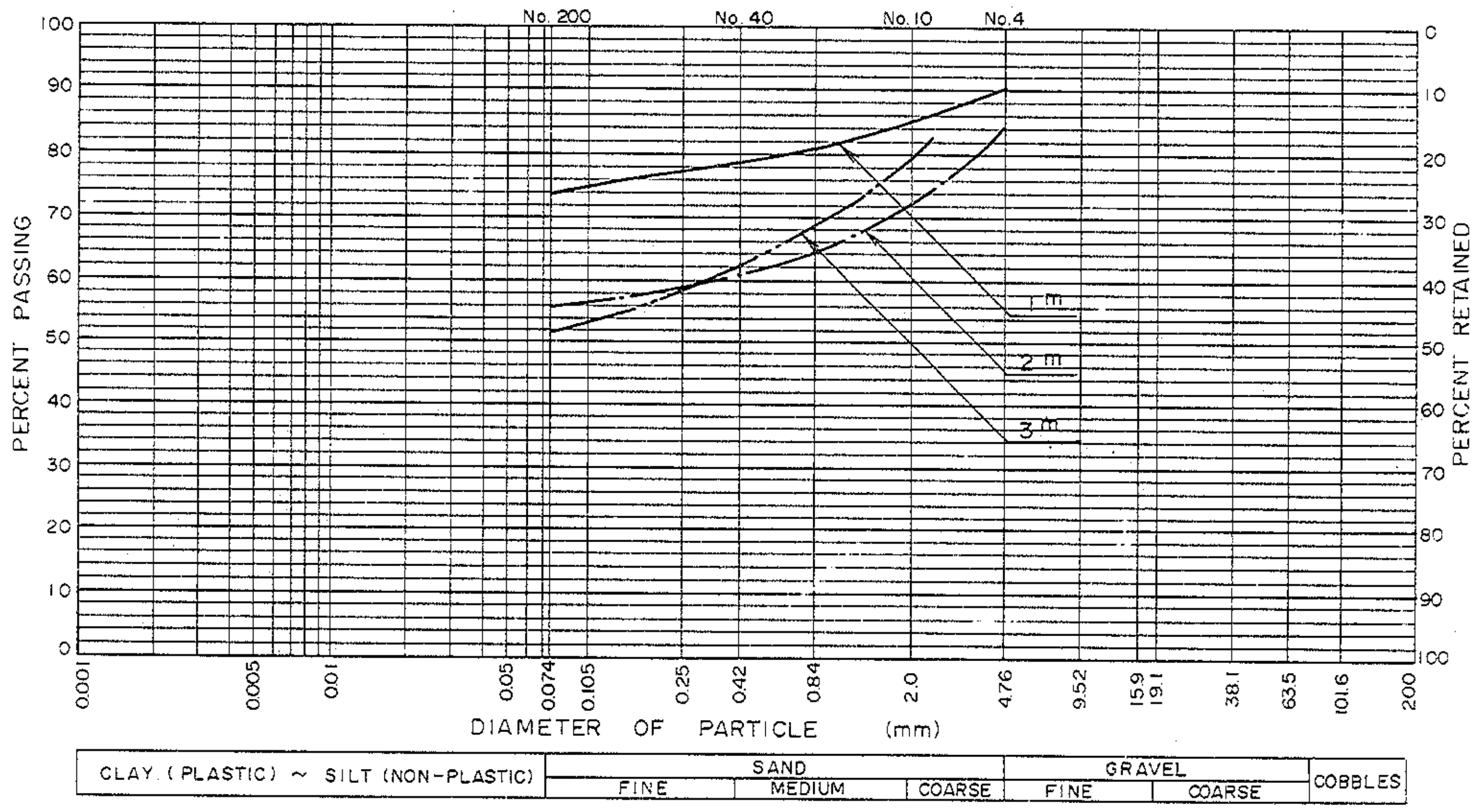

SAMPLE NO.		
MAX GRAIN SIZE		
mm (%)		
mm (%)		
mm 46 (%)		
mm 0.074 (%)		
D_{60} (mm)		
D_{30} (mm)		
D_{10} (mm)		
Cu		
Cc		

$Cu = \frac{D_{60}}{D_{10}}$ COEFFICIENT OF UNIFORMITY

$Cc = \frac{(D_{30})^2}{(D_{60}) \times (D_{10})}$ COEFFICIENT OF CURVATURE

SAMPLE		SOIL CLASSIFICATION		SPECIFIC GRAVITY		ATTERBERG LIMITS			
NUMBER	DEPTH (m)	UNIFIED SYSTEM	REVISED P.R. SYSTEM			LL	PL	PI	SL

Fig.1-6 Grain Size Distribution Curve Sample A-7

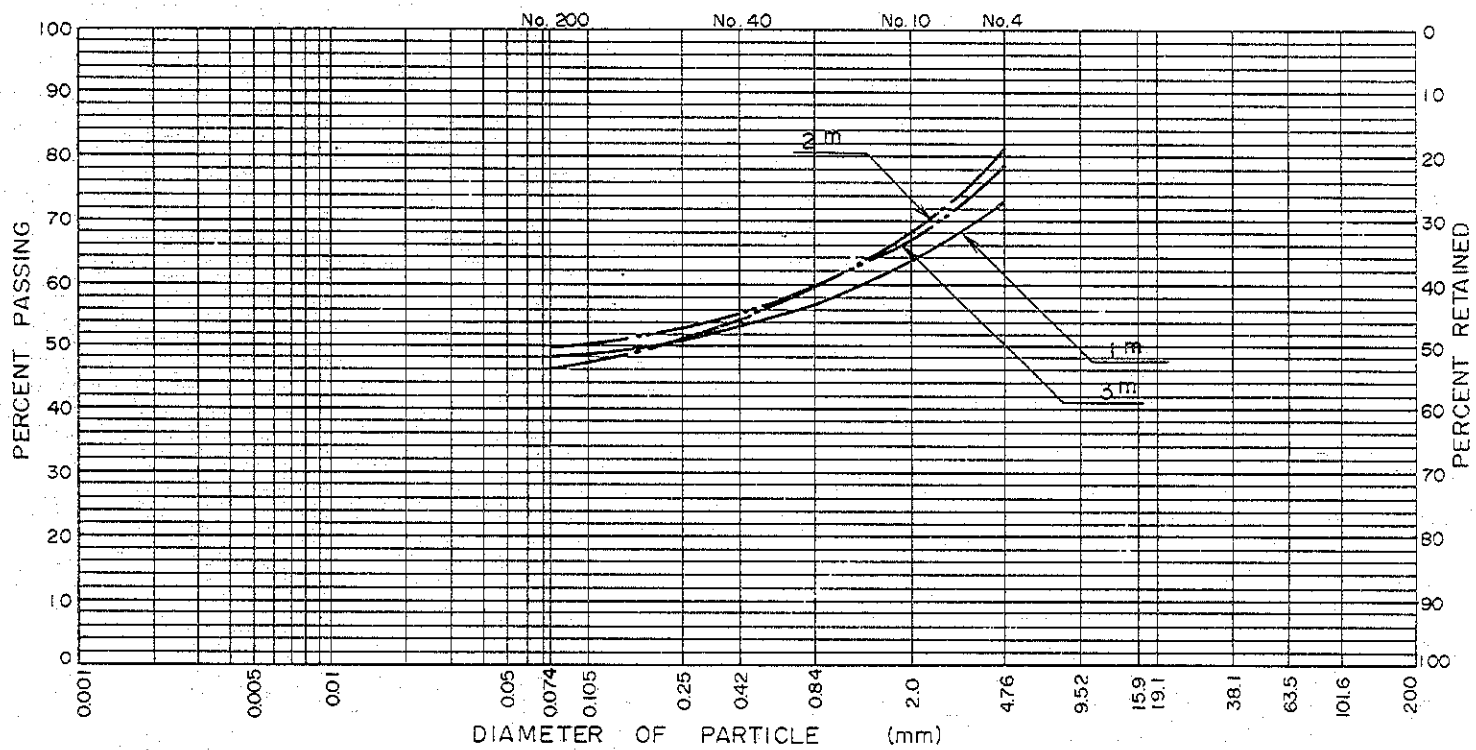

CLAY (PLASTIC) ~ SILT (NON-PLASTIC)	SAND			GRAVEL		COBBLES
	FINE	MEDIUM	COARSE	FINE	COARSE	

SAMPLE NO.		
MAX GRAIN SIZE		
mm (%)		
mm (%)		
mm 4.6 (%)		
mm 0.074 (%)		
D_{60} (mm)		
D_{30} (mm)		
D_{10} (mm)		
Cu		
Cc		

$Cu = \frac{D_{60}}{D_{10}}$ COEFFICIENT OF UNIFORMITY

$Cc = \frac{(D_{30})^2}{(D_{60}) \times (D_{10})}$ COEFFICIENT OF CURVATURE

SAMPLE		SOIL CLASSIFICATION		SPECIFIC GRAVITY		ATTERBERG LIMITS			
NUMBER	DEPTH (m)	UNIFIED SYSTEM	REVISED P.R. SYSTEM			LL	PL	PI	SL

Fig. I-7 Grain Size Distribution Curve Sample A-8

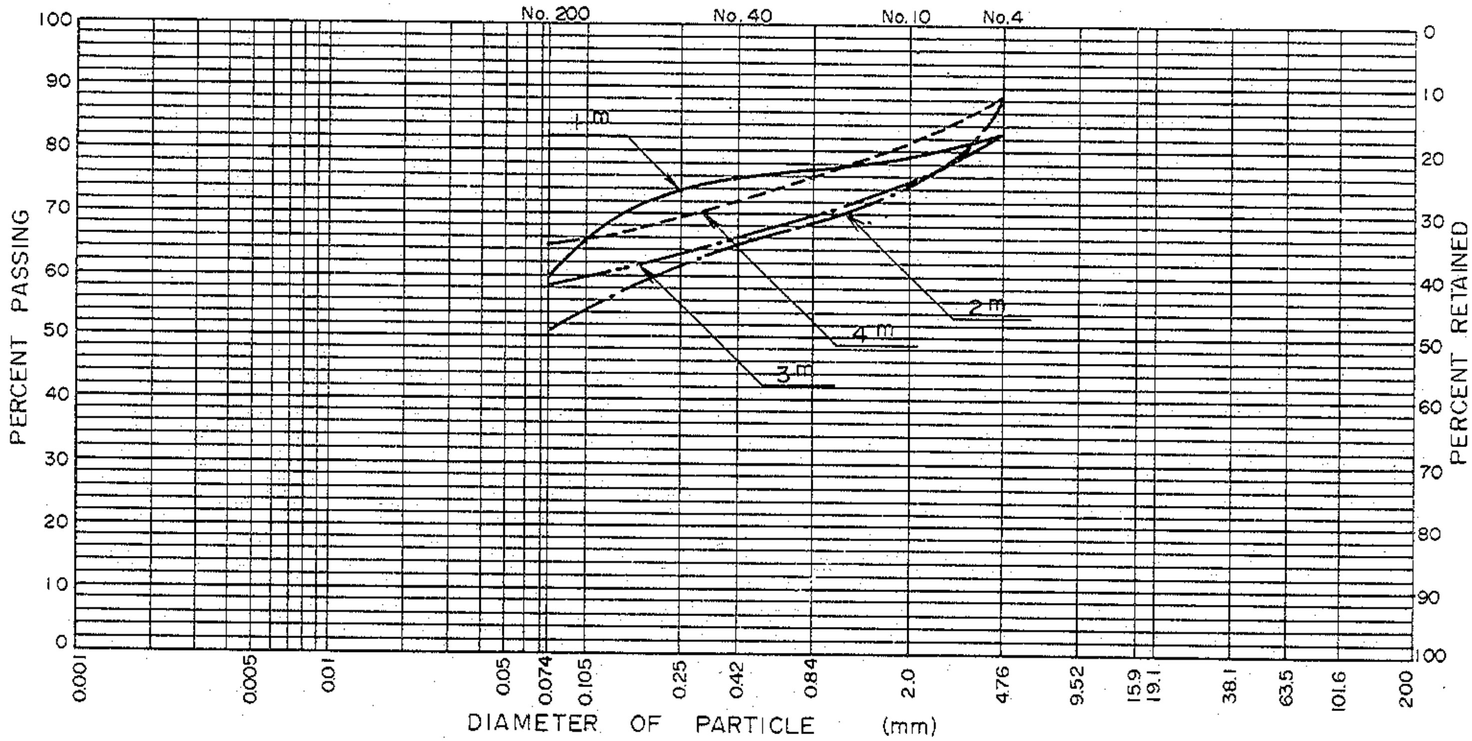

CLAY (PLASTIC) ~ SILT (NON-PLASTIC)	SAND			GRAVEL		COBBLES
	FINE	MEDIUM	COARSE	FINE	COARSE	

SAMPLE NO.		
MAX GRAIN SIZE		
mm (%)		
mm (%)		
mm 46 (%)		
mm 0.074 (%)		
D_{60} (mm)		
D_{30} (mm)		
D_{10} (mm)		
Cu		
Cc		

$Cu = \frac{D_{60}}{D_{10}}$ COEFFICIENT OF UNIFORMITY

$Cc = \frac{(D_{30})^2}{(D_{60}) \times (D_{10})}$ COEFFICIENT OF CURVATURE

SAMPLE		SOIL CLASSIFICATION		SPECIFIC GRAVITY		ATTERBERG LIMITS			
NUMBER	DEPTH (m)	UNIFIED SYSTEM	REVISED P.R. SYSTEM			LL	PL	PI	SL

Fig. I-8 Grain Size Distribution Curve Sample A-9

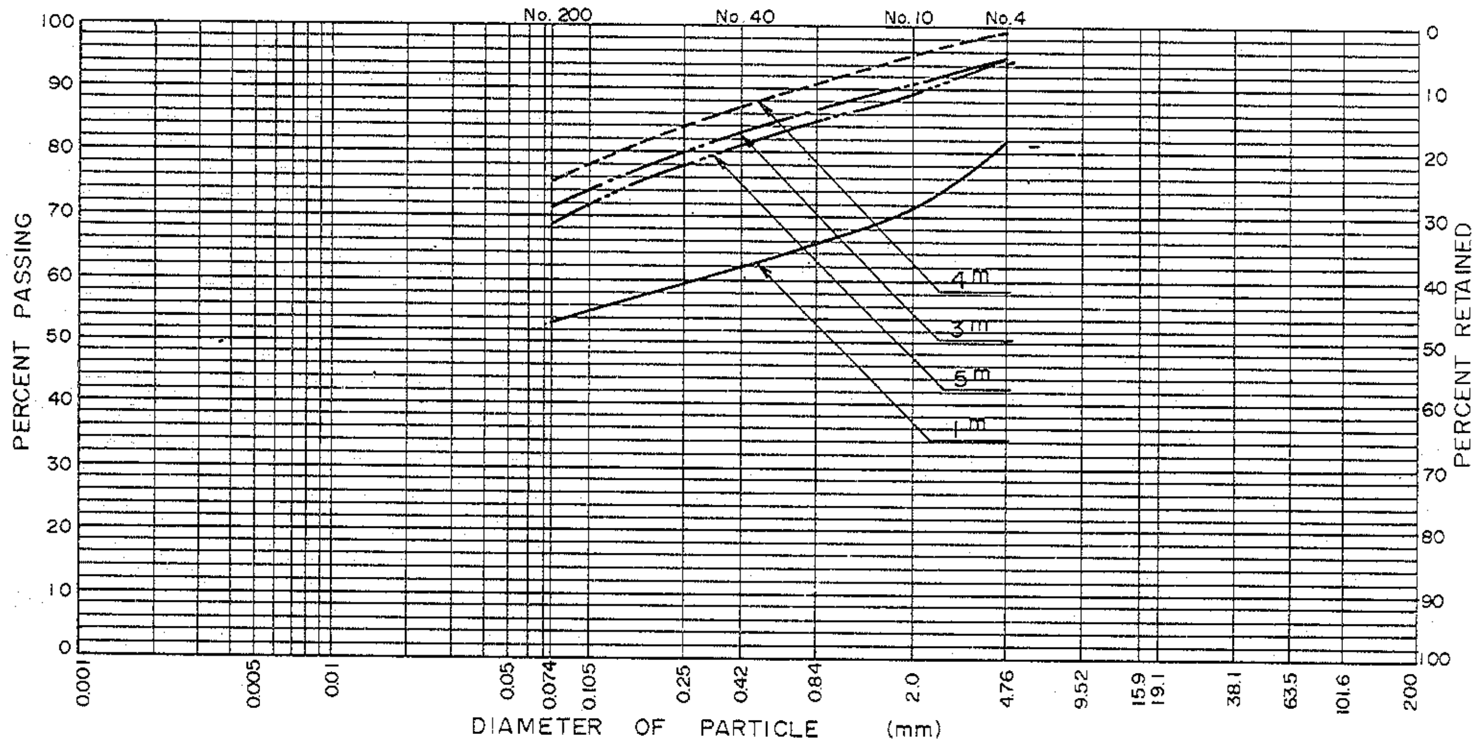

SAMPLE NO.		
MAX GRAIN SIZE		
mm (%)		
mm (%)		
mm 46 (%)		
mm 0.074 (%)		
D_{60} (mm)		
D_{30} (mm)		
D_{10} (mm)		
Cu		
Cc		

$Cu = \frac{D_{60}}{D_{10}}$

COEFFICIENT OF UNIFORMITY

$Cc = \frac{(D_{30})^2}{(D_{60}) \times (D_{10})}$

COEFFICIENT OF CURVATURE

CLAY (PLASTIC) ~ SILT (NON-PLASTIC)	SAND			GRAVEL		COBBLES
	FINE	MEDIUM	COARSE	FINE	COARSE	

SAMPLE		SOIL CLASSIFICATION		SPECIFIC GRAVITY		ATTERBERG LIMITS			
NUMBER	DEPTH (m)	UNIFIED SYSTEM	REVISED P.R. SYSTEM			LL	PL	PI	SL

Fig. I-9 Grain Size Distribution Curve Sample A-10

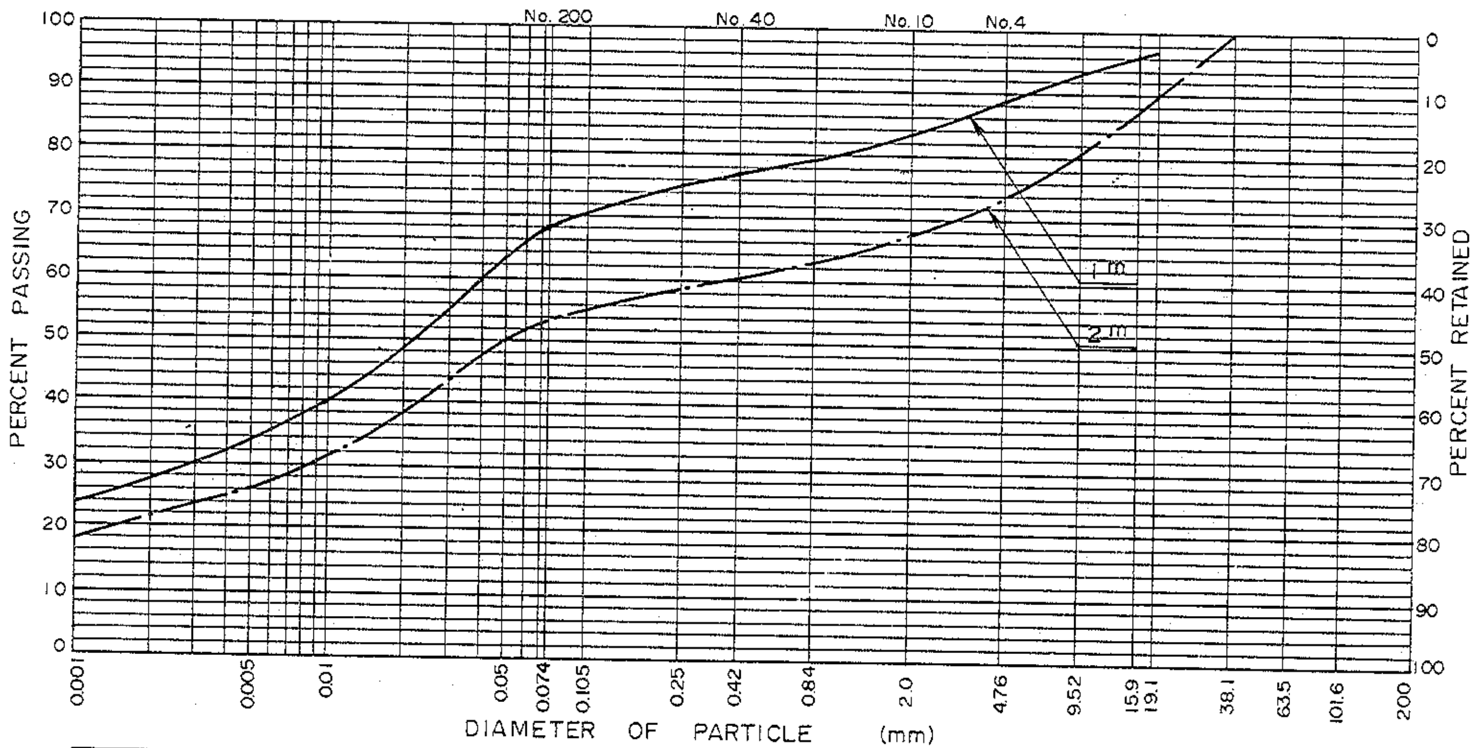

SAMPLE NO.		
MAX GRAIN SIZE		
mm (%)		
mm (%)		
mm 46 (%)		
mm 0.074 (%)		
D_{60} (mm)		
D_{30} (mm)		
D_{10} (mm)		
Cu		
Cc		

$Cu = \frac{D_{60}}{D_{10}}$ COEFFICIENT OF UNIFORMITY

$Cc = \frac{(D_{30})^2}{(D_{60}) \times (D_{10})}$ COEFFICIENT OF CURVATURE

CLAY (PLASTIC) ~ SILT (NON-PLASTIC)	SAND			GRAVEL		COBBLES
	FINE	MEDIUM	COARSE	FINE	COARSE	

SAMPLE		SOIL CLASSIFICATION		SPECIFIC GRAVITY		ATTERBERG LIMITS			
NUMBER	DEPTH (m)	UNIFIED SYSTEM	REVISED P.R. SYSTEM			LL	PL	PI	SL

Fig. I-10 Grain Size Distribution Curve Sample B-1

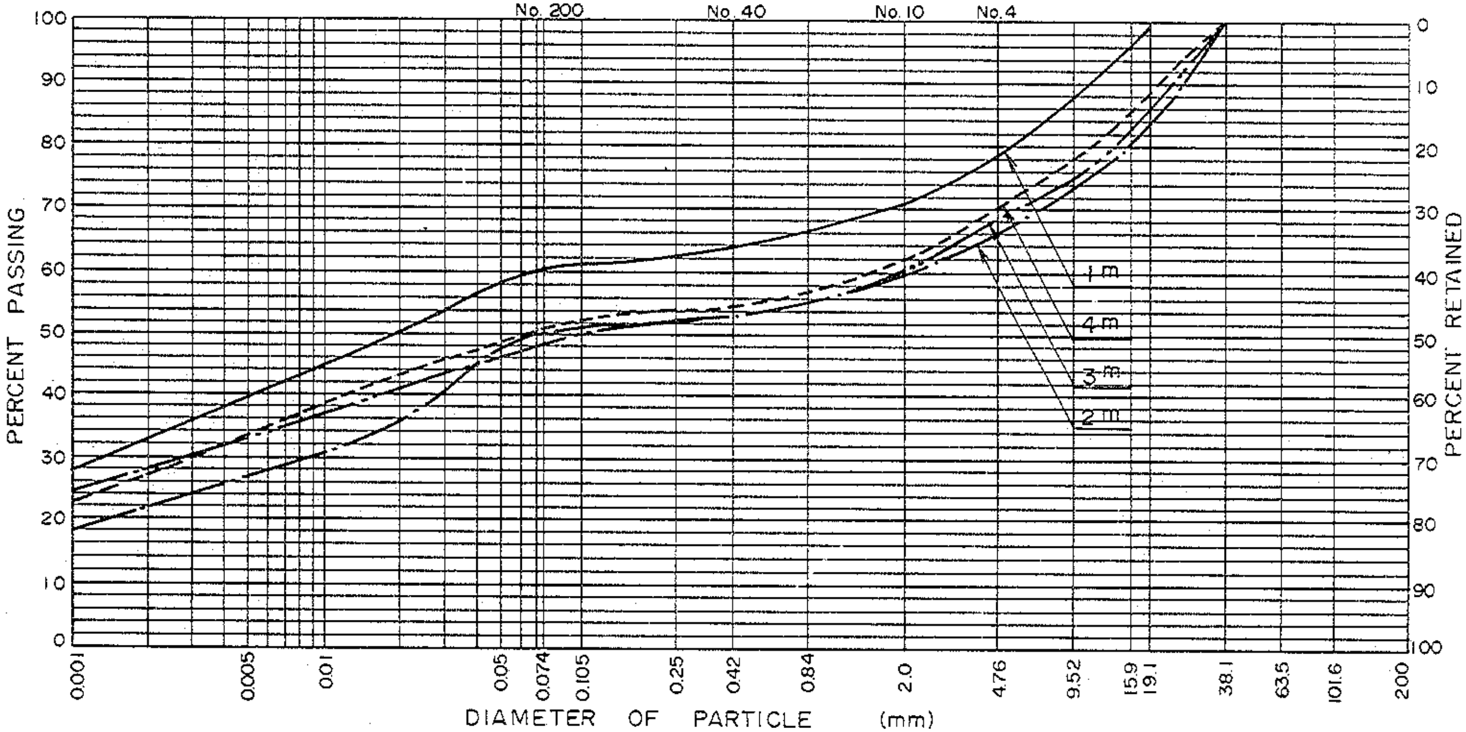

CLAY (PLASTIC) ~ SILT (NON-PLASTIC)	SAND			GRAVEL		COBBLES
	FINE	MEDIUM	COARSE	FINE	COARSE	

SAMPLE NO.		
MAX GRAIN SIZE		
mm (%)		
mm (%)		
mm 46 (%)		
mm 0.074 (%)		
D_{60} (mm)		
D_{30} (mm)		
D_{10} (mm)		
Cu		
Cc		

$Cu = \frac{D_{60}}{D_{10}}$

COEFFICIENT OF UNIFORMITY

$Cc = \frac{(D_{30})^2}{(D_{60}) \times (D_{10})}$

COEFFICIENT OF CURVATURE

SAMPLE		SOIL CLASSIFICATION		SPECIFIC GRAVITY		ATTERBERG LIMITS			
NUMBER	DEPTH (m)	UNIFIED SYSTEM	REVISED PR. SYSTEM			LL	PL	PI	SL

Fig.I-11 Grain Size Distribution Curve Sample C-1

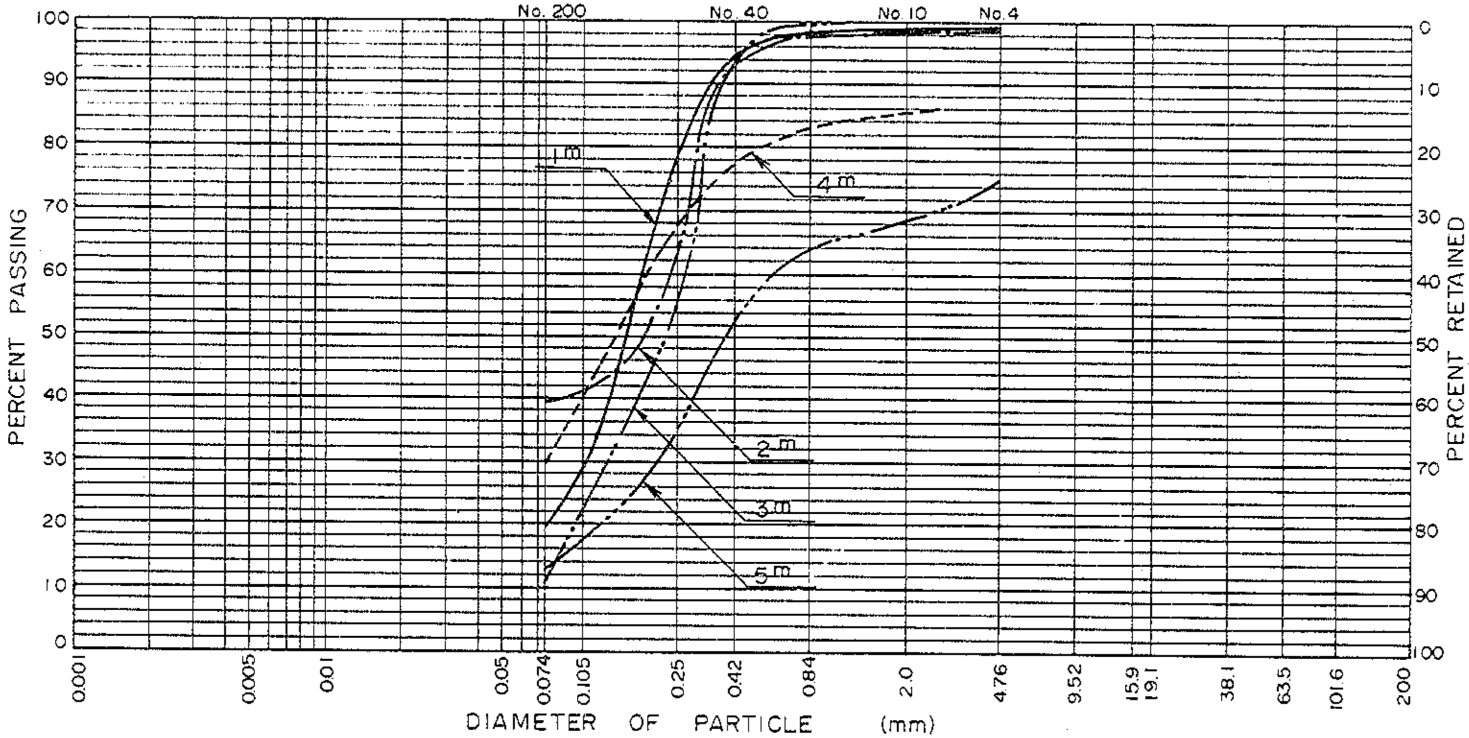

CLAY (PLASTIC) ~ SILT (NON-PLASTIC)	SAND			GRAVEL		COBBLES
	FINE	MEDIUM	COARSE	FINE	COARSE	

SAMPLE NO.		
MAX GRAIN SIZE		
mm (%)		
mm (%)		
mm 46 (%)		
mm 0.074 (%)		
D60 (mm)		
D30 (mm)		
D10 (mm)		
Cu		
Cc		

$Cu = \frac{D_{60}}{D_{10}}$

COEFFICIENT OF UNIFORMITY

$Cc = \frac{(D_{30})^2}{(D_{60}) \times (D_{10})}$

COEFFICIENT OF CURVATURE

SAMPLE		SOIL CLASSIFICATION		SPECIFIC GRAVITY		ATTERBERG LIMITS			
NUMBER	DEPTH (m)	UNIFIED SYSTEM	REVISED PR. SYSTEM			LL	PL	PI	SL

Fig. 1-12 Grain Size Distribution Curve Sample C-6

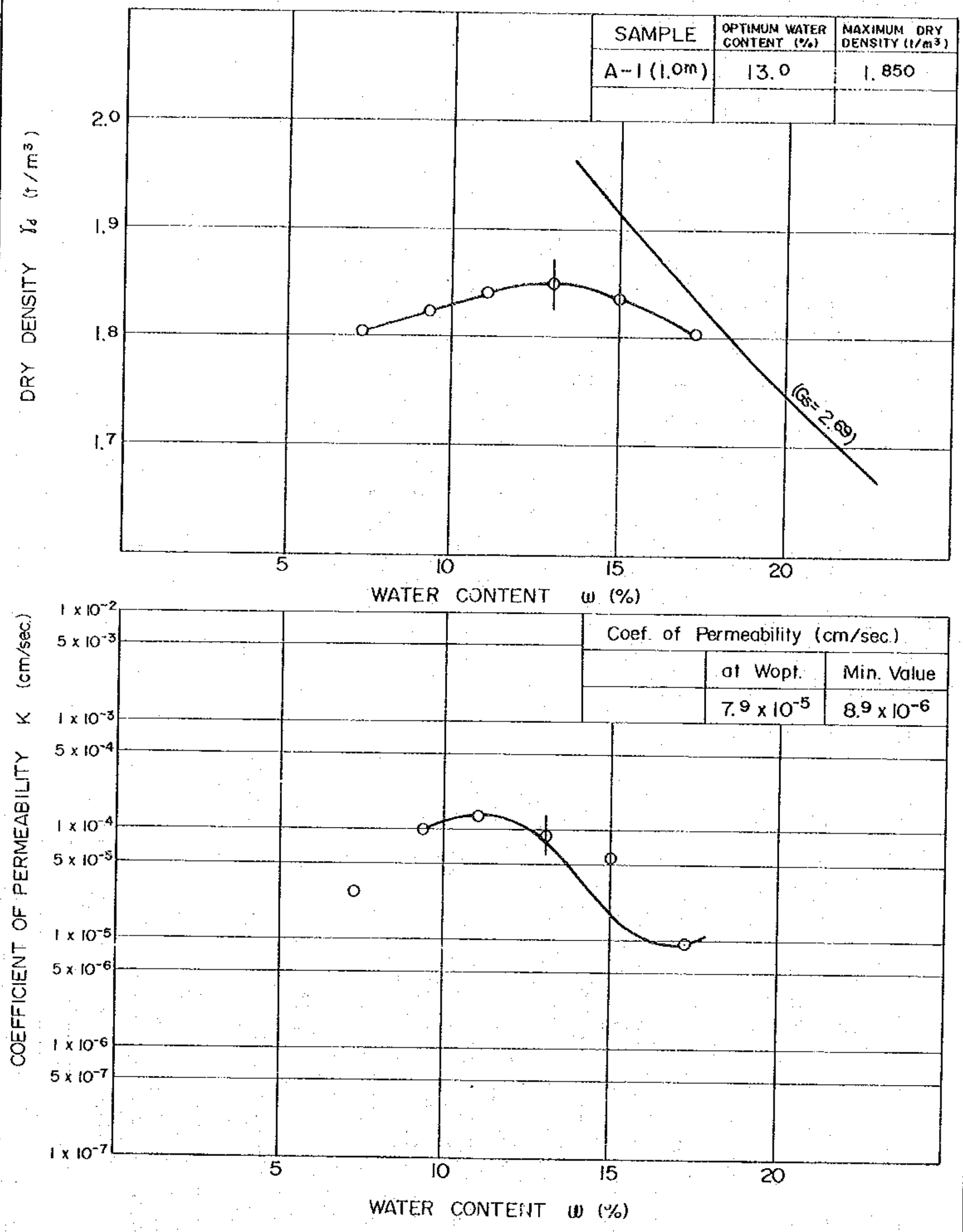

Sample A-1 1.00m

Fig.2-1 Compaction and Permeability Test

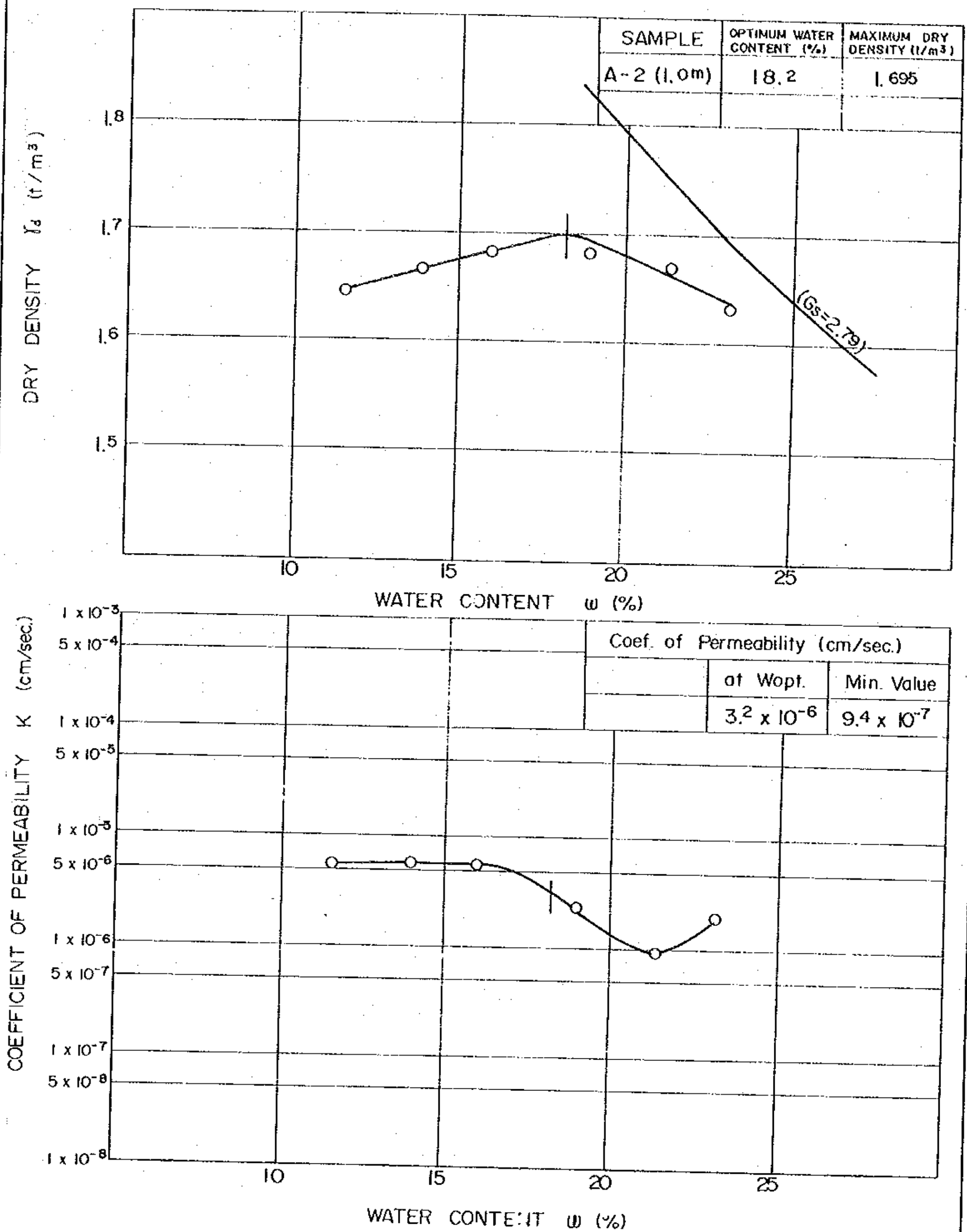

Sample A-2 1.00m

Fig.2-2 Compaction and Permeability Test

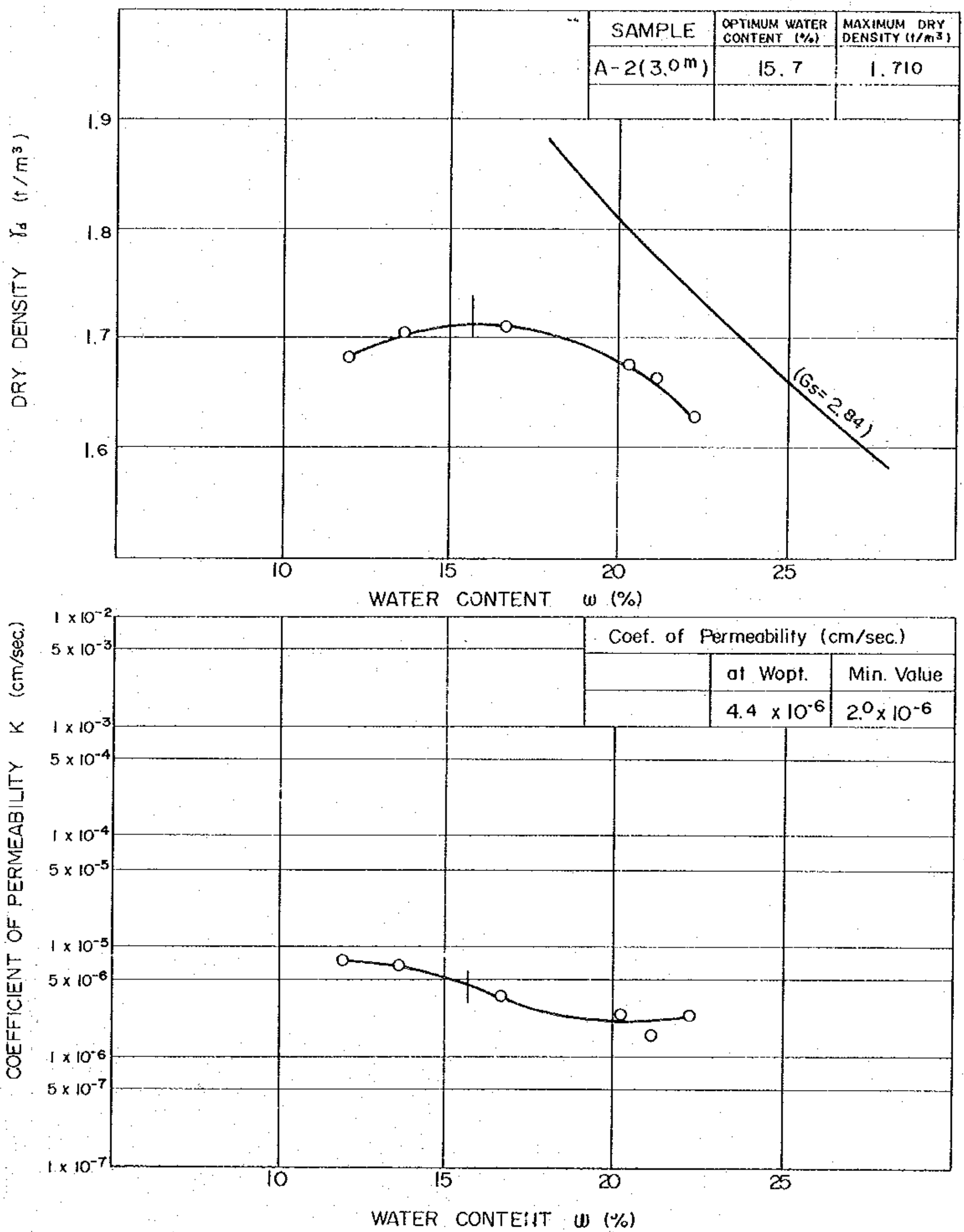

Sample A-2 3.00m

Fig.2-3 Compaction and Permeability Test

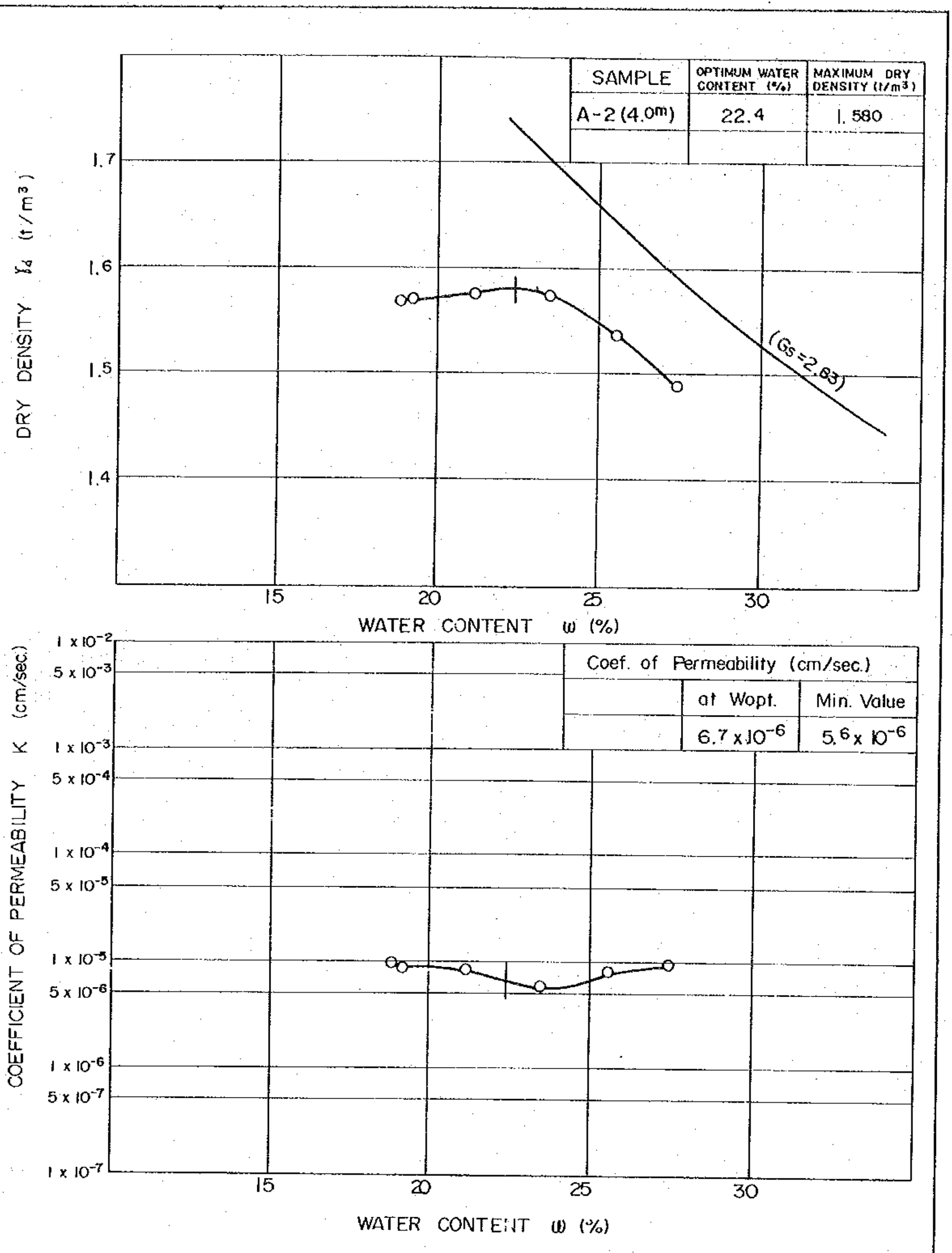

Sample A-2 4.00m

Fig.2-4 Compaction and Permeability Test

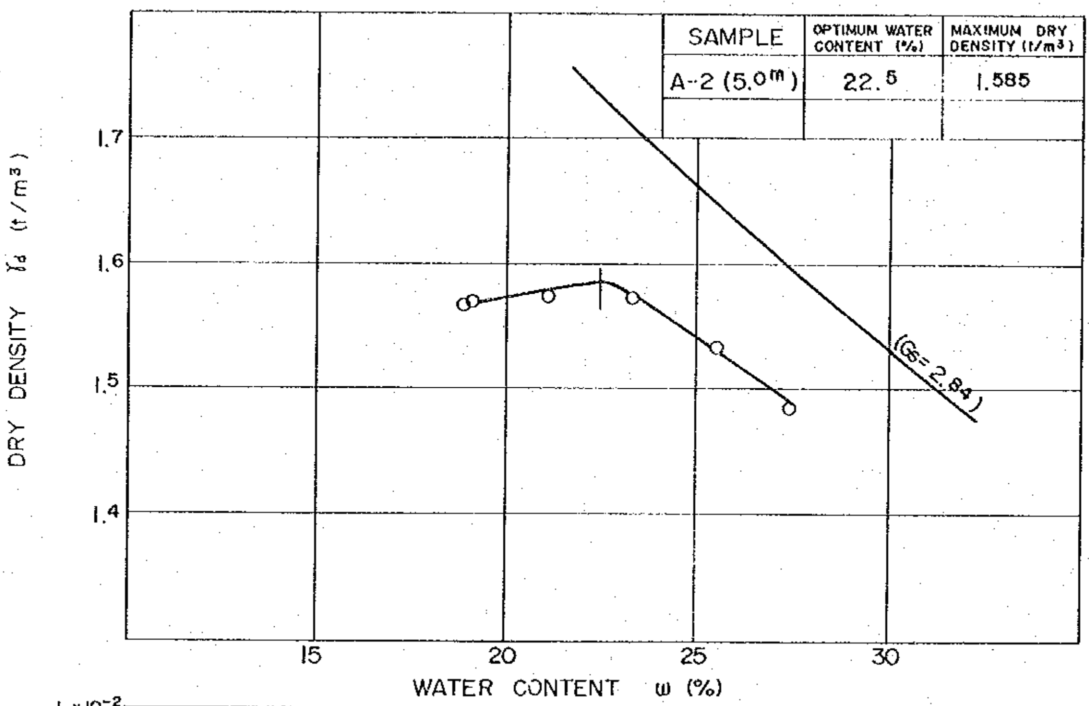

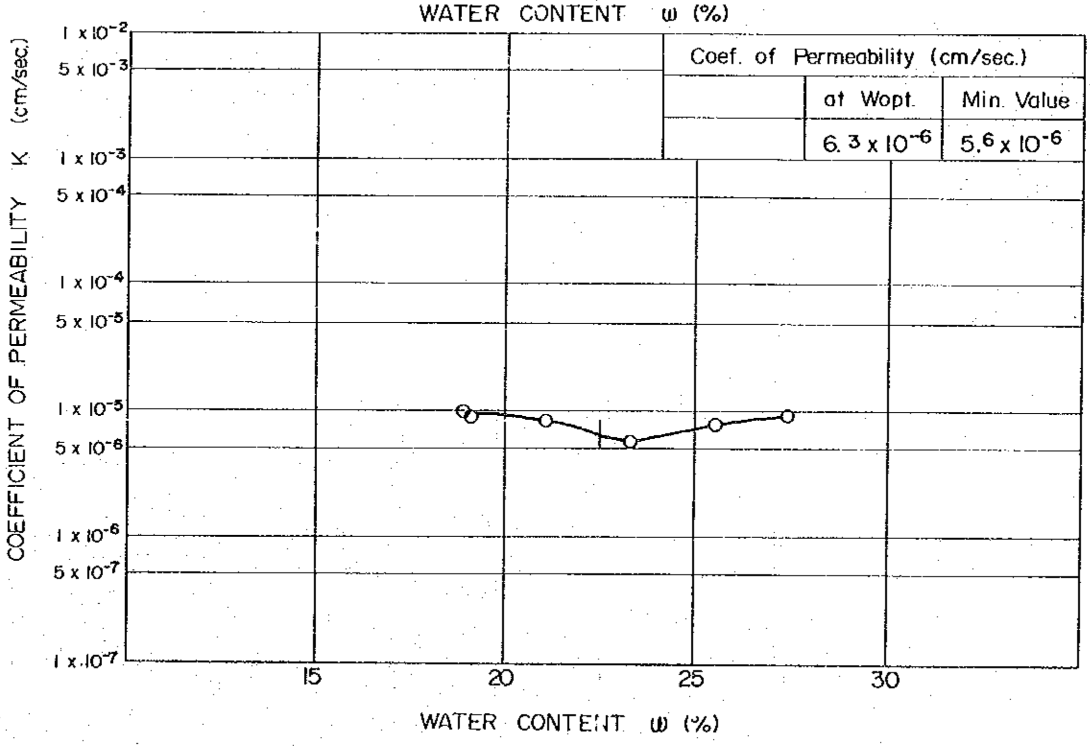

Sample A-2 5.00m

Fig.2-5 Compaction and Permeability Test

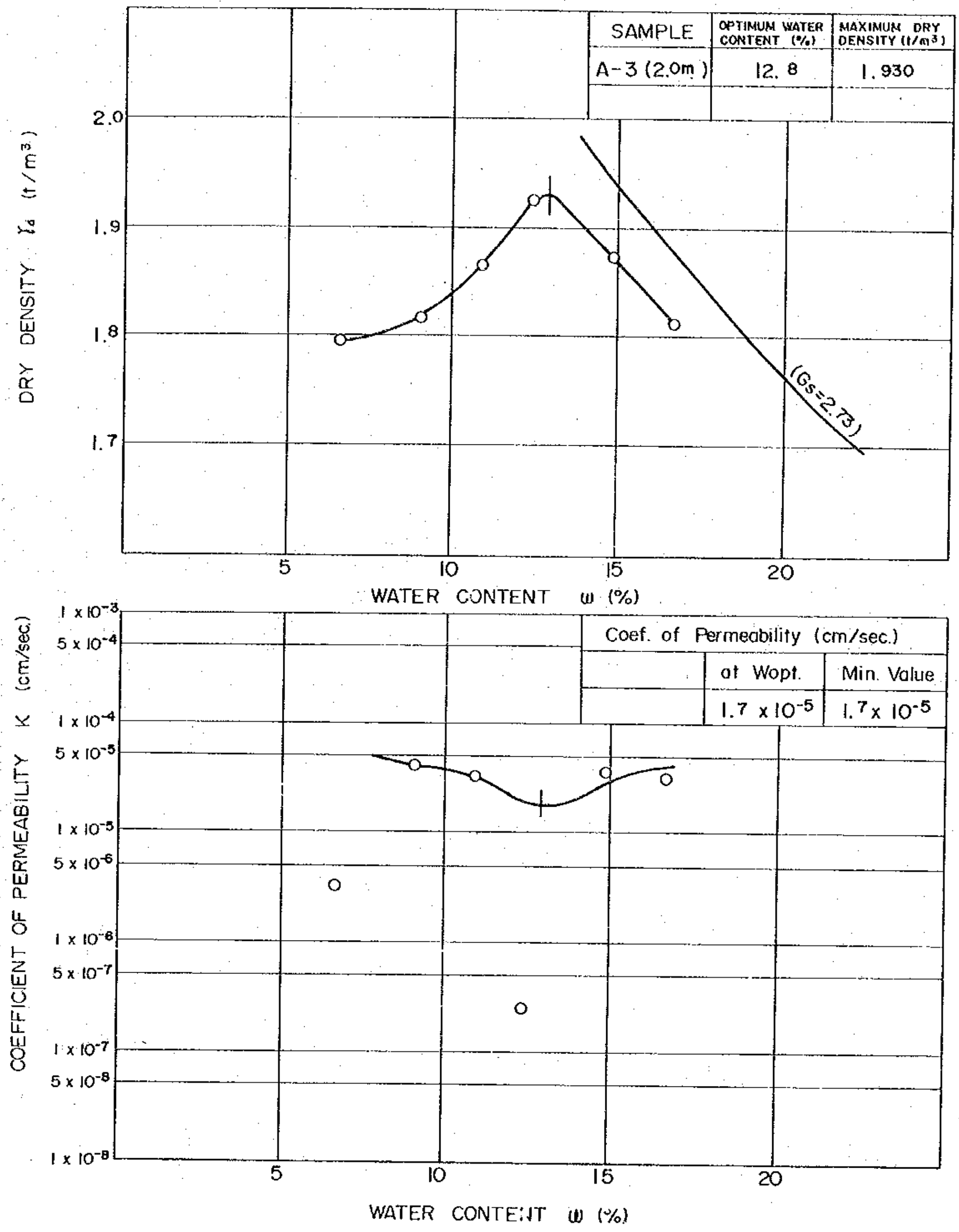

Sample A-3 2.00m

Fig.2-6 Compaction and Permeability Test

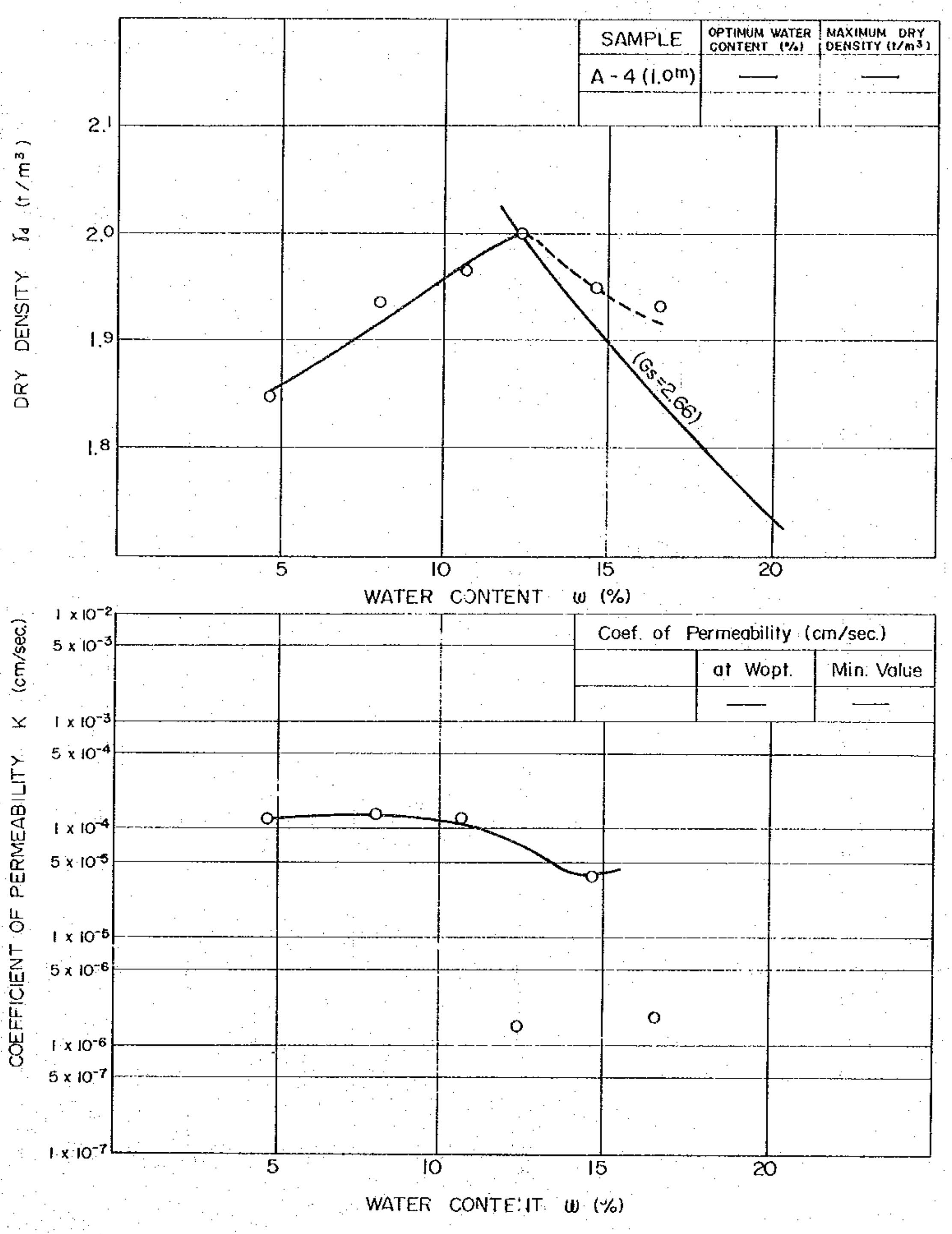

Sample A-4 1.00m

Fig.2-7 Compaction and Permeability Test

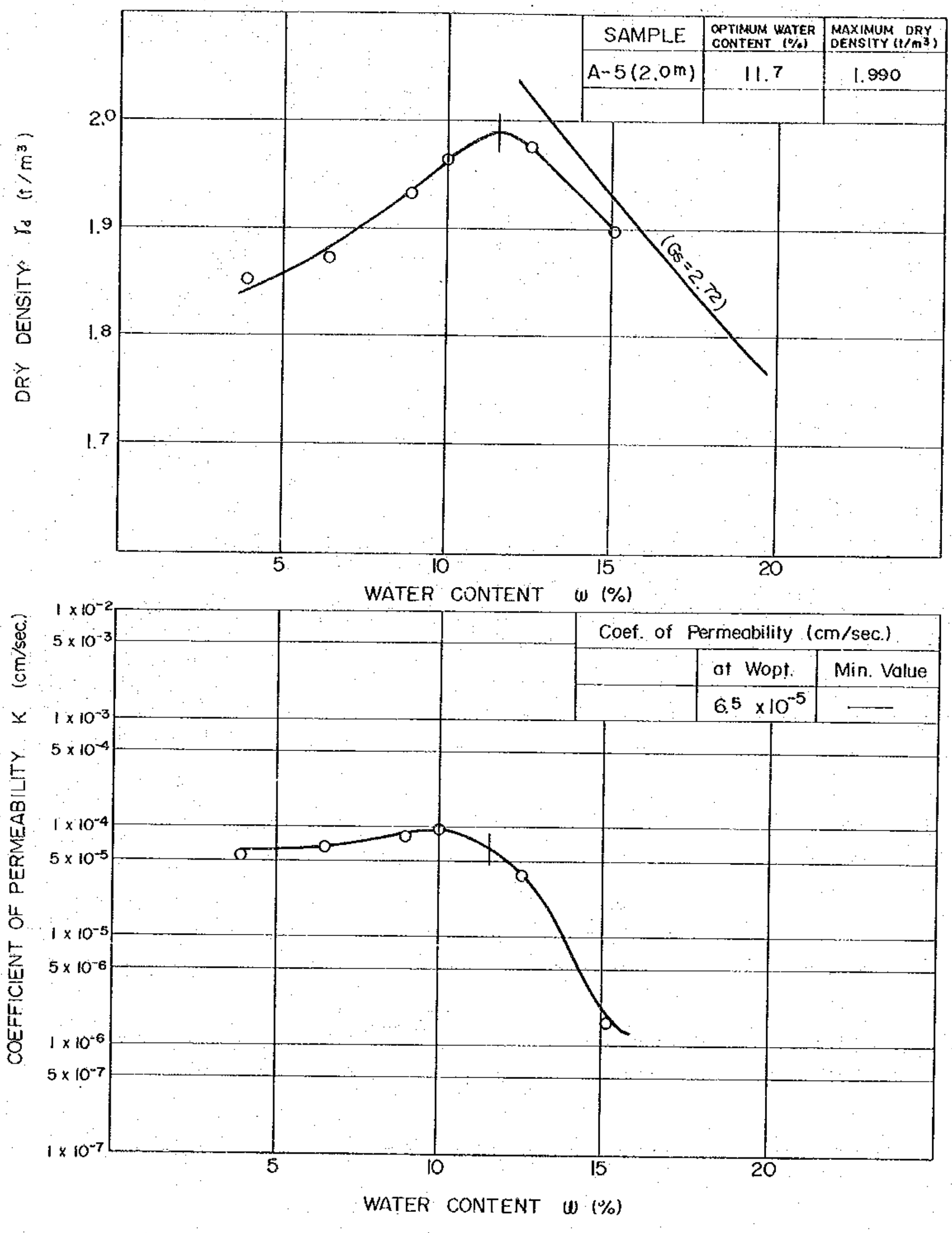

Sample A - 5 2.00m

Fig. 2-8 Compaction and Permeability Test

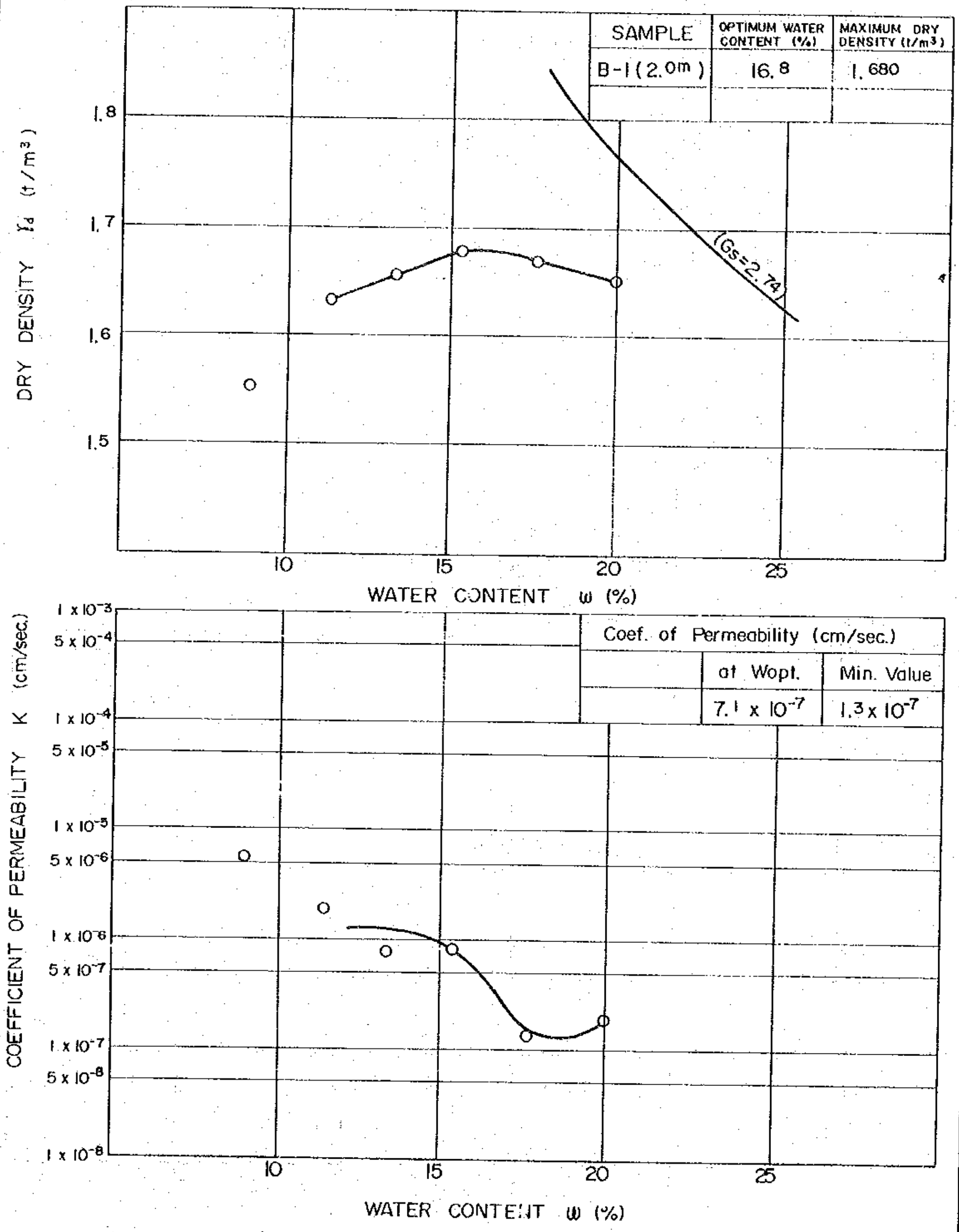

Sample B-1 2.00m

Fig.2-9 Compaction and Permeability Test

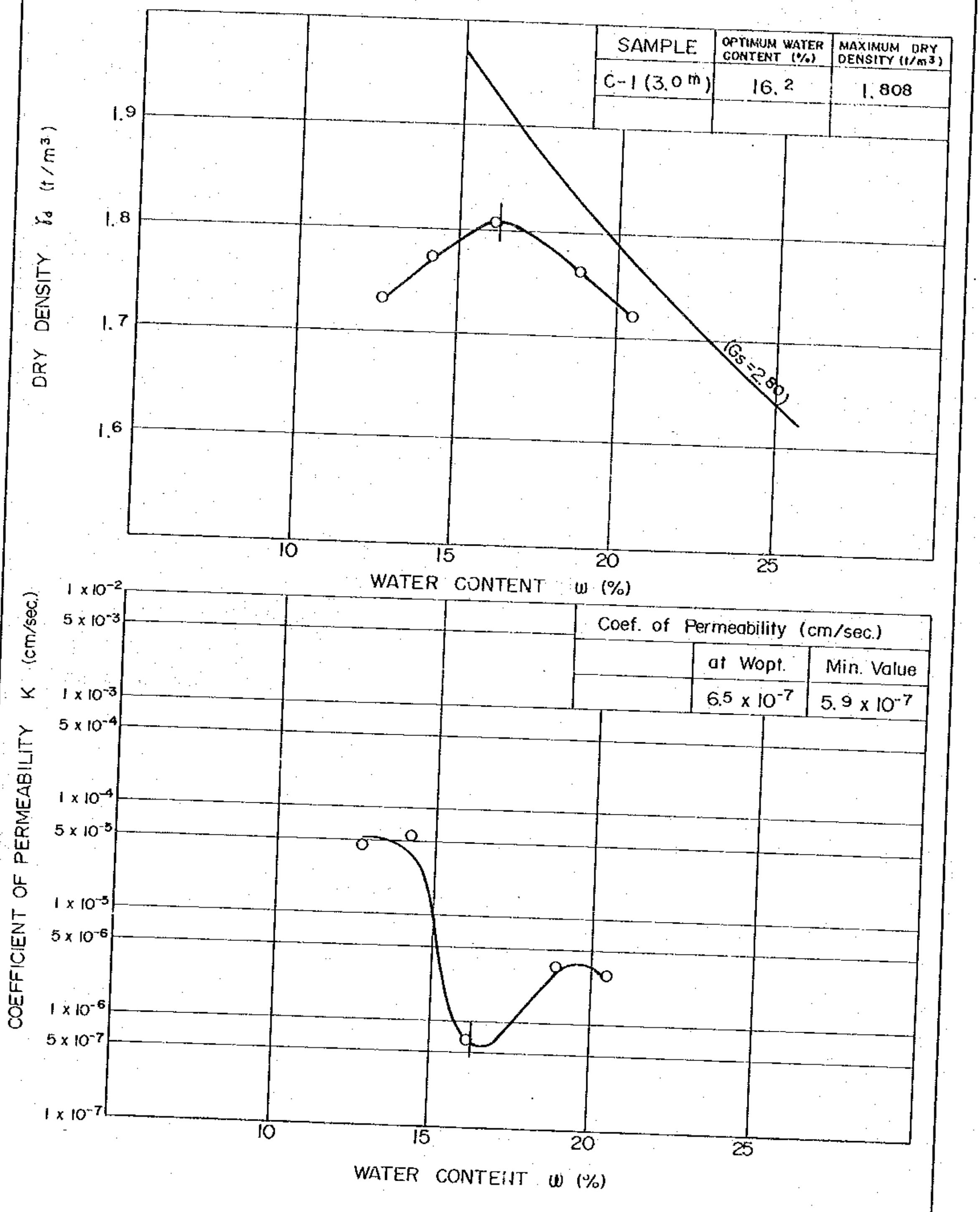

Sample C-1 3.00m

Fig. 2-10 Compaction and Permeability Test

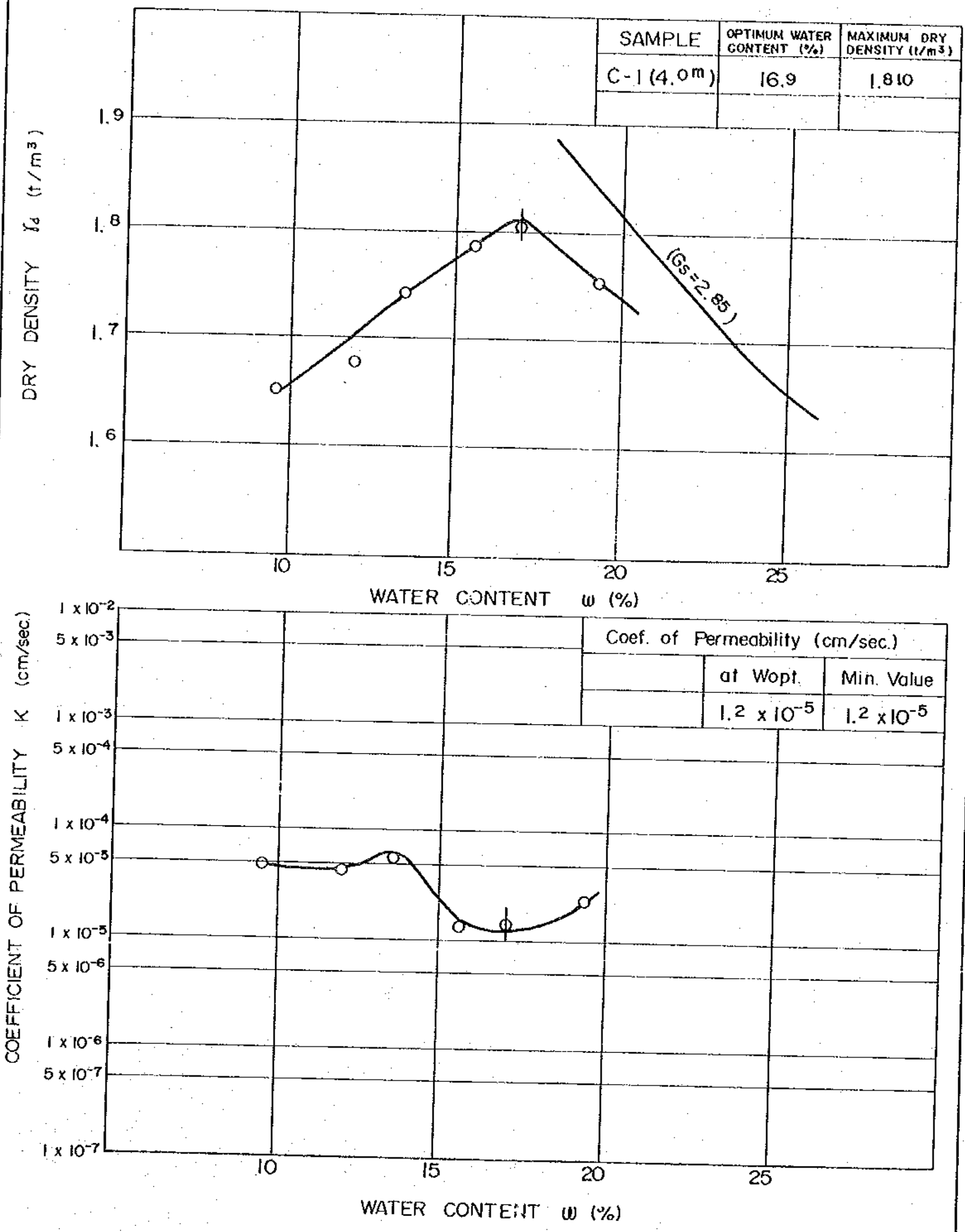

Sample C-1 4.00m

Fig.2-11 Compaction and Permeability Test

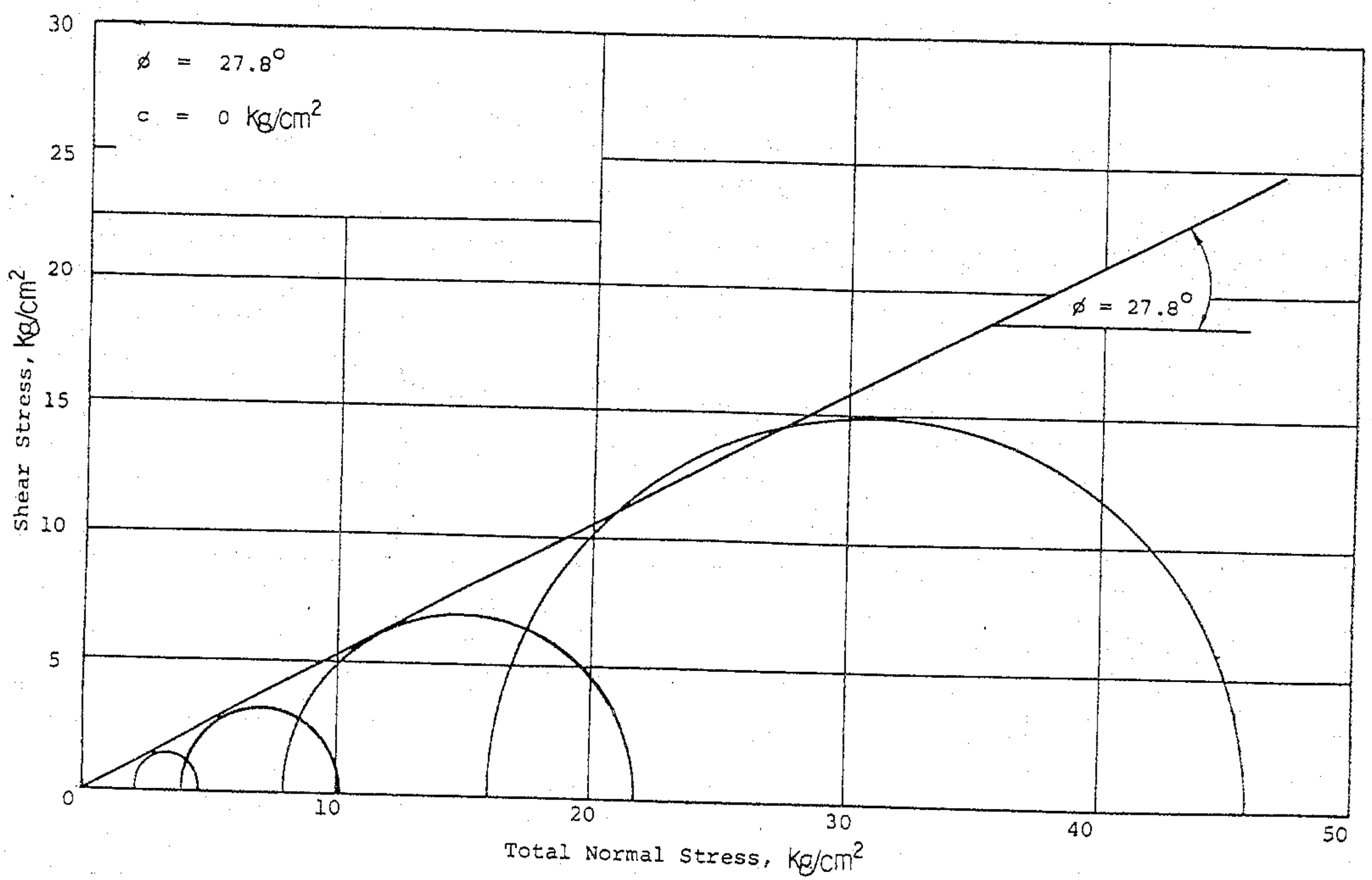

Fig. 3-1 Mohr Envelope in Terms of Total Stresses for $\overline{CU}$ Triaxial Tests on Compacted Samples No. A-1, Depth 1.00 m.

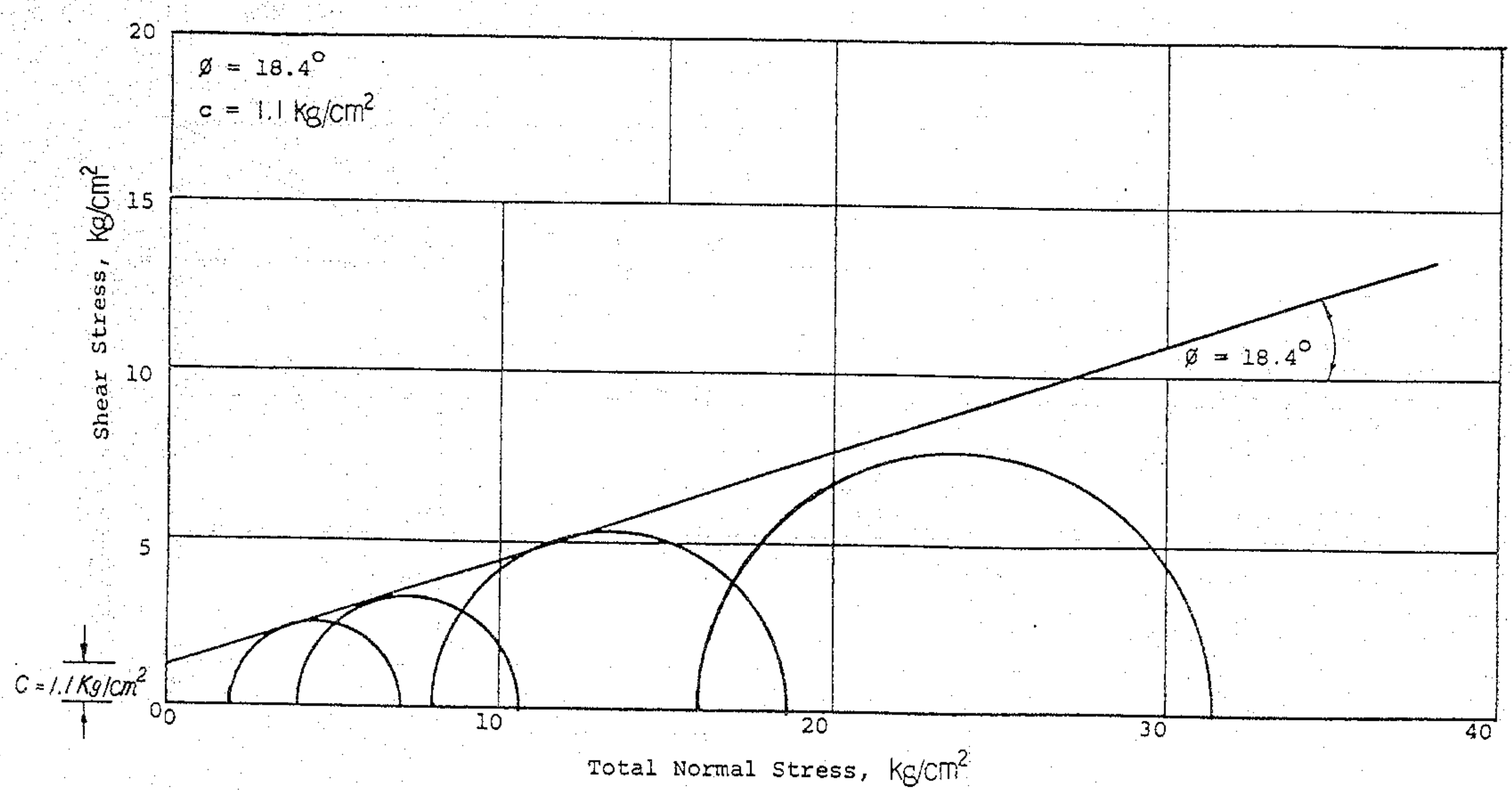

Fig. 3-2 Mohr Envelope in Teams of Total Stresses for $\overline{CU}$ Triaxial Tests on Compacted Sample No. A-2, Depth 3.00 m.

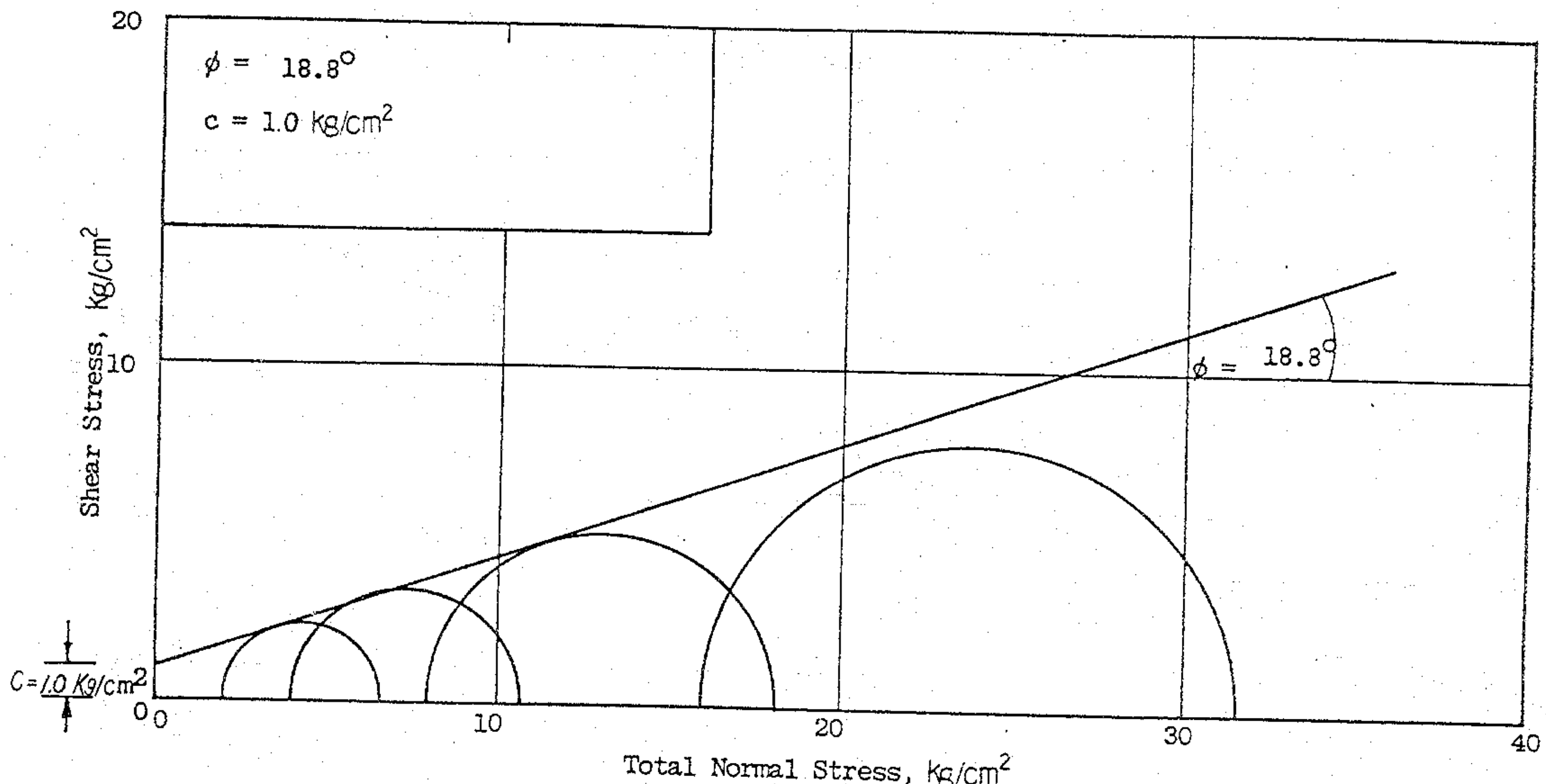

Fig. 3-3 Mohr Envelope in Terms of Total Stresses for $\overline{CU}$ Triaxial Tests on Sample No. A-2, Depth 5.00 m.

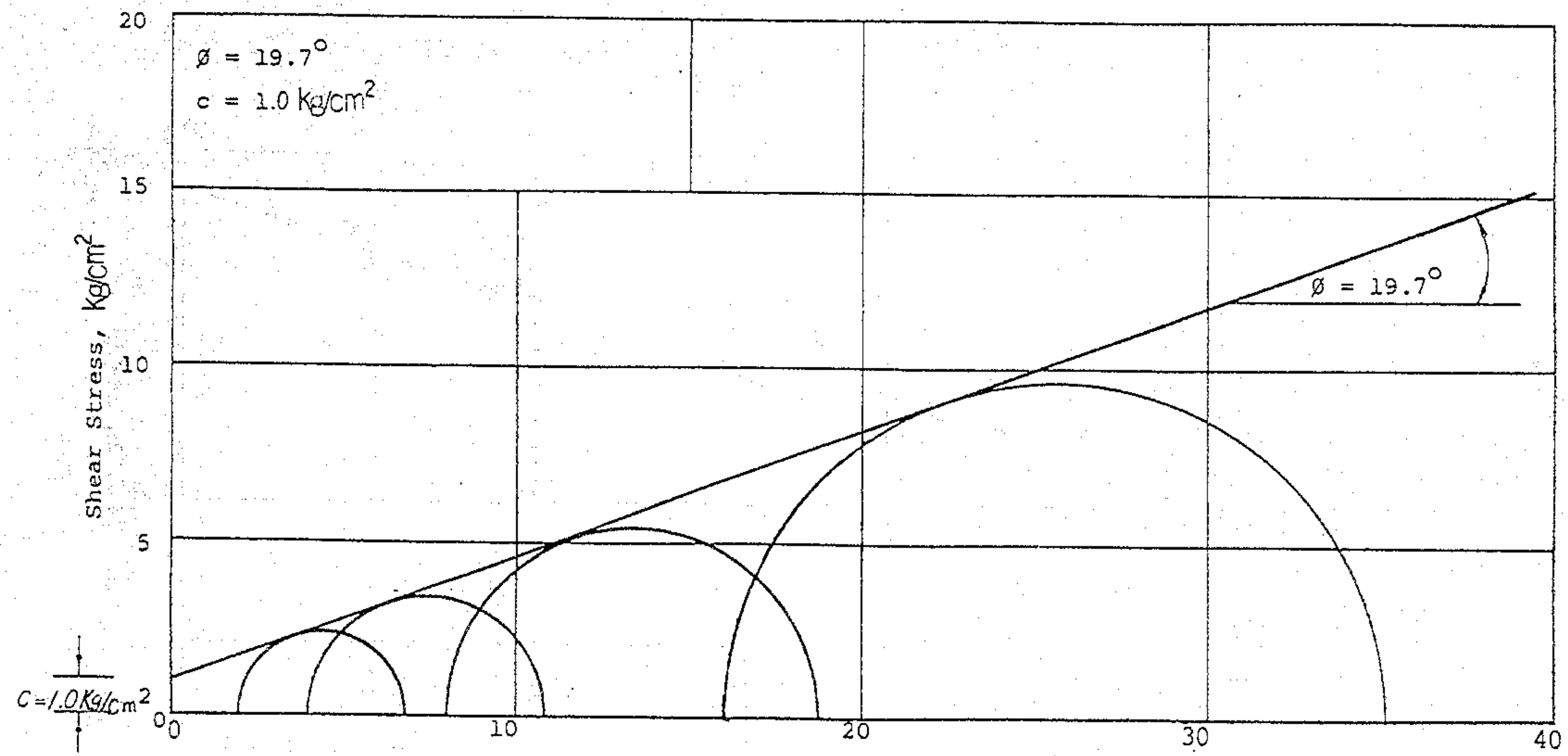

Fig.3-4 Mohr Envelope in Terms of Total Stresses for $\overline{C}\overline{U}$ Triaxial Tests on Compacted Sample No. A-3, Depth 2.00 m.

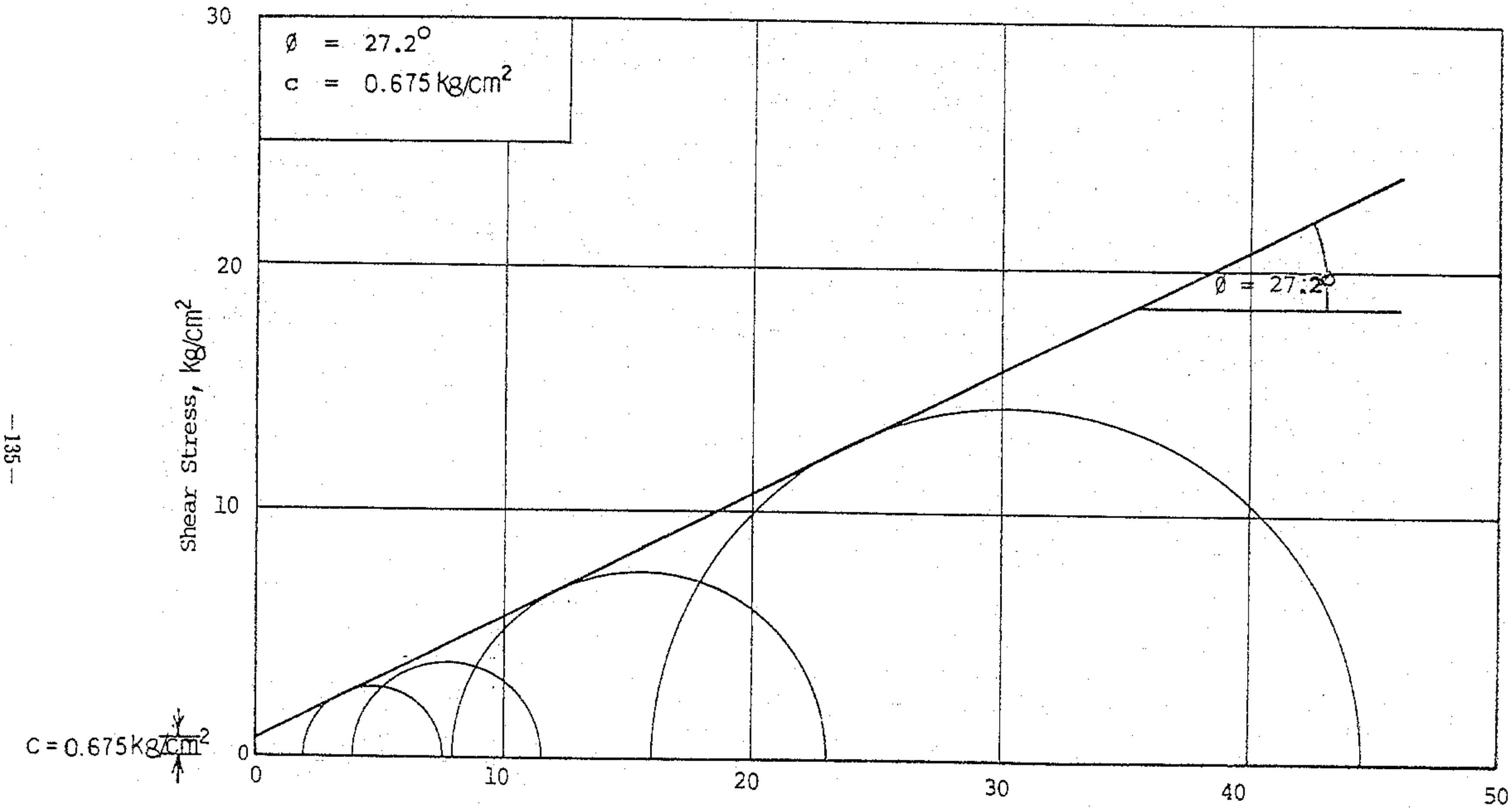

Fig. 3-5 Mohr Envelope in Terms of Total Stresses for $\overline{CU}$ Triaxial Tests on Sample No. A-5, Depth 2.00 m.

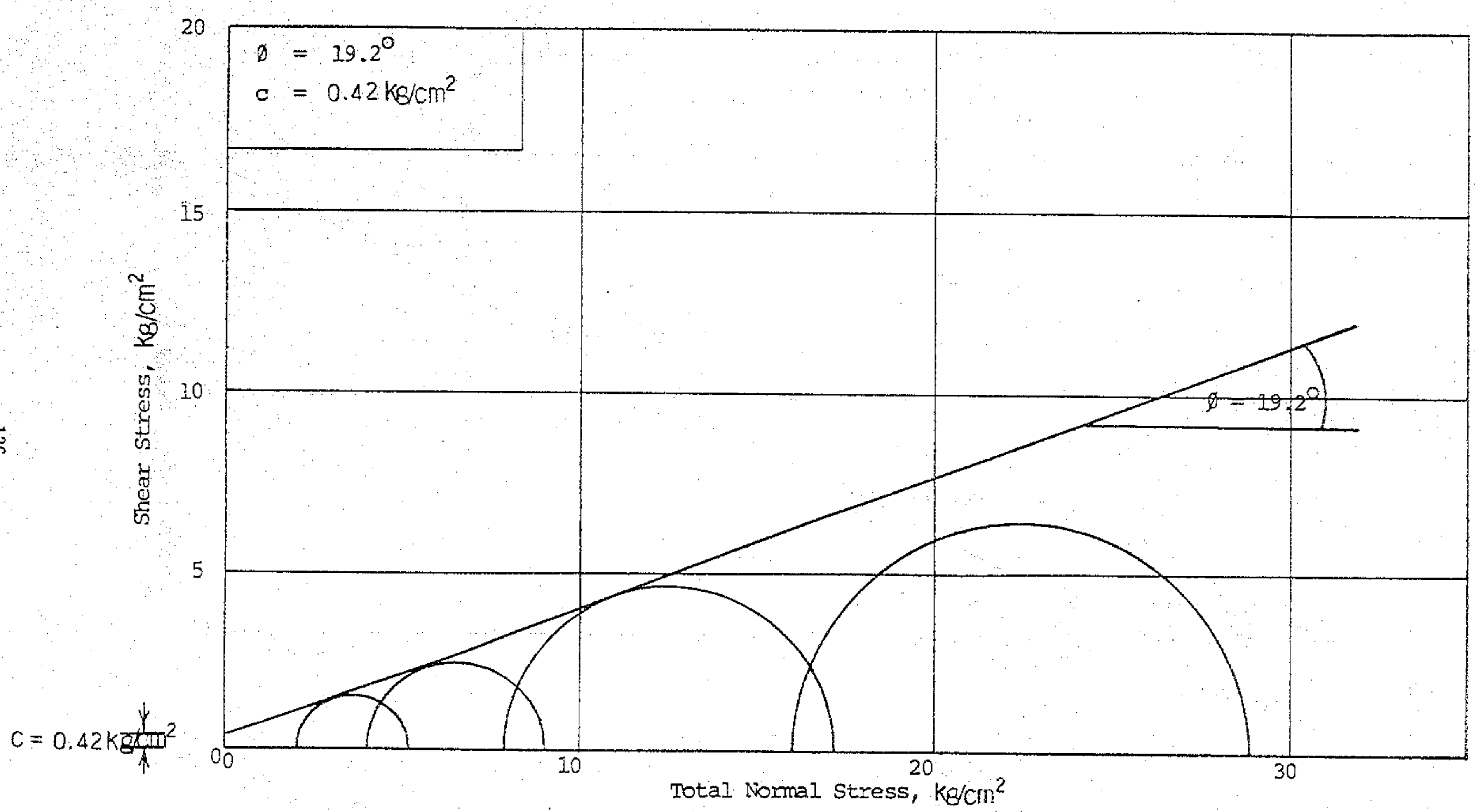

Fig. 3－6 Mohr Envelope in Terms of Total Stresses for $\overline{CU}$ Triaxial Tests on Compacted Sample No. B-1, Depth 2.00 m.

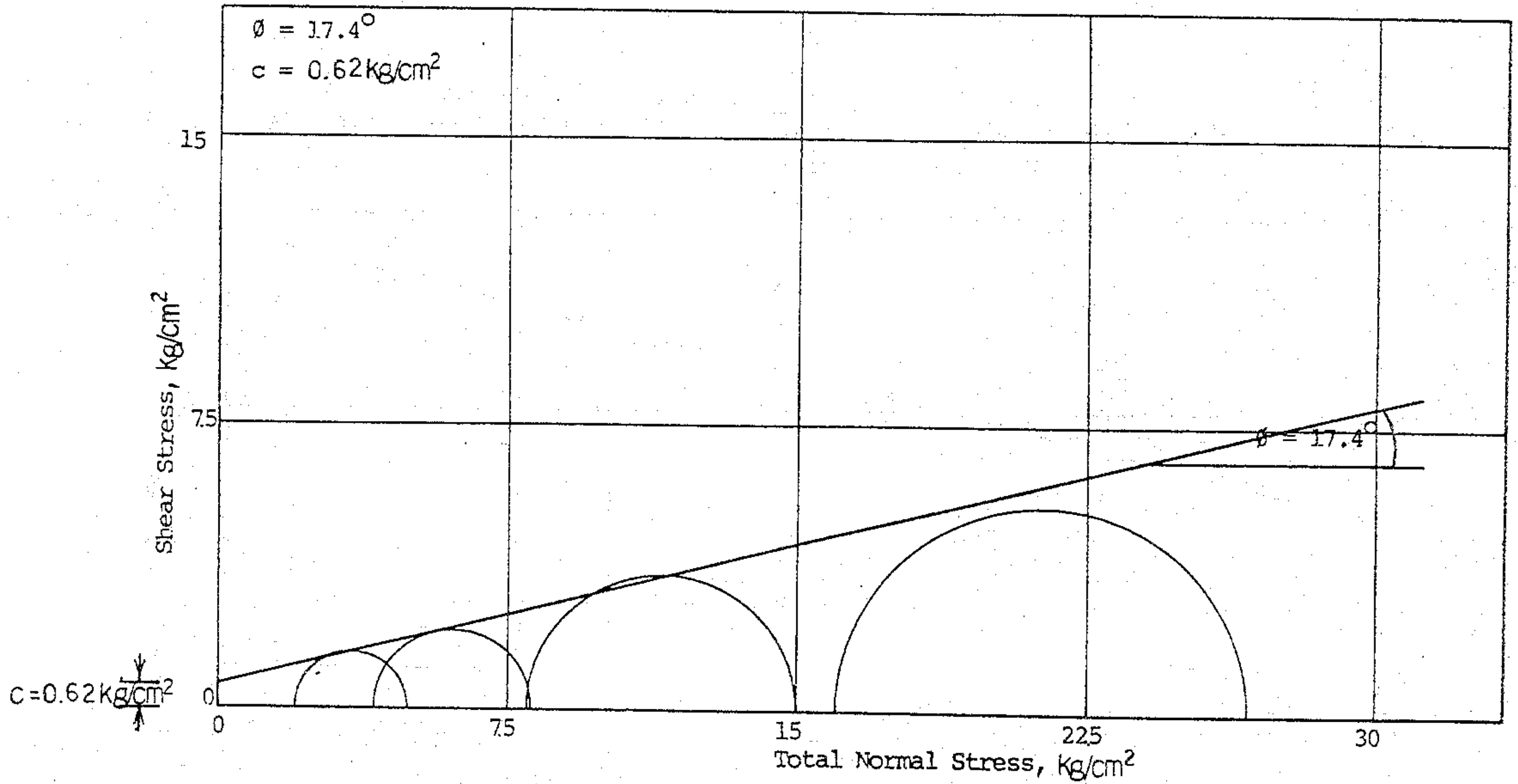

Fig. 3-7 Mohr Envelope in Terms of Total Stresses for $\overline{CU}$ Triaxial Tests on Sample No. C-1, Depth 3.00 m.

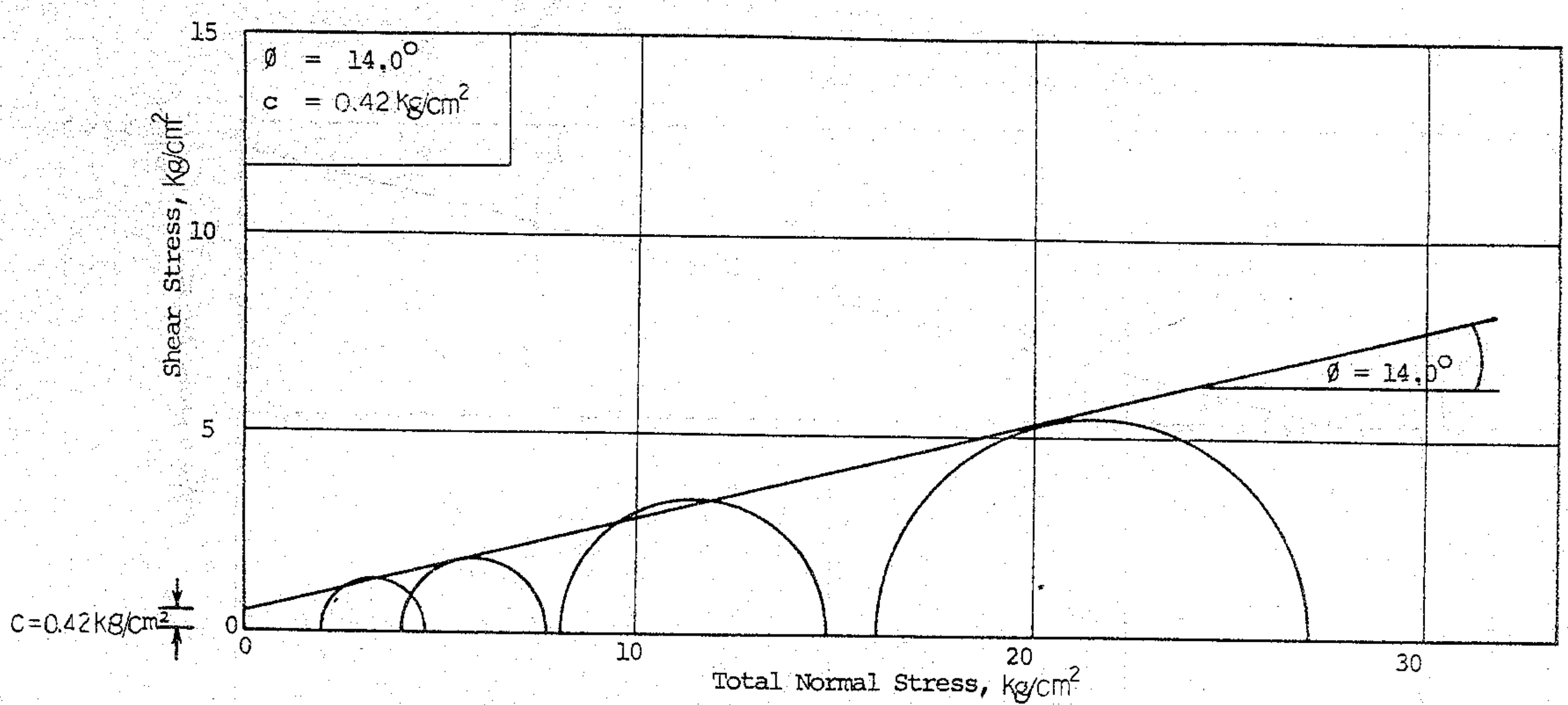

Fig. 3-8 Mohr Envelope in Terms of Total Stress for $\overline{CU}$ Triaxial Tests on Compacted Sample No. C-1, Depth 4.00 m.

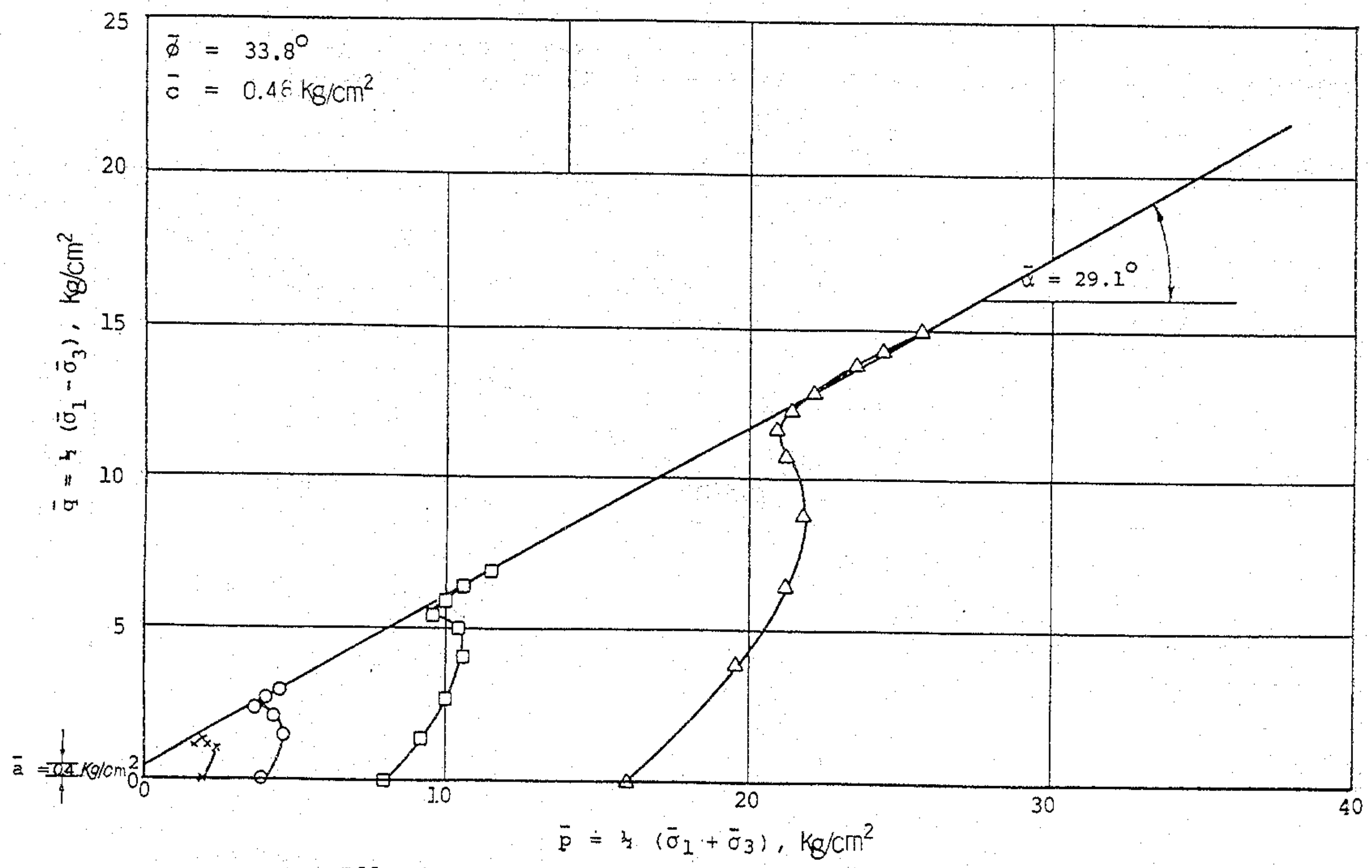

Fig. 4-1 Effective Stress Paths and Strength Envelope for $\overline{CU}$ Triaxial Tests on Compacted Sample No. A-1, Depth 1.00 m.

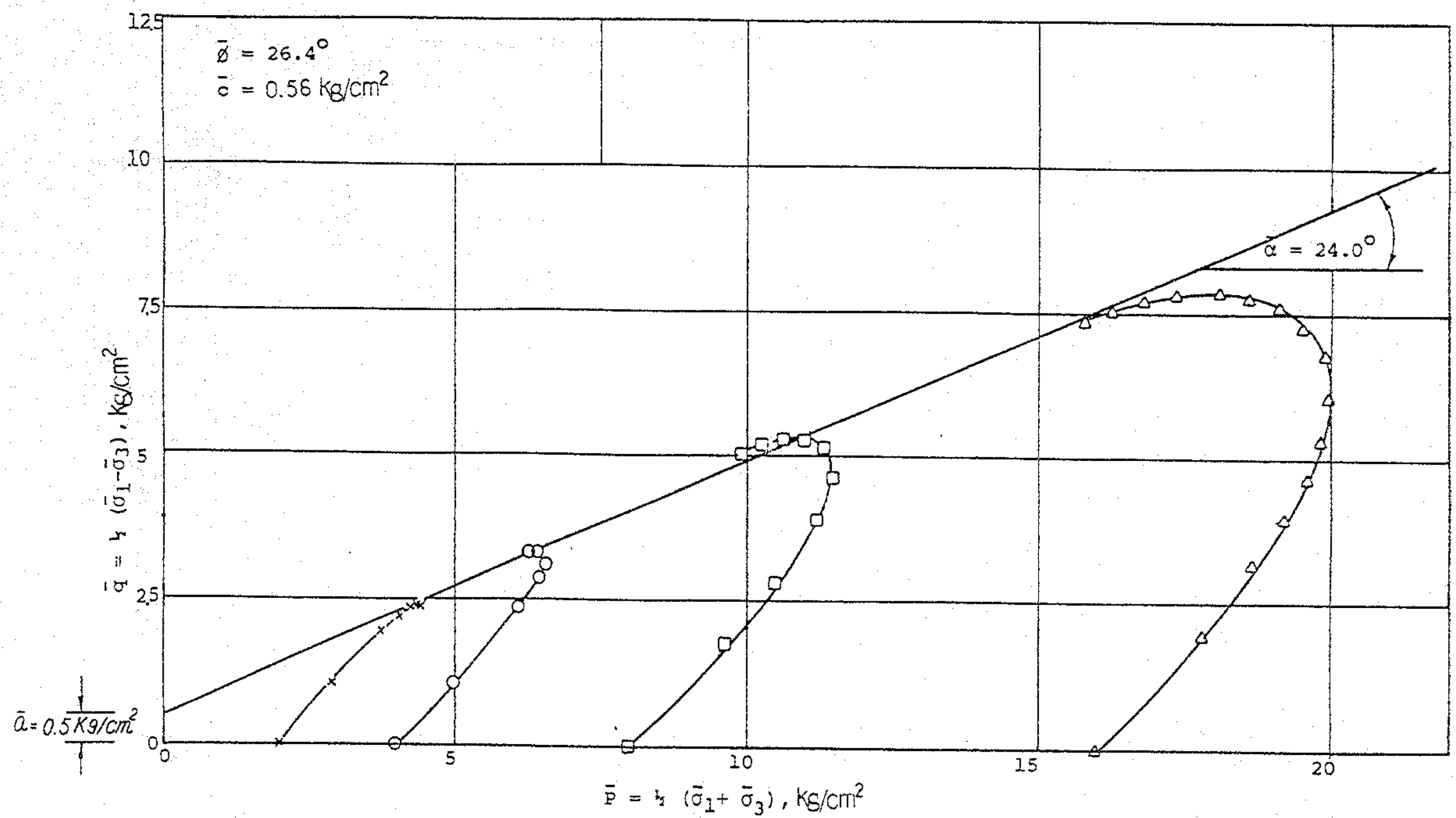

Fig. 4-2 Effective Stress Paths and Strength Envelope for $\overline{CU}$ Triaxial Tests on Compacted Sample No. A-2, Depth 3.00 m.

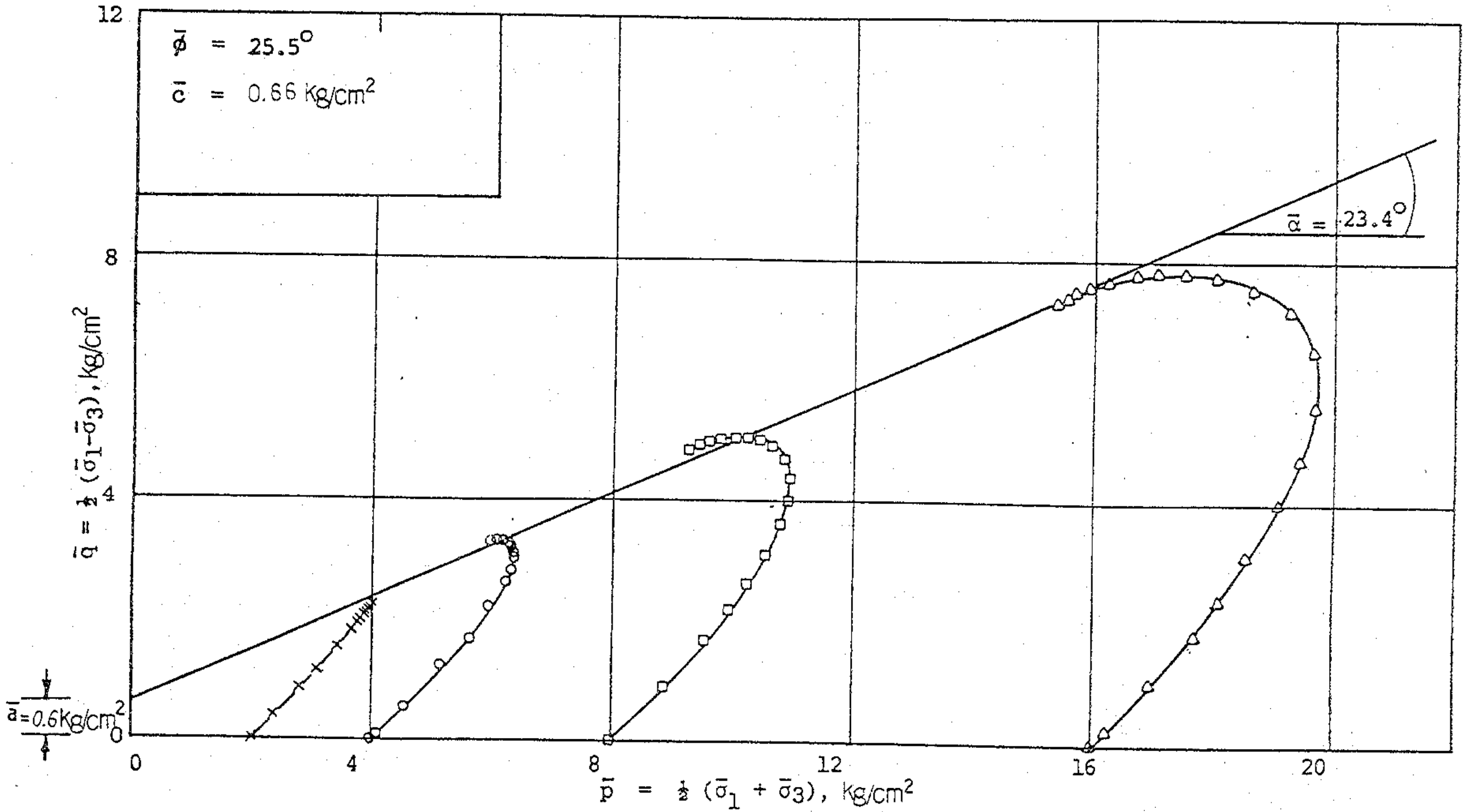

Fig. 4-3 Effective Stress Paths and Strength Envelope for $\overline{CU}$ Triaxial Tests on Sample No. A-2, Depth 5.00 m.

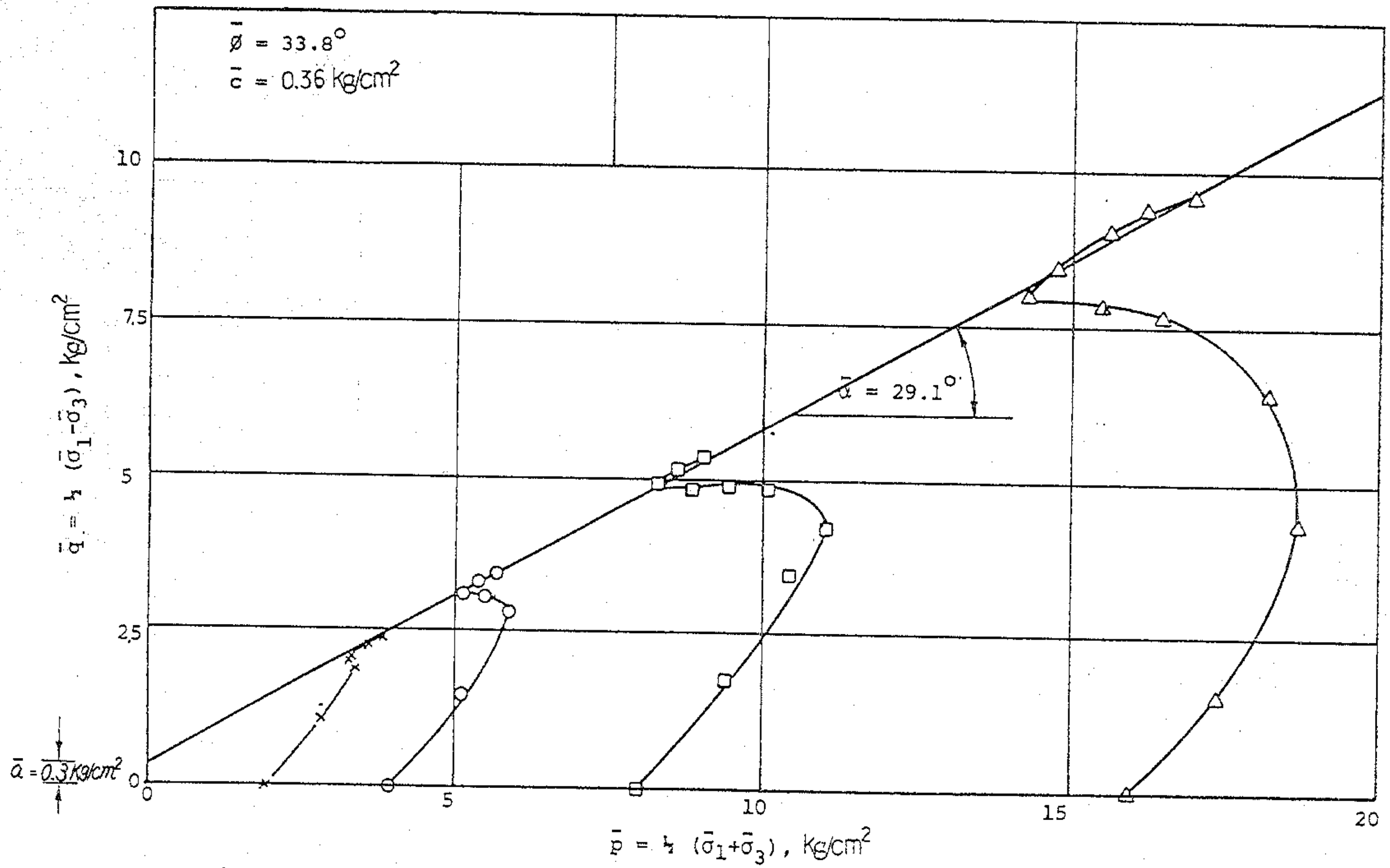

Fig. 4-4 Effective Stress Paths and Strength Envelope for $\overline{CU}$ Triaxial Tests on Compacted Sample No. A-3, Depth 2.00 m.

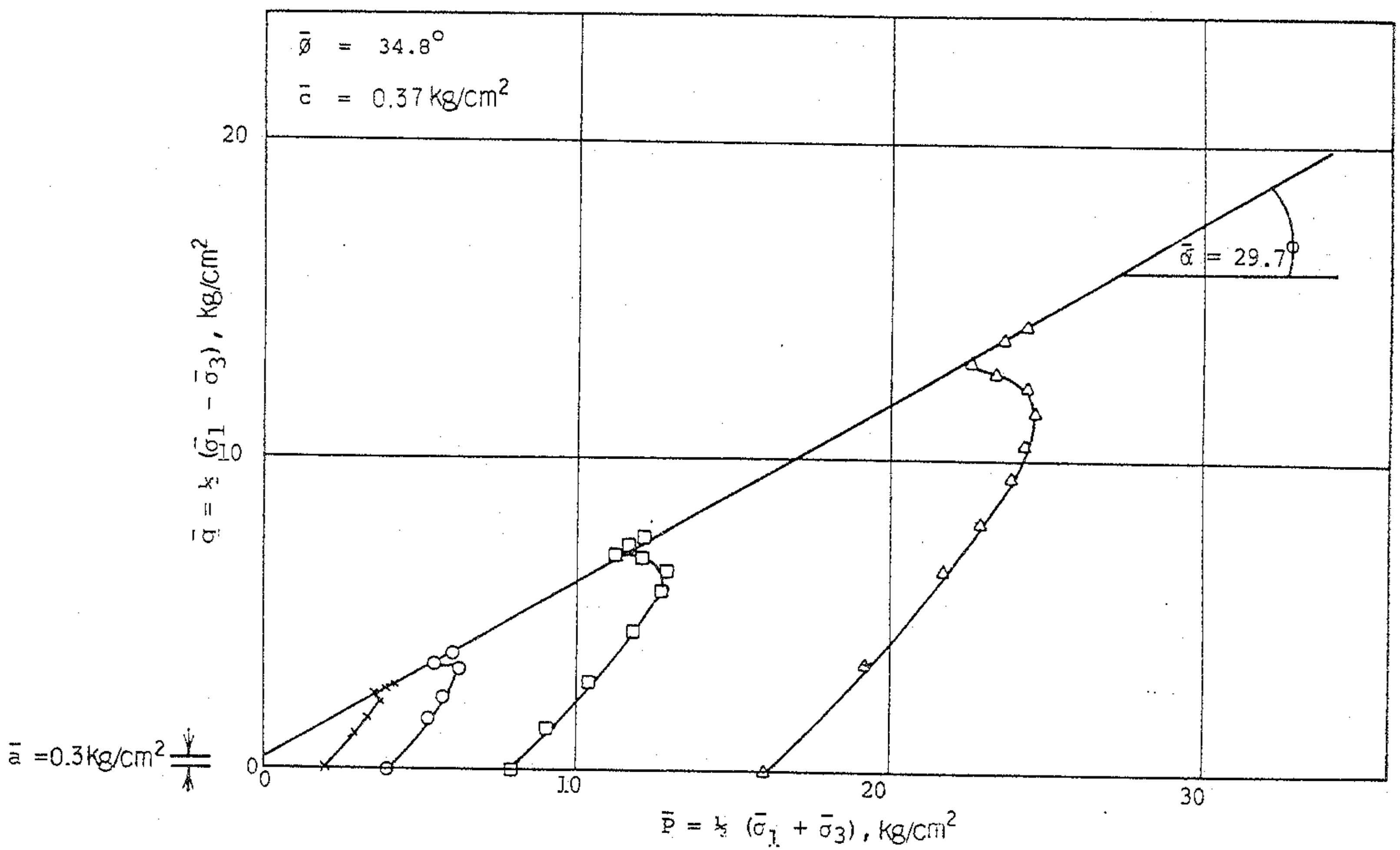

Fig. 4 - 5 Effective Stress Paths and Strength Envelope for $\overline{CU}$ Triaxial Tests on Sample No. A-5, Depth 2.00 m.

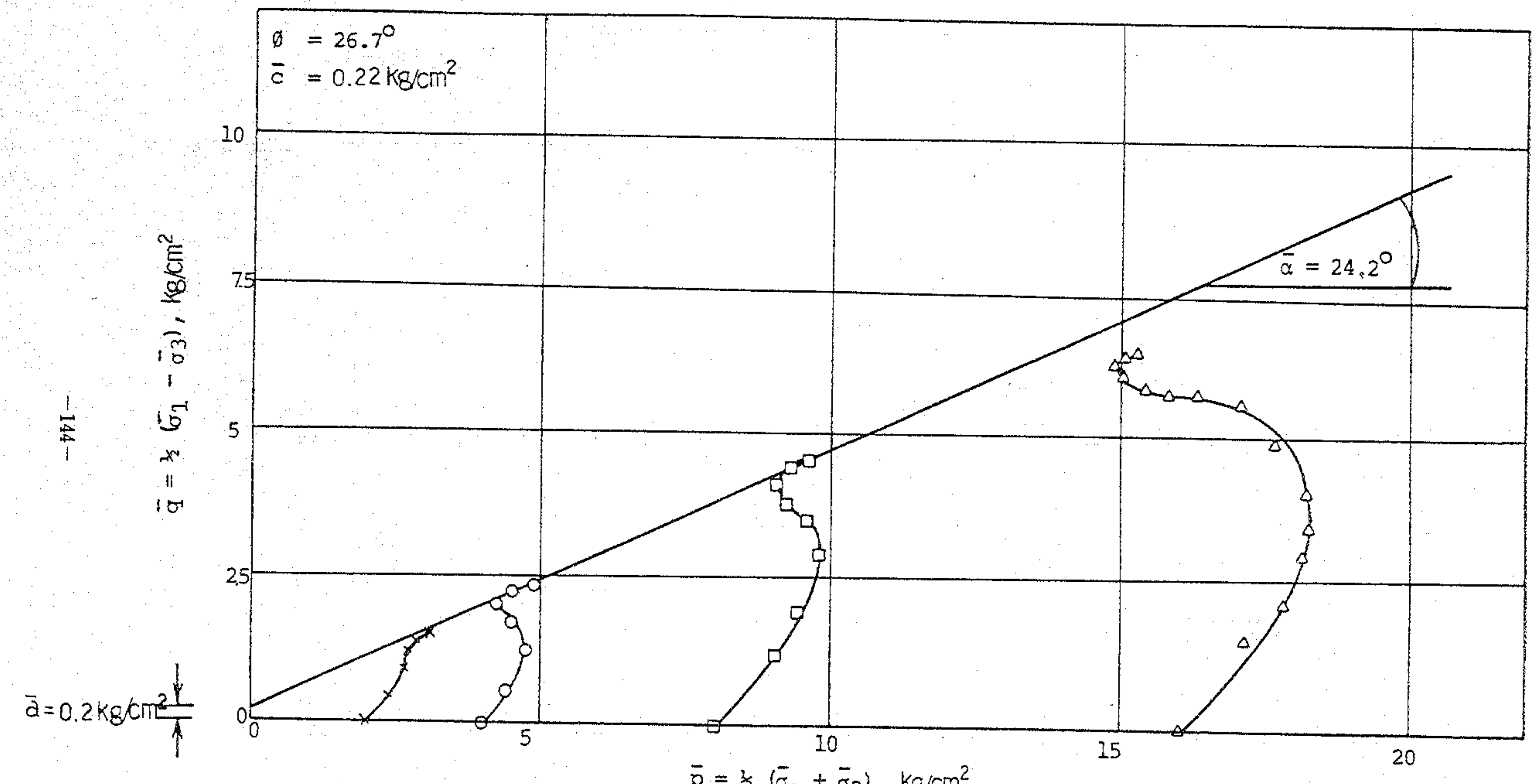

Fig. 4 - 6 Effective Stress Paths and Strength Envelope for $\overline{CU}$ Triaxial Tests on Compacted Sample No. B-1, Depth 2.00 m.

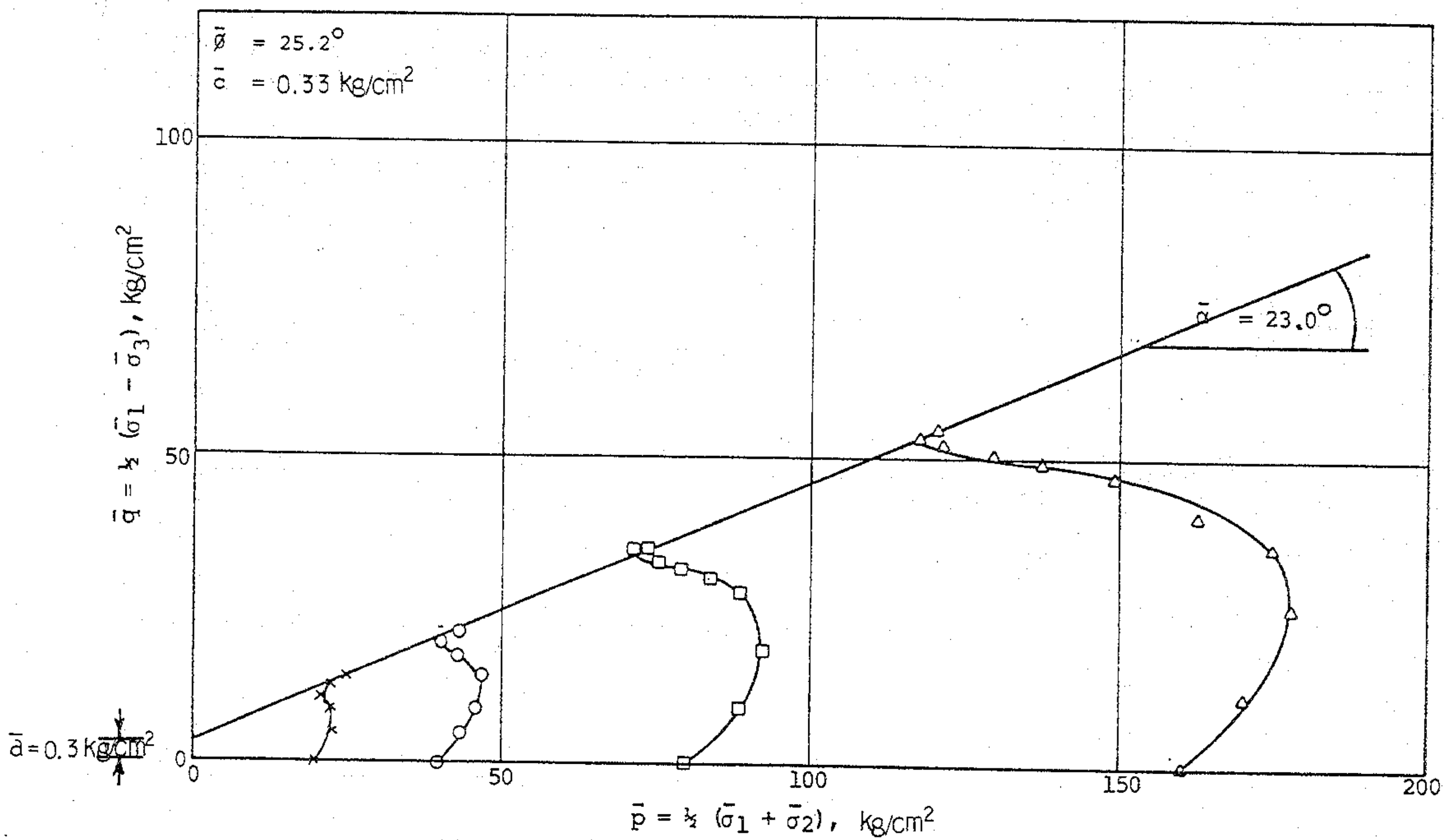

Fig. 4-7 Effective Stress Paths and Strength Envelope for $\overline{CU}$ Triaxial Tests on Sample No. C-1, Depth 3.00 m.

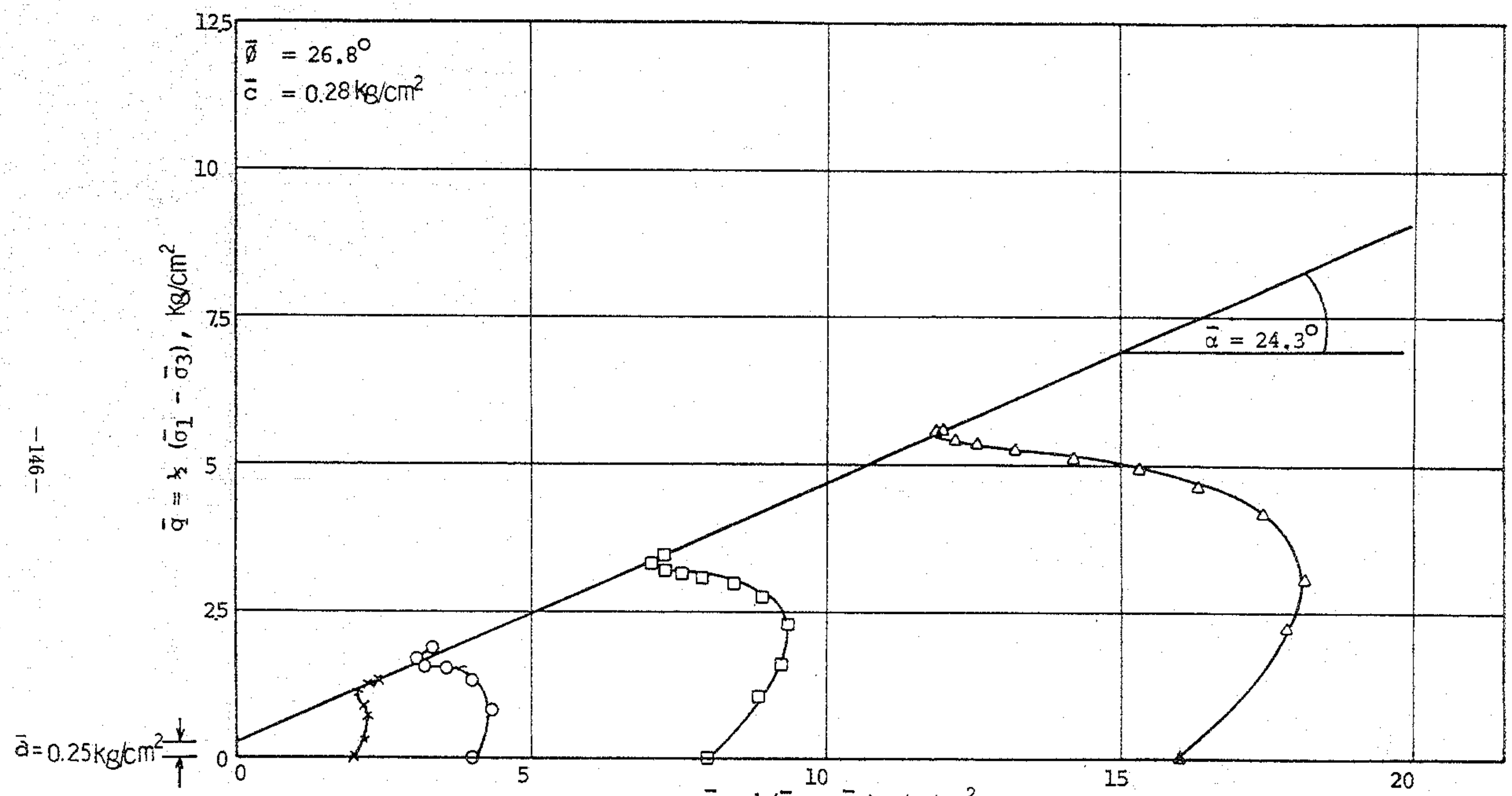

Fig. 4-8 Effective Stress Paths and Strength Envelope for $\overline{CU}$ Triaxial Tests on Compacted Sample No. C-1, Depth 4.00 m.

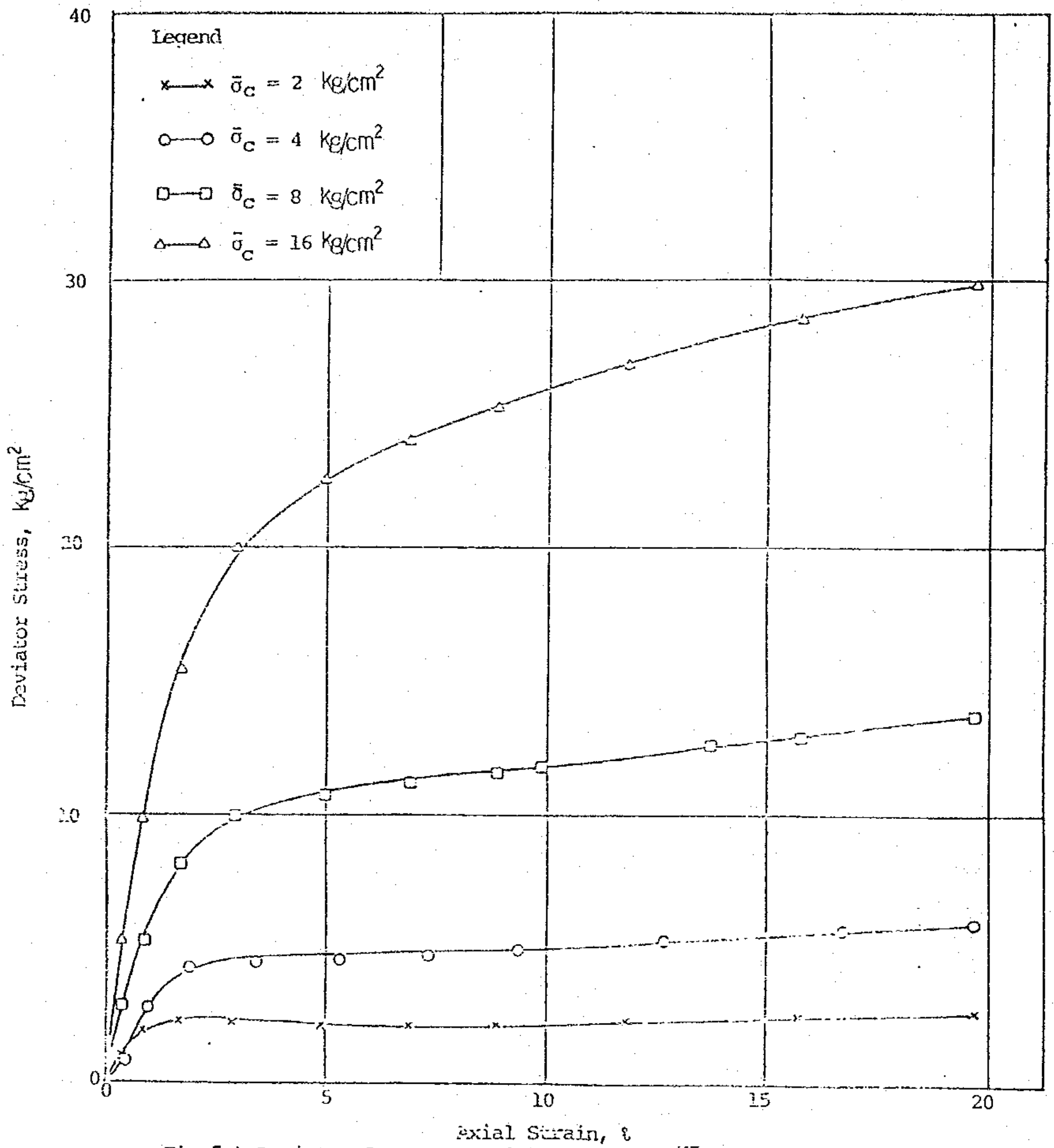

Fig.5-1 Deviator Stress vs Axial Strain for $\bar{C}\bar{U}$ Triaxial Tests on Compacted Sample No. A-1, Depth 1.00 m.

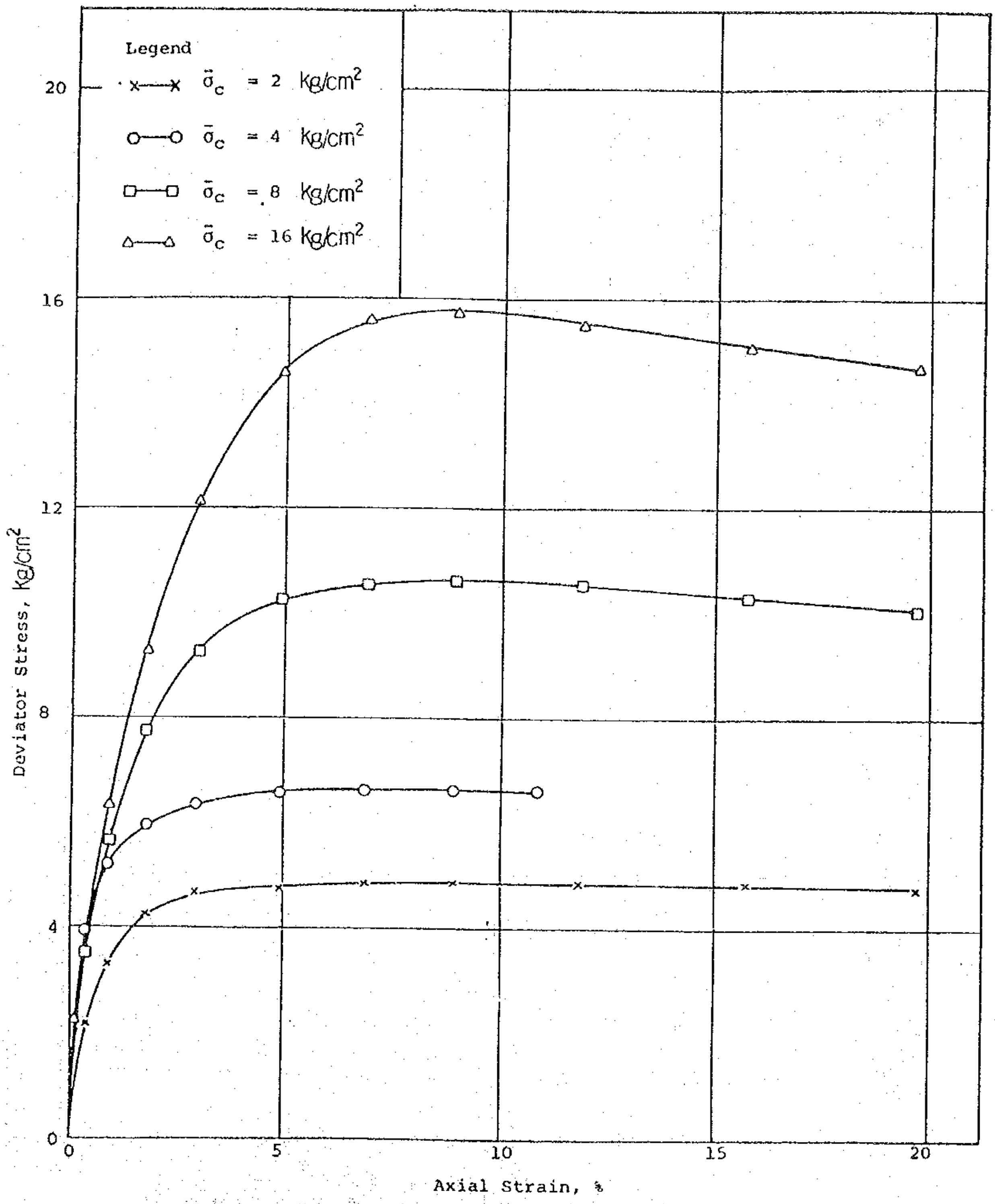

Fig. 5-2 Deviator Stress vs Axial Strain for $\overline{CU}$ Triaxial Tests on Compacted Sample No. A-2, Depth 3.00 m.

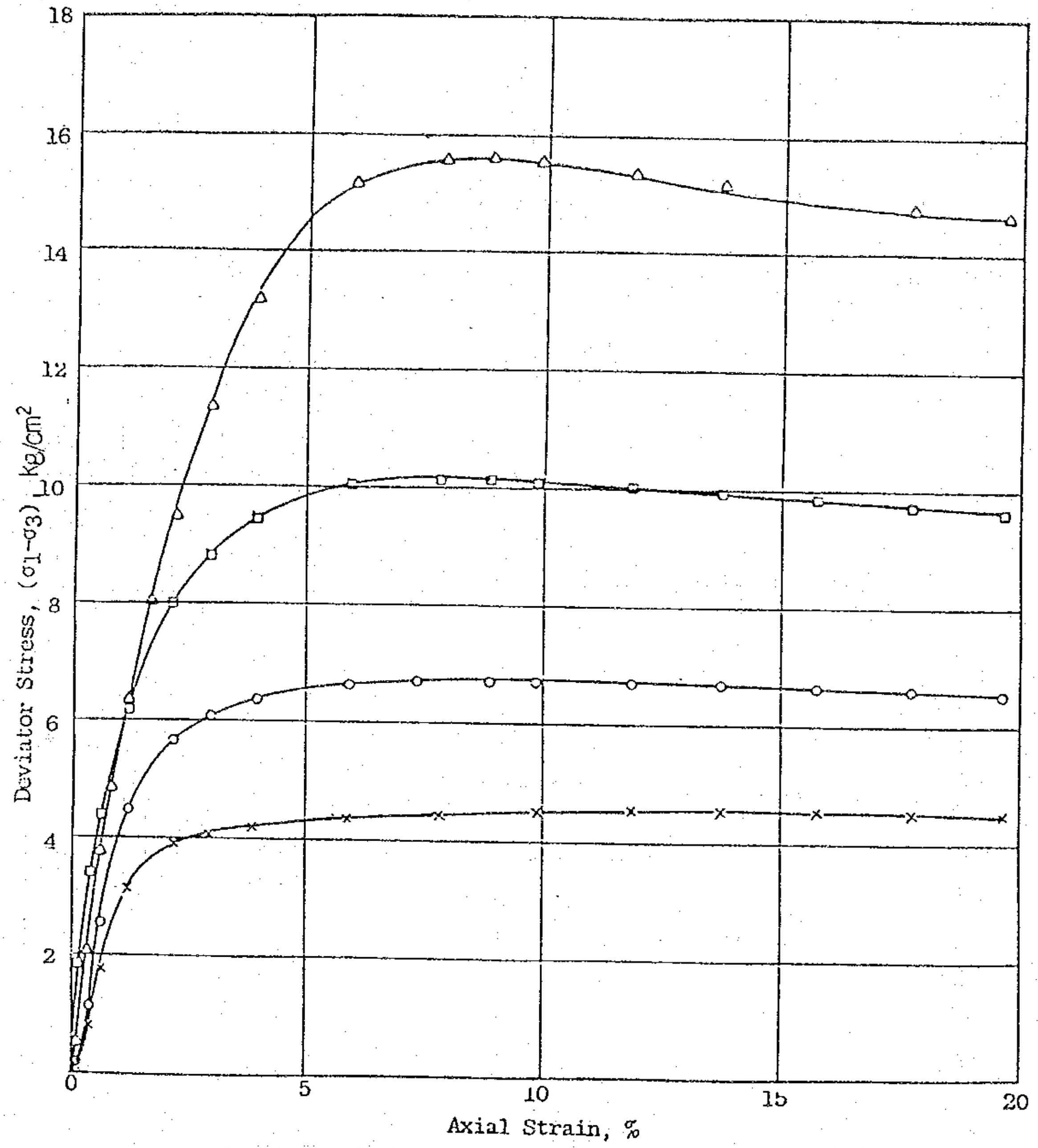

Fig. 5-3 Deviator Stress vs Axial Strain for $\overline{CU}$ Triaxial Tests on Compacted Sample No. A-2, Depth 5.00 m.

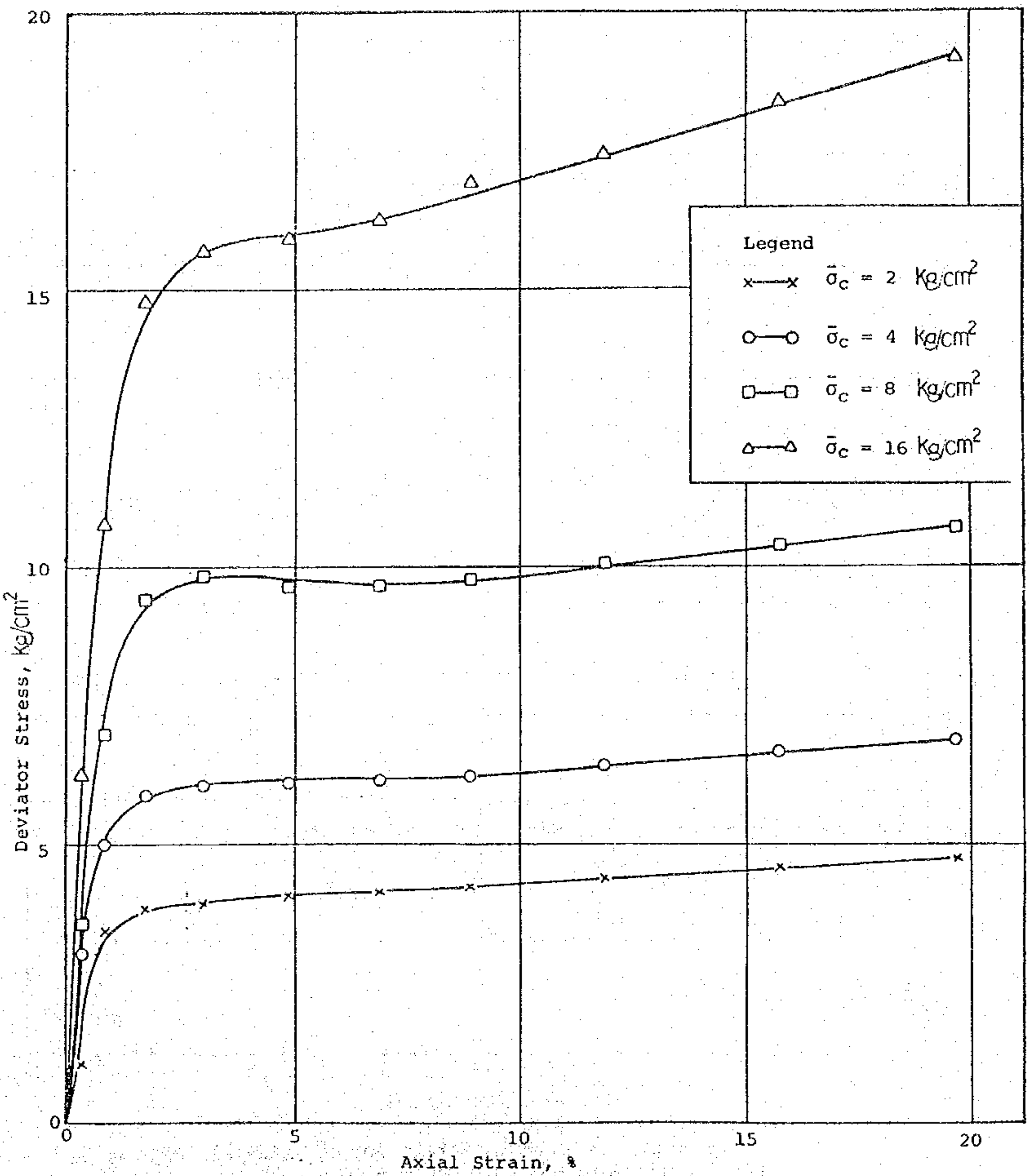

Fig. 5-4 Deviator Stress VS Axial Strain for $\bar{CU}$ Triaxial Tests on Compacted Sample No. A-3, Depth 2.00 m.

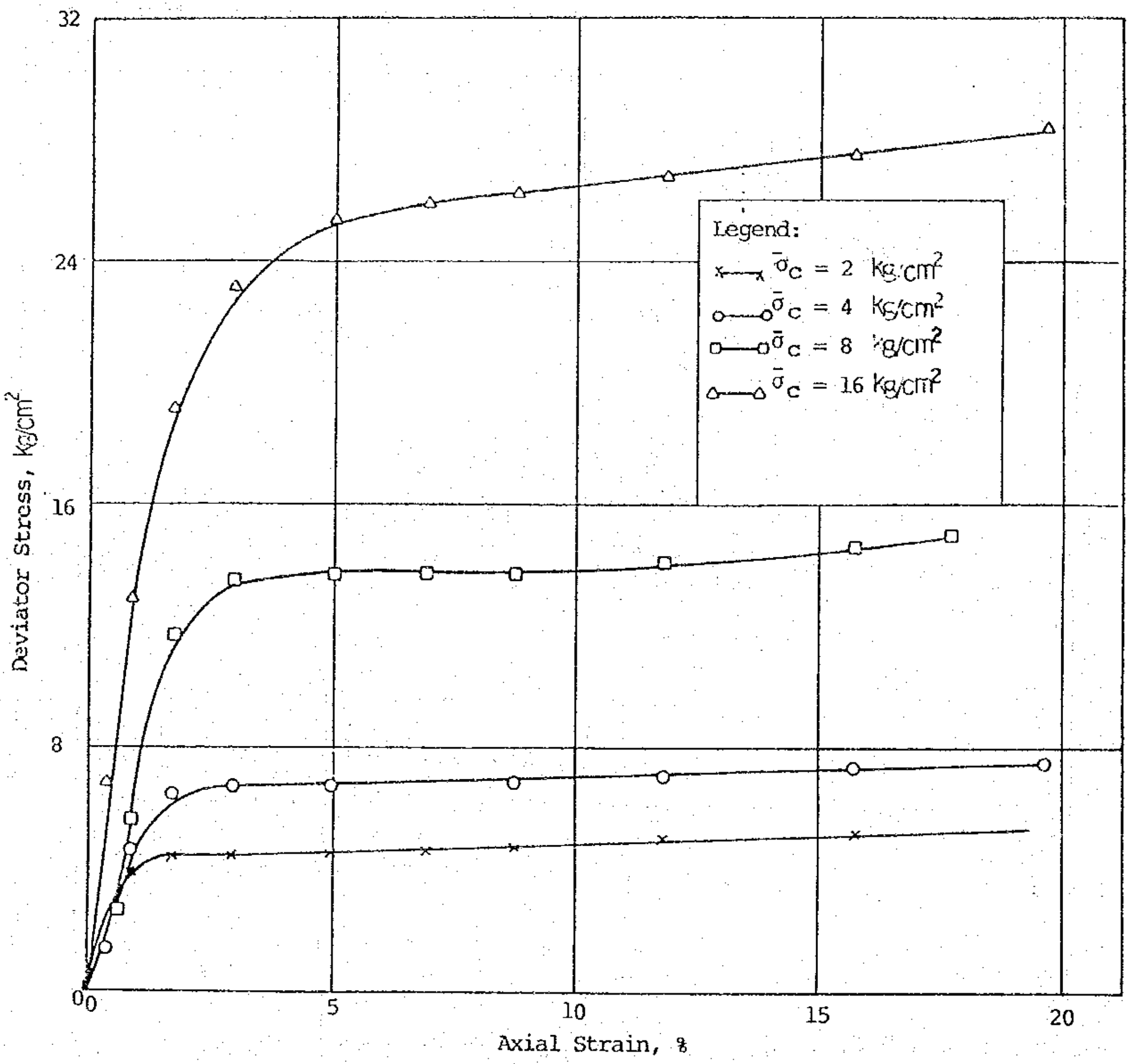

Fig. 5-5 Deviator Stress vs Axial Strain for $\overline{CU}$ Triaxial Tests on Sample No. A-5, Depth 2.00 m.

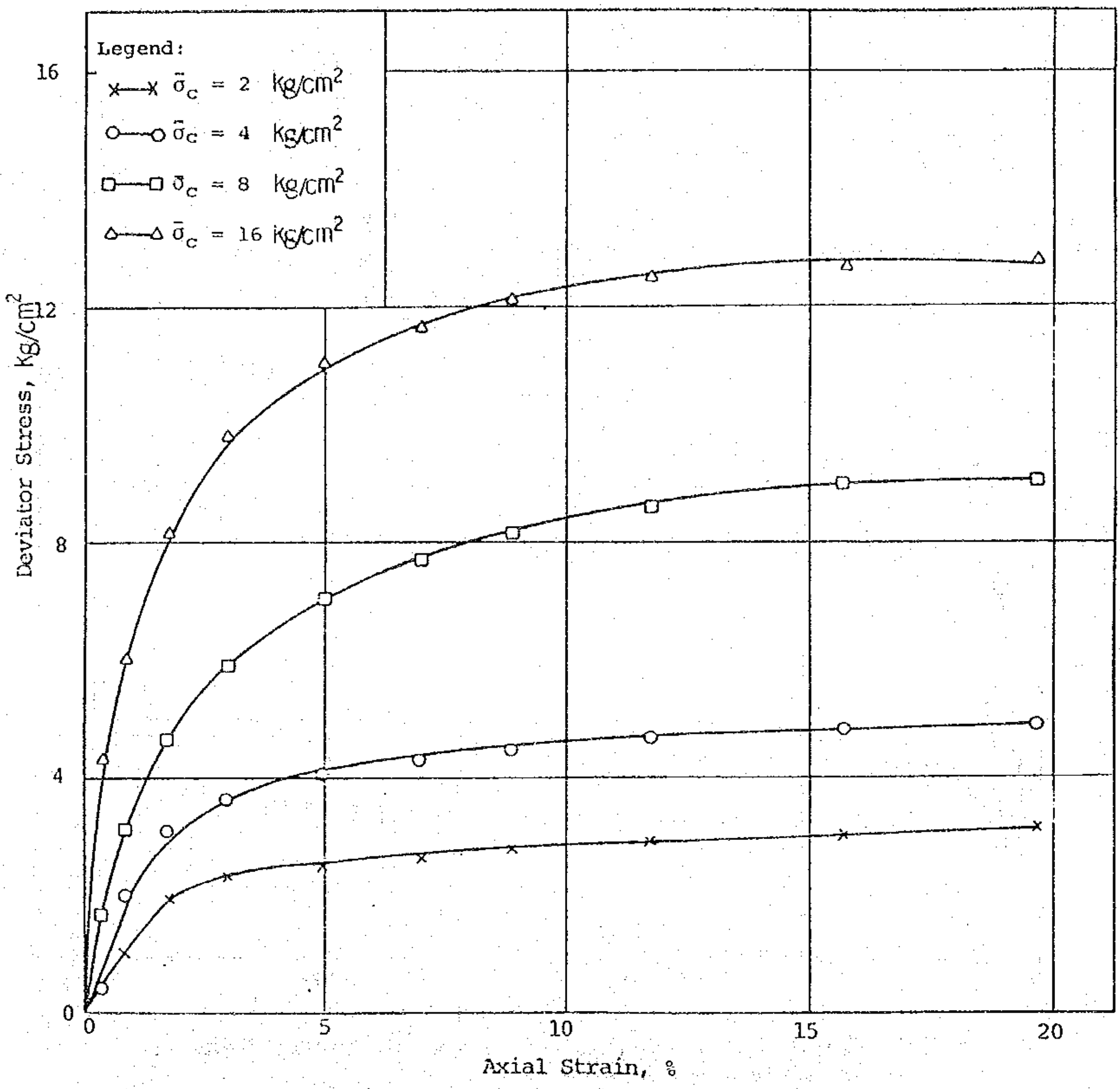

Fig. 5-6 Deviator Stress vs Axial Strain for $\overline{CU}$ Triaxial Tests on Compacted Sample No. B-1, Depth 2.00 m.

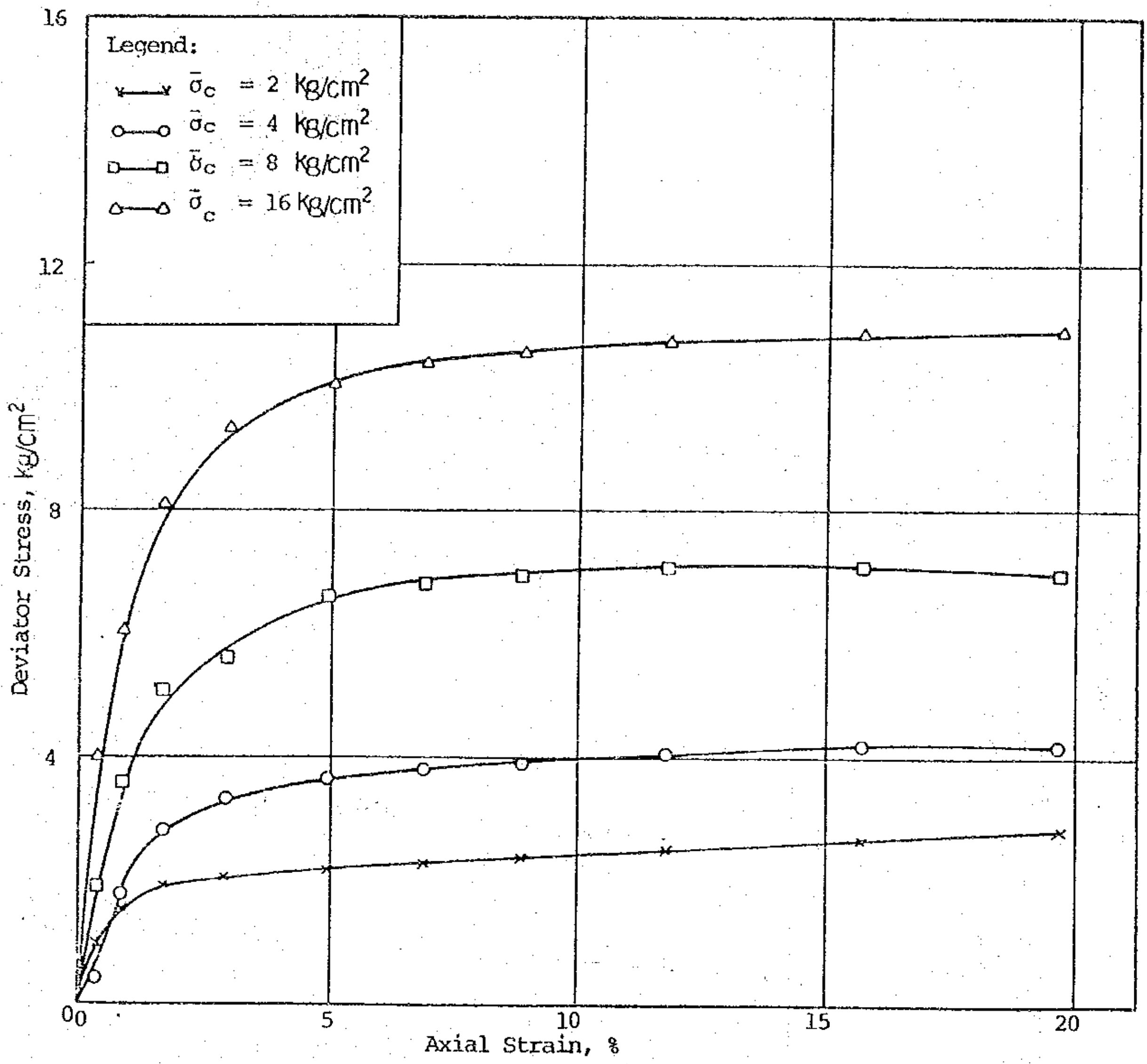

Fig. 5-7 Deviator Stress vs Axial Strain for $\overline{CU}$ Triaxial Tests on Sample No. C-1, Depth 3.00 m.

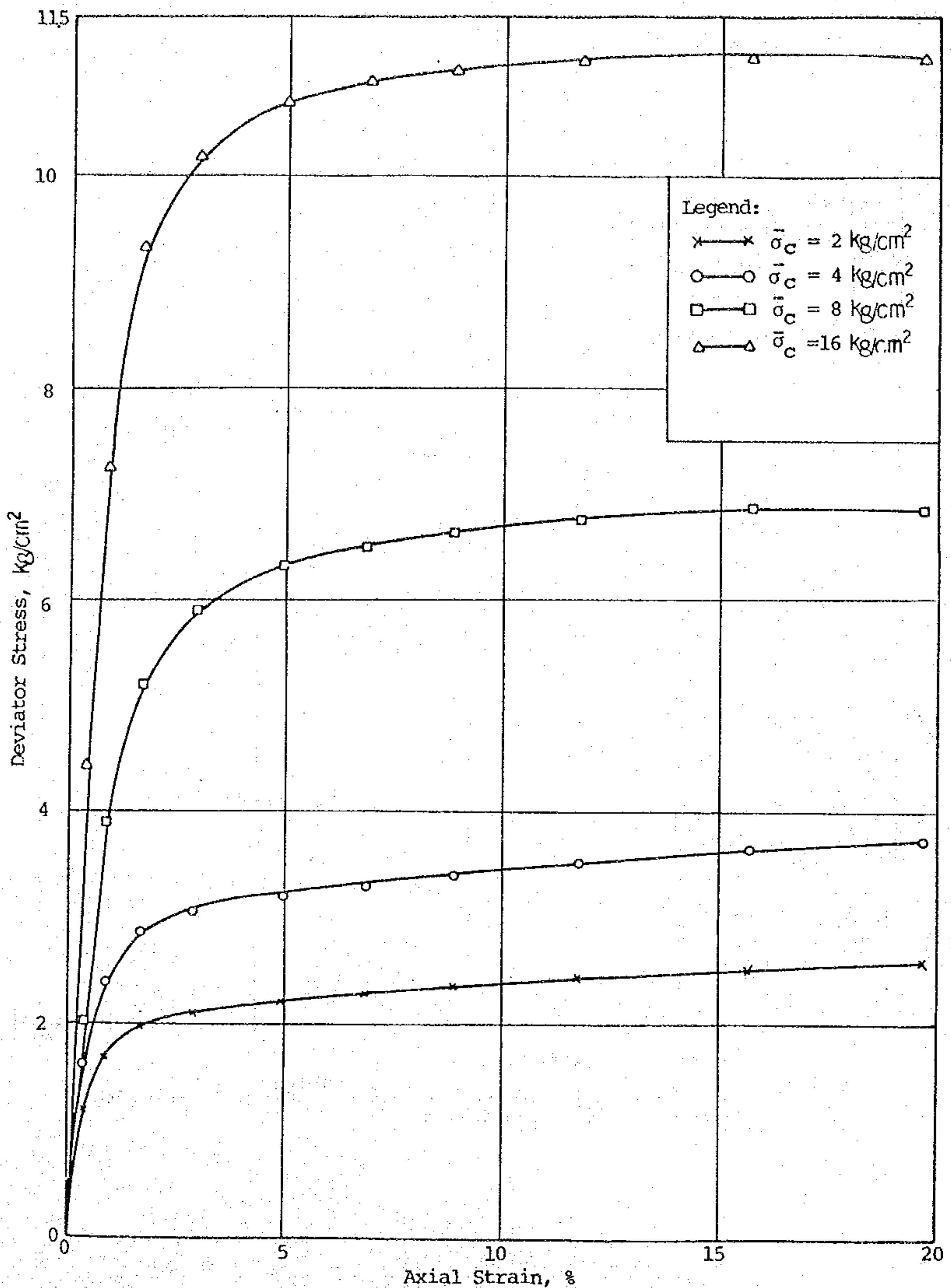

Fig. 5-8 Deviator Stress vs Axial Strain for $\overline{CU}$ Triaxial Tests on Compacted Sample No. C-1, Depth 4.00 m.

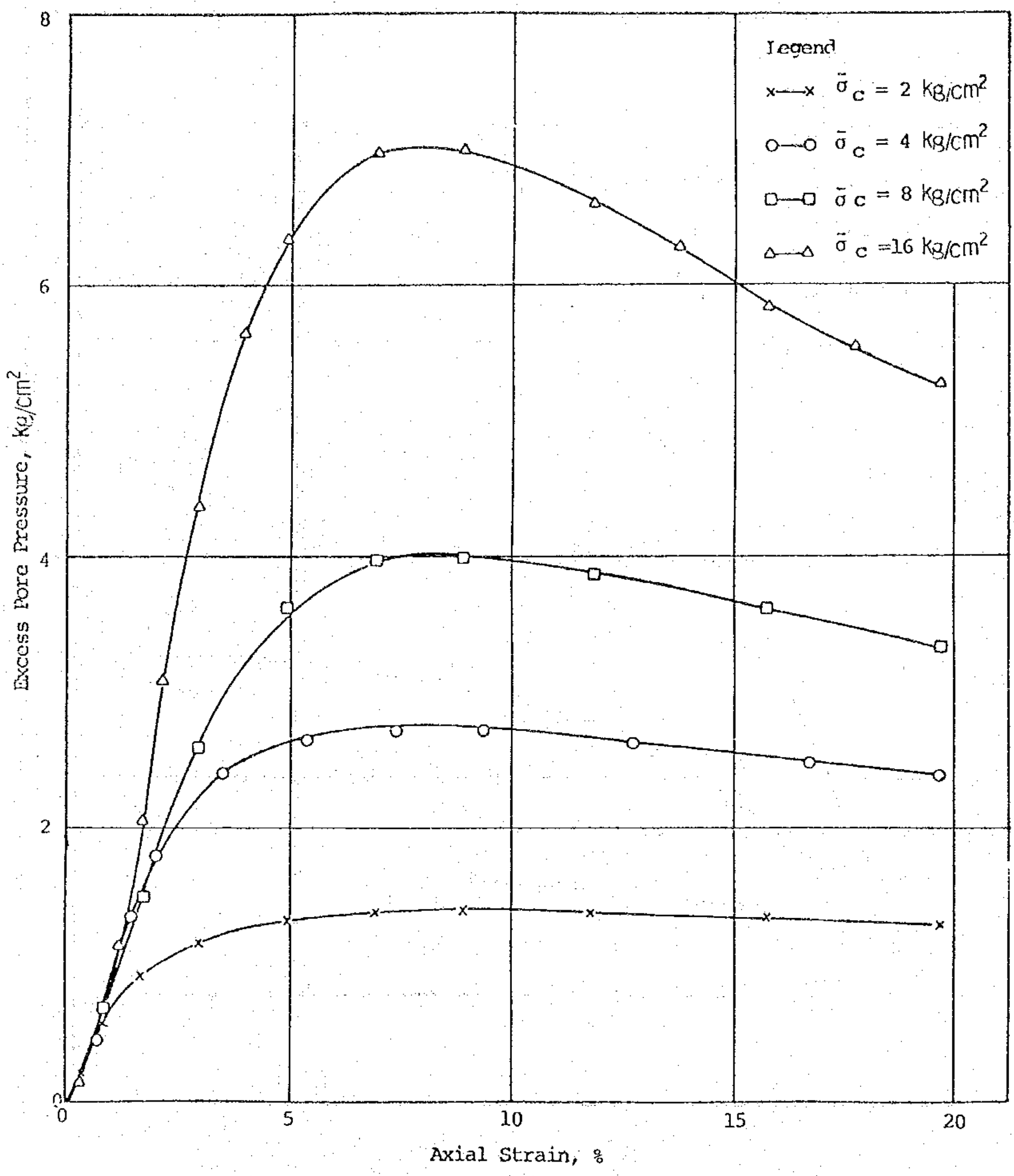

Fig. 6-1 Excess Pore Pressure vs Axial Strain for $\overline{CU}$ Triaxial Tests on Compacted Sample No. A-1, Depth 1.00 m.

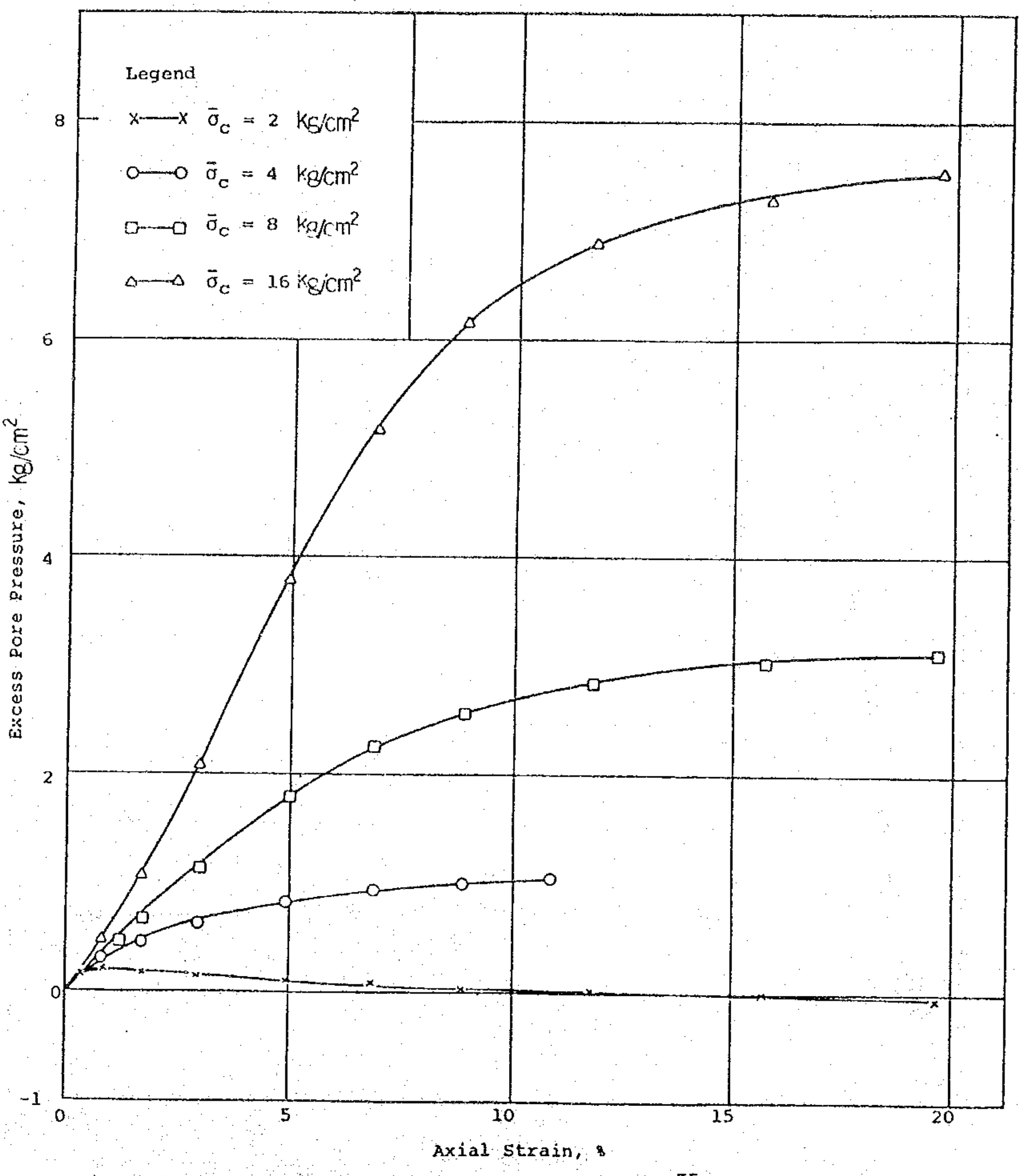

Fig. 6-2 Excess Pore Pressure vs Axial Strain for $\bar{C}\bar{U}$ Triaxial Tests on Compacted Sample No. A-2, Depth 3.00 m

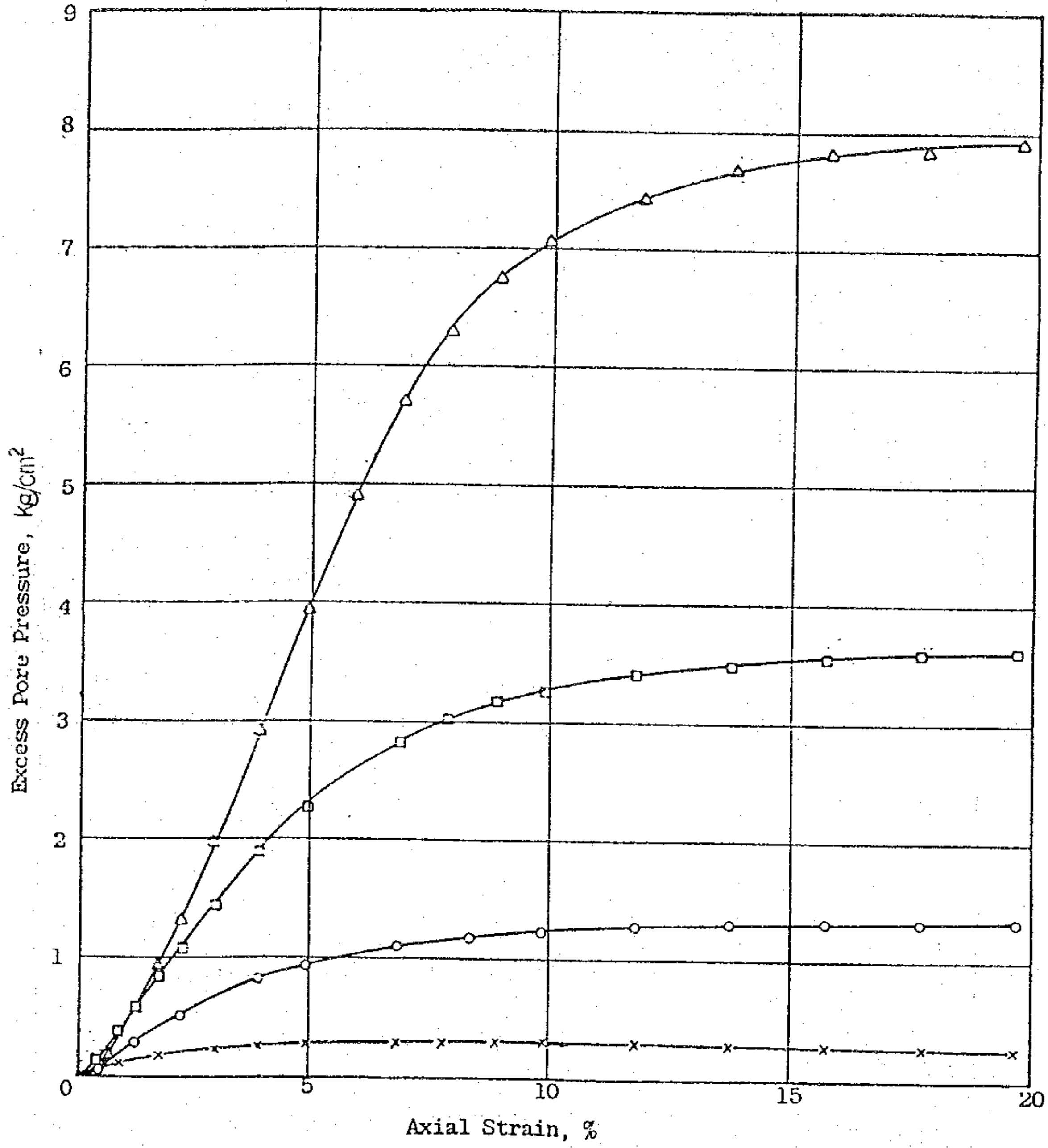

Fig.6-3 Excess Pore Pressure vs Axial Strain for $\overline{CU}$ Triaxial Tests on Sample No. A-2, Depth 5.00 m.

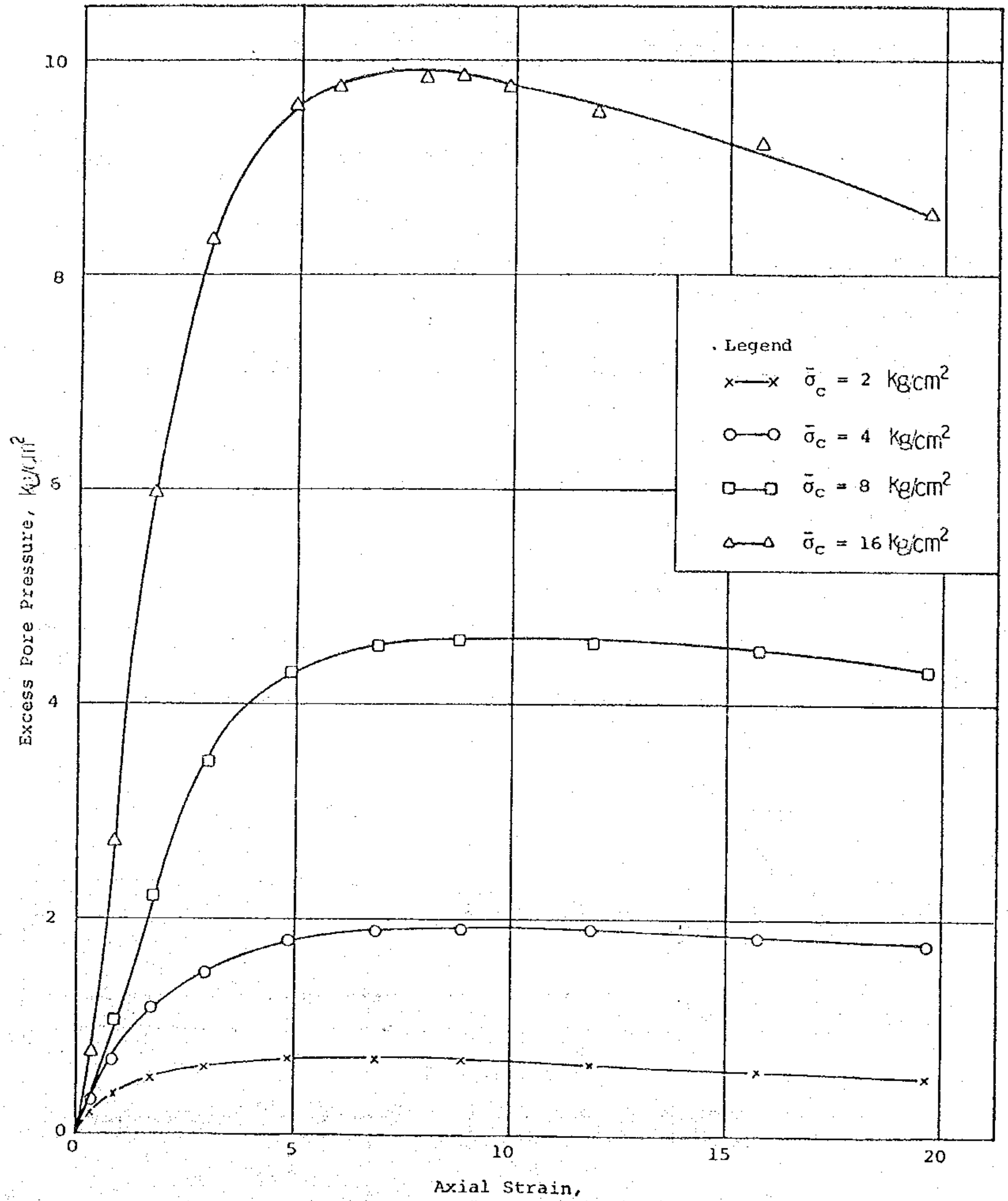

Fig. 6-4 Excess Pore Pressure vs Axial Strain for $\overline{CU}$ Triaxial Tests on Compacted Sample No. A-3, Depth 2.00 m.

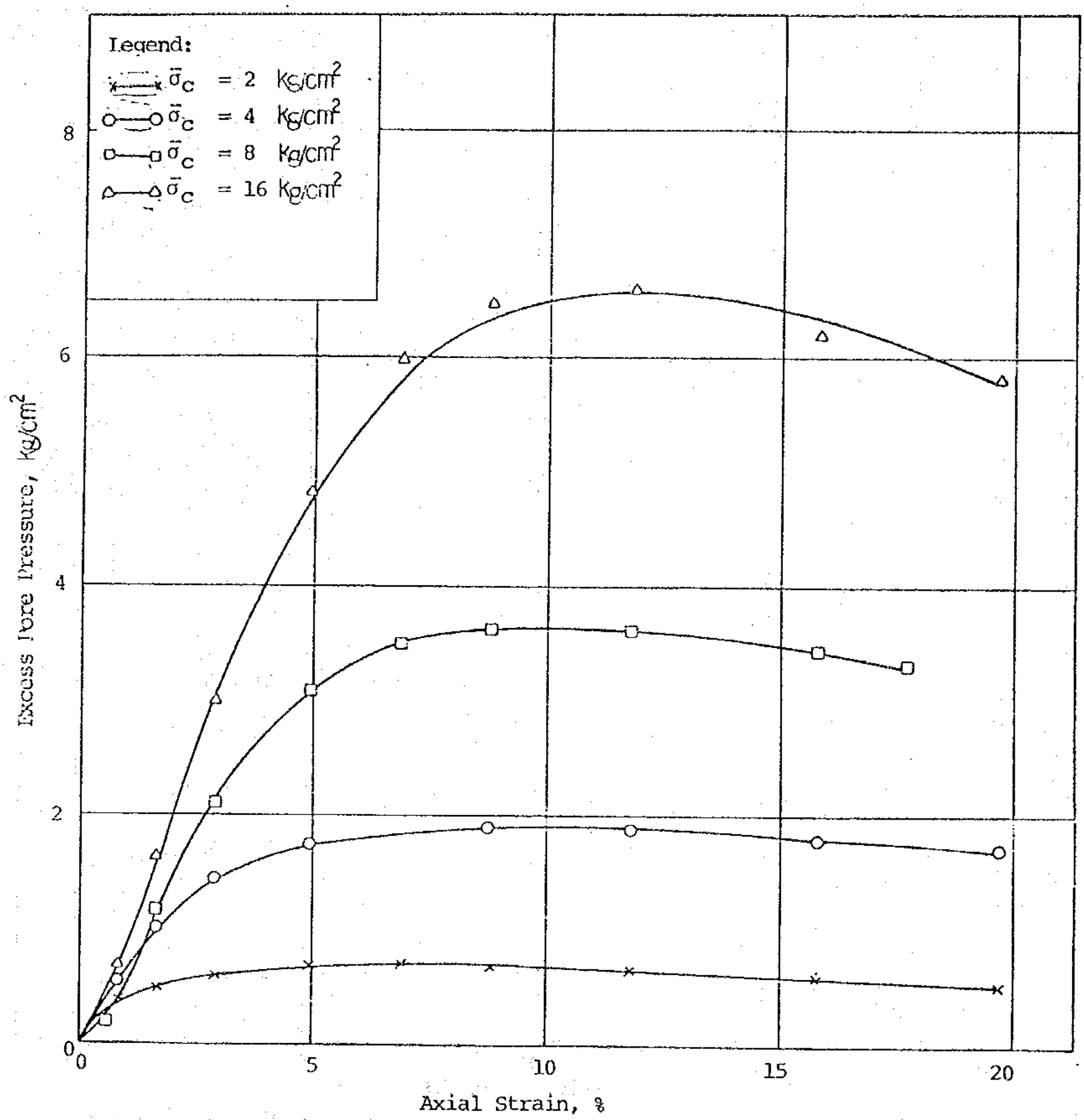

Fig. 6-5 Excess Pore Pressure vs Axial Strain for $\bar{C}\bar{U}$ Triaxial Tests on Sample No. A-5, Depth 2.00 m.

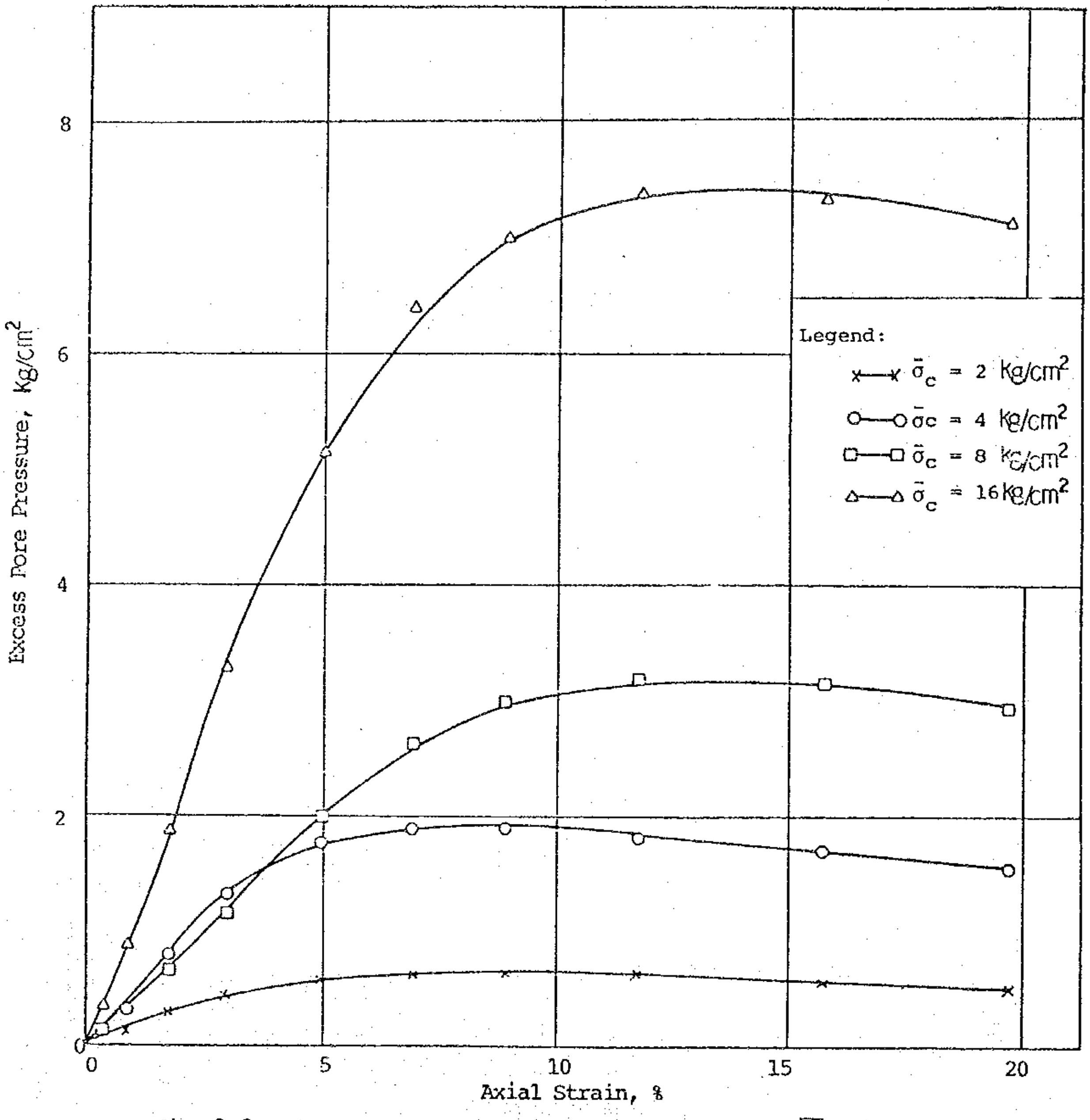

Fig. 6-6 Excess Pore Pressure vs Axial Strain for $\overline{CU}$ Triaxial Tests on Compacted Sample No. B-1, Depth 2.00 m.

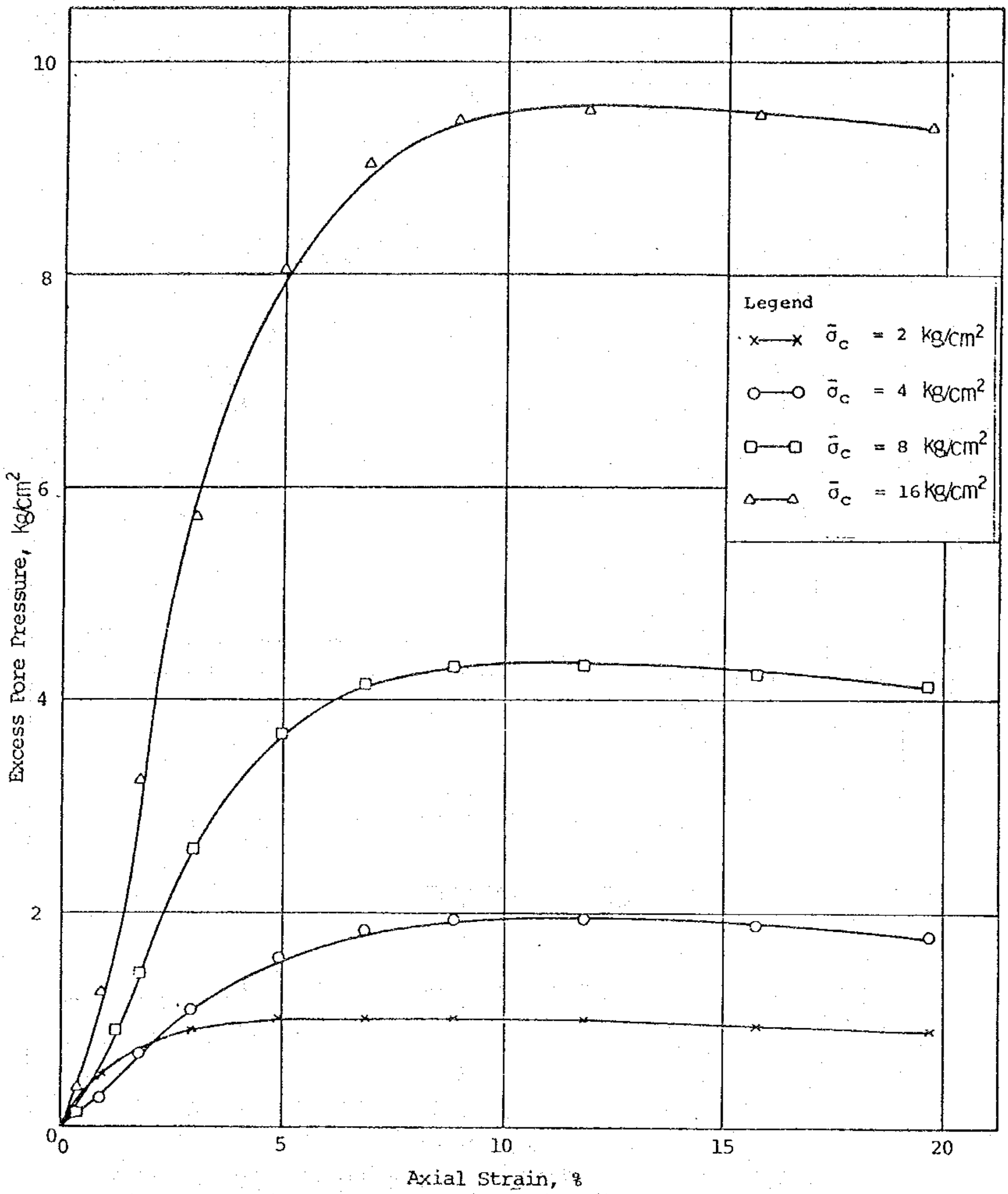

Fig. 6-7 Excess Pore Pressure vs Axial Strain for $\overline{CU}$ Triaxial Tests on Sample No C-1, Depth 3.00 m.

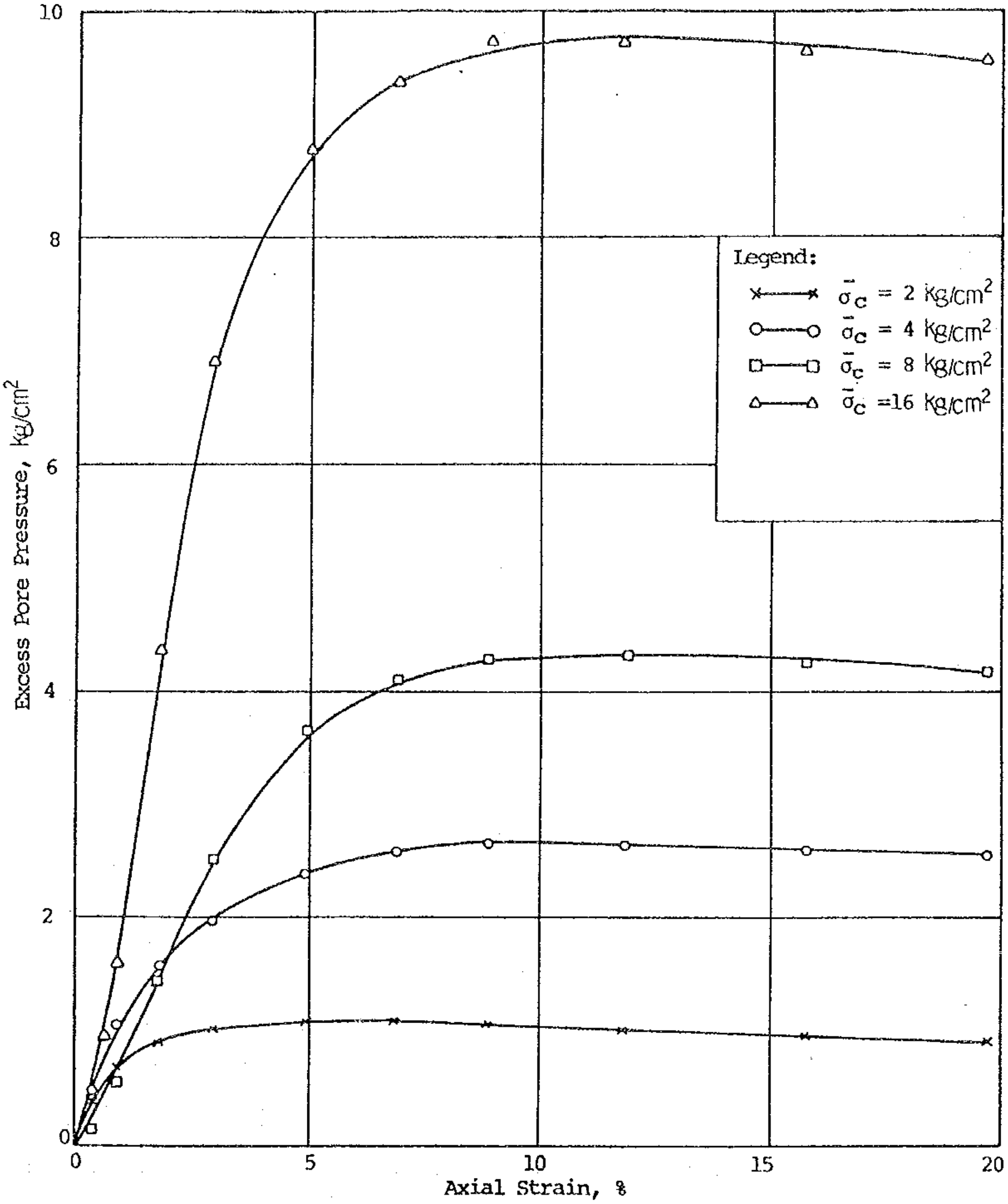

Fig. 6-8 Excess Pore Pressure vs Axial Strain for $\overline{CU}$ Triaxial Tests on Compacted Sample No. C-1, Depth 4.00 m.

A 5 CONSTRUCTION COST

Construction Cost Estimates

(1)

As of Dec. 1982 Price Level
Unit: Bath 10^3

Work Items	Unit	Unit Price	Quantities	Total Amount (10^3)	Foreign Currency (10^3)	Local Currency (10^3)
1) Preparation works						
1. Camp facilities	LS		1	122,500	38,700	83,800
2. Compensation	"		1	197,800	12,910	184,910
3. Access road	"		1	213,500	38,075	175,425
4. Clearing	"		1	19,440	-	19,440
5. Contingency	"		1	56,740	8,915	47,825
Sub-total				610,000	98,600	511,400
2) Civil works						
1. Diversion & care of river	LS		1	261,000	58,860	202,140
2. Dam	"		1	893,000	467,700	425,300
3. Spilway	"		1	519,000	81,000	438,000
4. Outlet works	"		1	41,000	5,900	35,100
5. Intake	"		1	25,000	2,700	22,300
6. Head-race	"		1	49,000	10,000	39,000
7. Surge tank	"		1	32,000	2,800	29,200
8. Penstock	"		1	69,000	13,000	56,000
9. Power station	"		1	213,000	20,900	192,100
10. Tail-race	"		1	31,700	5,200	26,500
11. Miscellaneous	"		1	93,800	35,500	58,300
12. Contingency	"		1	222,500	70,440	152,060
Sub-total				2,450,000	774,000	1,676,000
3) Hydraulic equipment						
1. Diversion gate	LS		1	9,800	490	9,310
2. Spillway gate	"		1	43,760	34,188	9,572
3. Intake gate	"		1	25,360	21,556	3,804
4. Tail-race gate	"		1	8,000	6,800	1,200

Construction Cost Estimates

As of Dec. 1982 Price Level
Unit: Bath 10^3

Work Items	Unit	Unit Price	Quantities	Total Amount (10^3)	Foreign Currency (10^3)	Local Currency (10^3)
(Continue from P-1)						
5. Outlet valve	LS		1	19,550	16,620	2,930
6. Penstock	"		1	90,000	67,500	22,500
7. Surge tank	"		1	66,000	49,500	16,500
8. Contingency	"		1	26,530	19,346	7,184
Sub-total				289,000	216,000	73,000
4) Electric equipment	LS		1	628,800	534,500	94,300
5) Telecommunication & Transmission Line	LS		1	606,600	424,600	182,000
Total				4,584,400	2,047,700	2,536,700
6) Engineering fee	LS			137,600	82,600	55,000
7) Interest during construction	LS			1,026,000	-	1,026,000
Ground-total				5,748,000	2,130,300	3,617,700

(3)

Construction Cost Estimates

As of Dec. 1982 Price Level
Unit: Bath 10^3

2) Civil Works

Work Items		Unit	Unit Price	Quantities	Total Amount (10^3)	Foreign Currency (10^3)	Local Currency (10^3)
1. Diversion & Care of river							
Excavation	Common	m^3	65	22,000	1,430	930	500
"	Rock	"	125	52,000	6,500	1,300	5,200
"	Tunnel	"	900	138,000	124,200	43,470	80,730
Concrete	Linning	"	2,900	28,000	81,200	8,120	73,080
Others		LS		1	47,670	5,040	42,630
Sub-total					261,000	58,860	202,140
2. Dam							
Excavation	Common	m^3	65	210,000	13,650	8,870	4,780
"	Rock	"	140	50,000	7,000	1,400	5,600
Embankment	Rock	"	120	3,550,000	426,000	255,600	170,400
"	Filter	"	200	412,000	82,400	49,440	32,960
"	Core	"	220	690,000	151,800	98,670	53,130
Drilling (not incl. grouting)		m	1,900	50,000	95,000	19,000	76,000
Others		LS		1	117,150	34,720	82,430
Sub-total					893,000	467,700	425,300
3. Spillway							
Excavation	Common	m^3	65	447,000	29,055	18,885	10,170
"	Rock	"	130	1,050,000	136,500	27,300	109,200
Concrete		"	2,300	102,000	234,600	23,460	211,140
Reinforcement		t	14,000	3,700	51,800	2,590	49,210
Others		LS		1	67,045	8,765	58,280
Sub-total					519,000	81,000	438,000

Construction Cost Estimates

As of Dec. 1982 Price Level
Unit: Bath 10^3

Work Items		Unit	Unit Price	Quantities	Total Amount (10^3)	Foreign Currency (10^3)	Local Currency (10^3)
(Continue from P-3)							
4. Outlet works							
Excavation	Common	m^3	65	3,200	208	135	73
"	Rock	"	140	7,500	1,050	210	840
"	Tunnel Access	"	1,500	1,600	2,400	840	1,560
Concrete	Plug	"	2,500	10,000	25,000	2,500	22,500
"	Linning	"	3,000	800	2,400	240	2,160
		LS		1	9,942	1,975	7,967
Sub-total					41,000	5,900	35,100
5. Intake							
Excavation	Common	m^3	65	6,000	390	254	136
"	Rock	"	140	13,000	1,820	364	1,456
Concrete	Open	"	2,500	6,000	15,000	1,500	13,500
Reinforcement		t	14,000	220	3,080	154	2,926
Others		LS		1	4,710	428	4,282
Sub-total					25,000	2,700	22,300
6. Head-race							
Excavation	Tunnel	m^3	930	17,000	15,810	5,534	10,276
Concrete		"	2,900	5,100	14,790	1,479	13,311
Reinforcement		t	14,500	280	4,060	203	3,857
Drilling		m	1,730	3,200	5,536	1,107	4,429
Grouting		t	7,900	320	2,528	632	1,896
Others		LS		1	6,276	1,045	5,231
Sub-total					49,000	10,000	39,000

Construction Cost Estimates

As of Dec. 1982 Price Level
Unit: Bath 10^3

Work Items		Unit	Unit Price	Quantities	Total Amount (10^3)	Foreign Currency (10^3)	Local Currency (10^3)
(Continue from P-4)							
7. Surge tank							
Concrete	Base	m^3	2,300	9,000	20,700	2,070	18,630
Reinforcement		t	14,000	330	4,620	231	4,389
Others		LS		1	6,680	499	6,181
Sub-total					32,000	2,800	29,200
8. Penstock							
Excavation	Common	m^3	65	140,000	9,100	5,915	3,185
"	Rock	"	140	60,000	8,400	1,680	6,720
Concrete		"	2,300	13,500	31,050	3,105	27,945
Reinforcement		t	14,000	490	6,860	343	6,517
Others		LS		1	13,590	1,957	11,633
Sub-total					69,000	13,000	56,000
9. Power station							
Excavation	Common	m^3	65	22,000	1,430	930	500
"	Rock	"	165	53,000	8,745	1,749	6,996
Concrete		"	2,600	40,000	104,000	10,400	93,600
Reinforcement		t	14,000	2,900	40,600	2,030	38,570
Others		LS		1	58,225	5,791	52,434
Sub-total					213,000	20,900	192,100

Construction Cost Estimates

As of Dec. 1982 Price Level
Unit: Bath 10^3

Work Items	Unit	Unit Price	Quantities	Total Amount (10^3)	Foreign Currency (10^3)	Local Currency (10^3)
(Continue from P-5)						
10. Tail-race						
Excavation Common	m^3	65	31,000	2,015	1,301	714
" Rock	"	125	72,000	9,000	1,800	7,200
Concrete	"	2,600	6,500	16,900	1,690	15,210
Others	LS		1	3,785	409	3,376
Sub-total				31,700	5,200	26,500
11. Miscellaneous (S.Y. & others)						
Excavation Common	m^3	65	252,000	16,380	10,647	5,733
Banking	"	120	250,000	30,000	18,000	12,000
Shotcrete	m^2	740	50,000	37,000	3,700	33,300
Others	LS		1	10,420	3,153	7,267
Sub-total				93,800	35,500	58,300

JICA